THE ROLE OF HEAT SHOCK PROTEINS IN $p56^{lck}$ KINASE FOLDING AND
FUNCTION

BY

BRADLEY TODD SCROGGINS

Bachelor of Science
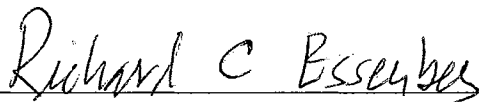
Oklahoma Baptist University

Shawnee, Oklahoma

1995

Submitted to the faculty of the
Graduate College of the
Oklahoma State University
in partial fulfillment of
requirements for the Degree of
DOCTOR OF PHILOSOPHY
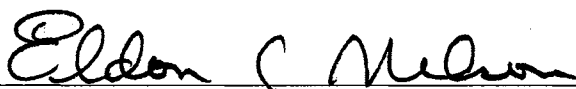August, 2002

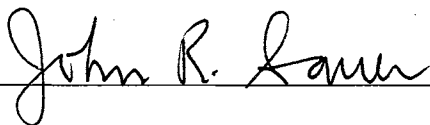THE ROLE OF HEAT SHOCK PROTEINS IN p56^{lck} KINASE FOLDING AND FUNCTION

Thesis Approved:

Robert L Matts

Thesis advisor

Richard C Essenberg

Eldon C Nelson

John R Sauer

Timothy J Pettibone

Dean of the Graduate College

ACKNOWLEDGMENTS

I wish to express my appreciation to my advisor Dr. Robert Matts for his supervision and guidance and for allowing me the opportunity to develop in his laboratory. He has been very patient and encouraging in my long stay, and has allowed and encouraged independence in thought and action at the bench. I have enjoyed the stimulating conversations we have had about research and life. I would also like to express my appreciation to my committee members Dr. Eldon C. Nelson, Dr. Richard Essenberg, and Dr. John Sauer for their guidance, supervision, and willingness to serve on my committee. To Dr. James Blair who was on my committee but has now moved, I also want to express my gratitude for his early involvement in my training both as an advisor and later as a committee member. I would like to thank the Department of Biochemistry and Molecular Biology and Oklahoma State University for financial support and for providing the equipment and laboratory facilities with which to work. Also, to the office staff of the Biochemistry Department I would like to express my appreciation for their assistance and kindness and helpfulness.

I wish to express my gratitude and say thank you to my fellow lab mates (Steve Hartson, Sheri Uma, Vanitha Thulasiraman, Jieya Shao, Bo-Geon Yun, Thomas Prince, and Angela Irwin) with whom I have shared common research interests, and whom have helped and encouraged me. To fellow colleagues and former fellow graduate students Drs. Aron Fenton and Eric Lehoux I wish to express my appreciation and say thank you for helpful and provoking discussion about all topics science and for their friendship and

encouragement. To my friend and colleague Kyle Rohde I wish to express my appreciation for his friendship and encouragement.

Finally, the best for last, I would like to express my special and profound gratitude to my immediate and extended family. To my parents who have given me their love and support through all things, including my education, and from whom I learned many things including the persistence and patience needed to complete my degrees. None of this would have been possible without their unquestionable love and support. Unfortunately, I do not have the words to express all they mean to me and so I will stop here. To my brothers Doug and Craig, I wish to thank for their support, encouragement, and brotherly love. I have and wish to continue to enjoy their friendship. To my extended family, Melissa and my niece and nephew Autumn and Kirkland, I wish to express my appreciation for their love and support and to let them know how near and dear they are to my heart.

TABLE OF CONTENTS

LIST OF TABLES

LIST OF FIGURES

Figure

LIST OF ABBREVIATIONS

ATP	adenosine triphosphate
ADP	adenosine diphosphate
BA	benzoquinone ansamycin
BHK	baby hampster kidney cells
BSA	bovine serum albumin
ClA	clofibric acid
Con A	Concanavalin A
CsA	cyclosporin A
Cyp40	40-kDa cyclophilin
DMSO	dimethylsulfoxide
DTT	dithiothreitol
EDTA	ethylenediamine-tetra acetic acid
eIF2α	eukaryotic initiation factor 2-α
FBS	fetal bovine serum
FK506	immunosuppressant drug
FKBP	FK506 binding protein
GA	geldanamycin
HRI	heme-regulated eIF-2α kinase or heme-regulated inhibitor of protein synthesis
Hsp	heat shock protein
IL-2	interleukin-2
IL-2R	interleukin-2 receptor

kDa	kilodaltons
NEM	N-ethylmaleimide
pepφ	FYQLALT
p50^{cdc37}	50-kDa homolog of the yeast cdc37 gene product
p56^{lck}	56-kDa lymphoid cell specific kinase
p60^{HOP}	60kDa Hsp70/Hsp90 organizing protein
PPI	peptidyl-prolyl cis-trans isomerase
PR	Progesterone receptor
PVDF	polyvinyldifluoride
RCM-BSA	reduced carboxymethylated bovine serum albumin
RRL	rabbit reticulocyte lysate
SDS-PAGE	sodium dodecyl sulfate poylacrylamide gel electrophoresis
SHR	steroid hormone receptor
TCR	T cell receptor
TPR	tetratricopeptide repeat

CHAPTER 1

INTRODUCTION

One biological function shared by all competent proteins is the ability to fold

properly. This function must be performed effectively before other productive functions

are possible [1]. The growing list of diseases attributed to protein misfolding underscores

this importance and demonstrates the consequences of ineffective folding [2, 3]. For this

reason as well as its fundamental importance to biology, protein folding has been the

focus of much study. How proteins achieve proper folding is still unknown. Anfinsen [4]

proposed that all of the information needed for protein folding to a native active

conformation was contained in its primary amino acid sequence. This process occurred

spontaneously *in vitro* without the aid of other proteins, a concept referred to as self-

assembly. Some researchers assumed protein folding *in vivo* occurred spontaneously and

unassisted as well. However, protein folding *in vitro*, even for simple monomeric proteins

under optimal conditions, takes place very slowly, much more slowly than seen *in vivo*.

An added complication of *in vivo* protein folding is molecular crowding, which may

change reaction rates and equilibria by more than an order of magnitude resulting in

unfavorable protein aggregation [5].

It is now appreciated that *in vivo* protein folding of some proteins (especially

large multi-domain proteins) is greatly enhanced by other proteins called molecular

chaperones. Molecular chaperones can facilitate protein folding usually via an ATP

dependent mechanism, which subsequently prevents improper interactions between

1

protein surfaces that lead to non-productive protein folding pathways. The concept of molecular chaperones does not refute the concept of self-assembly, rather it is thought chaperones assist proteins in self-assembly by reducing non-productive interactions that might compete with self-assembly interactions in a complex cellular environment [6]. Most molecular chaperones are stress proteins, meaning their synthesis is upregulated under stress conditions such as heat shock or hypoxia. More extensive reviews of the list of molecular chaperones can be found in the literature [1, 3, 7-9]. Only the chaperones studied in this report are reviewed below: Hsp90, Hsp70, Hsp40, p60[HOP], FKBPs, Cyp40, p23, and p50[cdc37].

Hsp90

Hsp90 structure and function

The 90-kDa Heat Shock Protein (Hsp90) family of proteins was originally identified, as indicated by the name heat shock protein, as a 90-kDa protein induced by heat stress. Under these conditions Hsp90 aids in protein refolding of thermally denatured proteins and prevents irreversible thermal aggregation. This indicates the importance for Hsp90 function under stress conditions. However, even when cells are unstressed constitutively expressed Hsp90 is one of the most abundant proteins in the cell [10]. In most eukaryotes, two cytosolic isoforms Hsp90α and β, have been identified. While both isoforms may be constitutively expressed in some cell types, Hsp90β is constitutively expressed in most cells, and Hsp90α expression is the primary isoform of Hsp90 induced by stress. The importance of Hsp90 for cell functions is underscored by its evolutionary

conservation from bacteria (called HtpG in *E. coli*) to higher eukaryotes. However, the role it plays in facilitating cellular processes may have changed over time, since Hsp90 is vital for eukaryotes from yeast on up, but is not essential for bacterial survival (reviewed by [11]). In eukaryotes, cytosolic Hsp90 is reported to function in many cellular processes including signal transduction, protein trafficking, chromatin condensation, cell cycle regulation, regulation of transcription and translation, protein degradation, and apoptosis [12]. Based on the abundance of Hsp90 in the cell and the multiple and varied functions one may expect Hsp90 to play a role in general protein folding. However, Hsp90 is not involved in folding of most proteins in the cell but rather seems to work on a select set of proteins that are critical for certain cell functions and survival. Cytosolic Hsp90 is the most highly expressed member of the Hsp90 gene family, but recently other organelle specific family members have been identified which add to the functions attributed to the family. Grp94/pg96 localizes to the endoplasmic reticulum and is involved in protein folding and transport in the ER, as well as antigen presentation to the major histocompatibility complex for mounting immune responses (reviewed in [13]). Hsp75/TRAP1 is found in the mitochondrial matrix and is also thought to function in transport and folding of mitochondrial proteins (reviewed in [14-16]). Hsp90 will be used to refer to the abundant cytosolic form and when generally referring to the whole family, specific members will be referred to by name when distinctions about function, structure, or location are necessary.

All family members share similar structural domain organization and are therefore expected to act by similar mechanisms. Hsp90 functions as a homodimer. Dimerization is attributed to its C-terminal 191 residues [14, 17]. The N-terminal domain is highly

conserved and binds ATP in an unusual kinked conformation [18, 19]. Bound ATP is

hydrolyzed, thus making it an ATPase. Structural comparisons of this domain with other

proteins have placed Hsp90 into the GHKL superfamily of homodimeric

ATPases/kinases including members such as DNA gyrase B, MutL, and the prokaryotic

histidine kinases Che A and Env Z (involved in E. coli osmosensing). Proteins in this

superfamily bind ATP by a structurally novel Bergerat fold [20, 21], which is probably

the reason for the unusual kinked conformation of the bound nucleotide [12, 19]. Based

on the similarity in structure to DNA gyrase and MutL a similar mechanism of action has

been proposed in which Hsp90 is dimerized by association of its C-terminal sites. Upon

binding ATP the N-terminal domains are induced to transiently dimerize forming a

"molecular clamp" around the unfolded protein substrate allowing it to fold or actively

participate in folding. The substrate protein is released when ATP hydrolysis disrupts the

dimerization of the N-terminal domains [14, 22, 23]. This is a useful model for nucleotide

regulated substrate binding based on the structural studies of these proteins, but more

work is needed to determine whether Hsp90 actually facilitates protein folding through

this mechanism.

Evidence that is consistent with a molecular clamp model demonstrates that

Hsp90 exists in at least two functional conformations that are regulated by nucleotide

binding. The two functional conformations are characterized by Hsp90's affinity for

phenyl sepharose when bound to ADP and its affinity for p23, a co-chaperone, when ATP

is bound [24, 25]. These conformations have been further characterized by the effect of

two Hsp90 binding drugs: benzoquinone ansamycins and molybdate. The benzoquinone

ansamycin geldanamycin (GA) mimics the kinked conformation of the nucleotide bound

to Hsp90 [18, 19]. GA locks Hsp90 in an open ADP conformation with high affinity for phenyl sepharose. Molybdate action depends on the presence of ATP and is thought to bind with ADP mimicking the γ-phosphate of ATP after hydrolysis, locking Hsp90 into an Hsp90:ADP+MoO$_4$ closed complex. Both of these conformations have characteristic protease fingerprints indicating distinct structural differences. Neither drug-induced conformation represents a productive folding complex, however, as indicated for the p56^{lck} kinase substrate [26, 27].

Two other structures identified in the cytosolic Hsp90 protein sequence are: a variable charged region and the MEEVD sequence at the C-terminus. The charged region is variable in sequence and length between family members, being completely absent in bacterial HtpG and Hsp75/TRAP, and separates the N-terminal ATPase domain from the conserved middle domain (M). One report indicates this region may function in regulating peptide substrate binding, although it is not vital for Hsp90 folding of transfected steroid receptors in yeast [28, 29]. The MEEVD sequence is conserved and is important for TPR (tetratricopeptide repeat) containing co-chaperone associations (to be discussed later). A graphical representation of the Hsp90 domain organization is shown below. The actual substrate binding site has not been identified although reports of both N-terminal and C-terminal substrate binding may indicate that there is more than one site [30]. This may explain why Hsp90 has such a diverse clientele (see Table 1) and may allow it to be more adaptable to client folding requirements. It also may explain the failure to identify a consensus binding motif among its clients. The only consistent theme to Hsp90 clients, to date, is that most are multi-domain regulatory signal transduction

proteins that can adopt more than one conformation, thus designating Hsp90 the "signal

transduction chaperone".

ATPase	Charged		Dimerization	
N-terminal domain		Middle domain	C-terminal domain	MEEVD
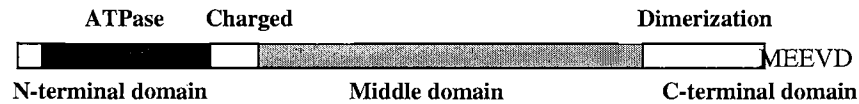
The Hsp90 chaperone cycle and co-chaperones

During active (ATP dependent) chaperoning Hsp90 associates with several

protein cohorts or co-chaperones forming more than one large multicomponent chaperone

complex. For the most part these co-chaperones appear to bind and dissociate in an

ordered ATP dependent fashion [31-34]. This has come to be known as the Hsp90

chaperone cycle [11]. Certainly some Hsp90 substrates are folded by a cycle of Hsp90

and co-chaperone binding and release; however, it is important to point out that Hsp90

does not nescessarily interact the same with each substrate. In fact, it is useful to compare

Hsp90/substrate interactions and to exploit differences to learn more about function. The

Hsp90 chaperone cycle model is based mostly on reconstitution studies of the steroid

hormone receptor family of substrates (see Figure 1). These studies indicate that during

biogenesis to a steroid binding state Hsp70 and its co-chaperone Hsp40 bind the receptor

forming the "early complex" [11, 34-37]. After an initial step where Hsp70 hydrolyzes

ATP and Hsp40 is released, the co-chaperone p60HOP (Sti1 in yeast) associates with the

complex [31, 32, 34, 38]. P60HOP interacts with Hsp70 through its N-terminal TPR1

domain. P60HOP also interacts with Hsp90 via its central TPR2A domain forming a

large Hsp70•p60HOP•Hsp90 complex called the "intermediate complex" [11, 34, 39, 40]. In this complex the steroid receptor passes from Hsp70 to Hsp90. The Hsp70 and p60HOP are replaced by at least one TPR containing immunophilin per Hsp90 monomer (FKBP51, FKBP52, or Cyclophilin 40) and the acidic p23 protein in the "late complex" [11, 41, 42]. Previous reports indicate that for kinase substrates, the kinase specific co-chaperone $p50^{cdc37}$ is substituted for the immunophilin component [43, 44]; however, work presented in chapter 2 indicates that is not necessarily true [45, 46]. Also at least one steroid receptor, androgen (AR), forms a complex with $p50^{cdc37}$ [47]. The mature complex is thought to keep the steroid receptors in a conformation capable of binding hormone but incapable of binding DNA as a transcription factor. In the presence of hormone, Hsp90 complex dissociation correlates with the formation of an active ligand bound receptor dimer.

As mentioned above Hsp90 interacts with several different proteins during folding. These proteins are thought to assist Hsp90 in ATP dependent client folding. All except Hsp70 and Hsp40 are referred to as Hsp90 cohorts or co-chaperones. Independently many co-chaperones facilitate protein folding or refolding indicating their importance may not be limited to Hsp90 mediated folding. The functions they play in Hsp90 mediated folding are just now being determined and are still largely unknown. More work is required to determine how they influence Hsp90 functions. To provide more detailed information for future reference a short section about each Hsp90 partner protein is included.

Figure 1. Hsp90 Chaperone Cycle Involved in Steroid Hormone Receptor (SHR) Folding and Activation.

Steroid receptors form heterocomplexes with many chaperones and co-chaperones in an ordered ATP dependent manner. The first components found to bind are Hsp70 and Hsp40 forming the "Early complex". Hsp90 is shown as a dimer. p60HOP also forms a dimer but only the monomer is shown for clarity. These components bind to form a second "Intermediate complex". Hsp70 hydrolyzes ATP during its binding and release of the SHR substrates. Both Hsp90 and Hsp70 have ADP bound in the intermediate complex. Hsp70 and p60HOP are released and p23 and immunophilins (IP) bind to form the "Late complex" in an ATP dependent step. Geldanamycin (GA) is shown as inhibiting the formation of the "Late complex". ATP is hydrolyzed and SHR is released and if hormone is not present (H) the cycle starts again. If hormone is present the receptor binds and becomes chaperone independent and able to bind DNA as a trascription factor. MoO_4 is shown as inhibiting the release of SHR from the "Late complex". MoO_4 would also inhibit activation of the receptor by hormone but, it is not shown in this diagram.

8
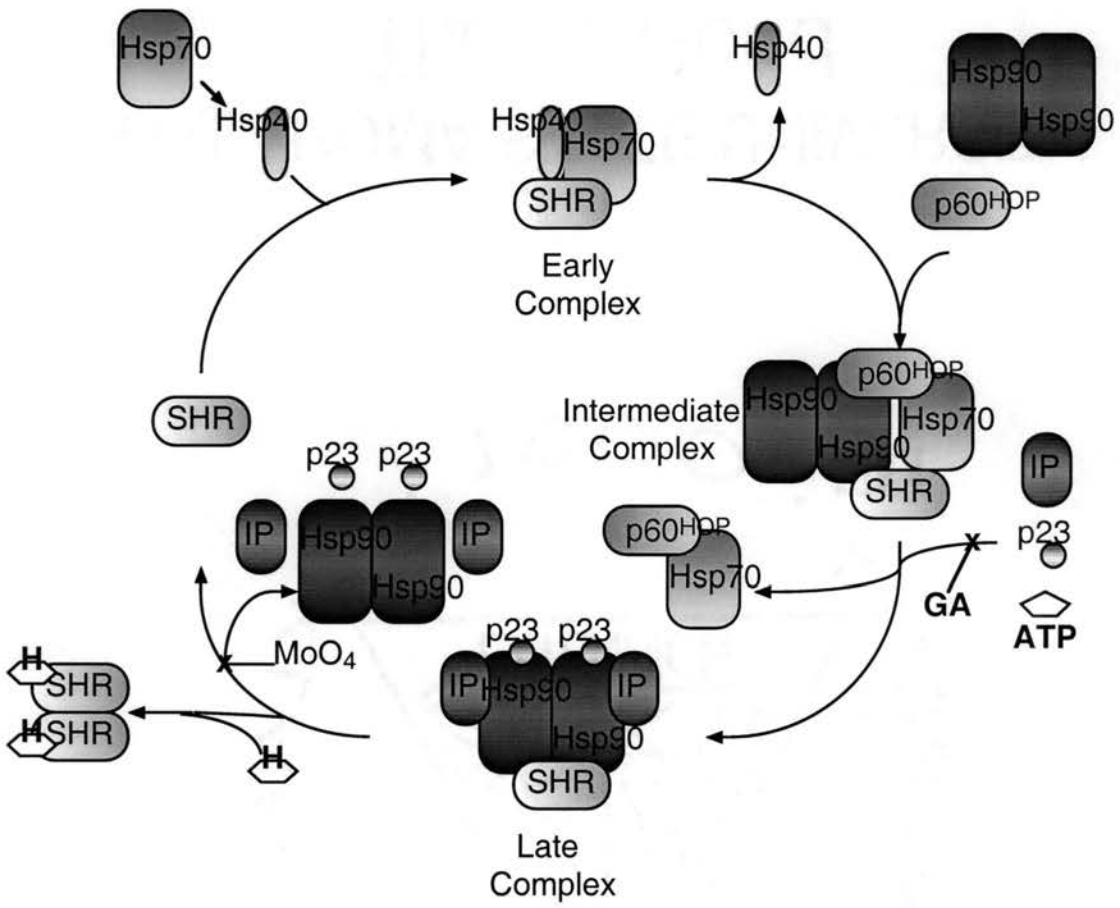
Hsp90 Partners

Hsp70 and Hsp 40

Like Hsp90, Hsp70 is just one member of a large family of proteins. Hsp70 facilitates ATP dependent protein folding in the cytosol of both prokaryotes and eukaryotes under stress and unstressed conditions. The reported functions of Hsp70 are wide and varied and include protein trafficking, apoptosis, protein degradation, translocation across membranes, regulation of transcription and translation, vesicle uncoating, and signal transduction [48]. Unlike Hsp90, Hsp70 is thought to play a more generic role in *de novo* protein folding, interacting with many folding substrates co-translationally [49-51]. An Hsp70 consensus binding motif has been identified indicating that a short hydrophobic stretch of amino acids in an extended conformation followed by a short region of basic residues provides a high affinity binding site for Hsp70 [52-54]. Estimates of the number of Hsp70 binding sites in the average protein (based on the common occurrence of amino acids for proteins in sequence databases) predict several sites per protein [55, 56]. This is consistent with a role for Hsp70 in general protein folding. Experimental evidence indicates Hsp70 dependent folding, while more common than Hsp90 mediated folding, is not as common as predicted [57] and actual cellular interactions and functions are more regulated (reviewed in [58]). Hsp70 regulated substrate folding is controlled by its co-chaperones, similar to Hsp90. There are several Hsp70 co-chaperones, but only Hsp40/DnaJ is reviewed here.

Hsp40 is a eukaryotic member of the DnaJ (*E. coli* Hsp40) family of proteins that are characterized by the presence of a conserved N-terminal J-domain. The J-domain meditates Hsp40's interaction with Hsp70. In *E. coli* the homolog DnaJ stimulates DnaK (*E. coli* Hsp70) ATPase activity and modulates substrate binding. Hsp70 chaperone function is referred to as a cycle of ATP regulated substrate binding and release much like the two state model of Hsp90. The ATP-bound open conformation of Hsp70 has a low affinity for substrate allowing rapid exchange. The ADP-bound closed conformation of Hsp70 has high affinity for substrate and a very slow exchange rate. It is thought that Hsp40 first binds the substrate in an ATP independent manner and conveys it to Hsp70 as the first step in the cycle. The Hsp40-substrate complex associates with Hsp70 via the J-domain interaction. Hsp40 can bind Hsp70 in either state although the exchange rate of substrate with the ATP-bound Hsp70 is higher and is therefore favored. Once the substrate is transferred to Hsp70 the ability of Hsp40 to stimulate ATPase activity converts Hsp70 into an ADP-bound high substrate affinity and slow exchange state, allowing prolonged interaction and folding. In *E. coli* an additional co-chaperone, GrpE, exchanges DnaK bound ADP for ATP stimulating substrate release and completing the cycle. A GrpE homolog in eukaryotes has not been identified suggesting the ADP exchange occurs independently or by some other mechanism. However, both p60/STI1/HOP and Bag1/RAP46 promote ADP dissociation and exchange for ATP, making them potential functional homologs even though they do not replace GrpE function in bactieria.

Hsp40 substrate binding is attributed to its C-terminal domain, which is variable among family members. The C-terminal domain variability is thought to impart substrate

specificity and regulation to the Hsp70 folding cycle. Since the DnaJ family of chaperones is large (over 150 proteins so far) there is potential for functional diversity in Hsp70 machinery as well [58]. Eukaryotic Hsp40 alone assists in processes such as steroid hormone receptor folding and regulation, co-translational folding, protein renaturation, tumor suppression, and cell cycle regulation [36, 37, 59-62]. Other DnaJ proteins may allow Hsp70 to function in other processes.

P60/HOP/STI1

P60/HOP (HOP-Hsp70/Hsp90 Organizing Protein) was originally identified as the nonessential yeast protein STI1 (stress inducible mediator of heat shock response)[63]. Later its human homolog, up regulated in SV40-transformed cells, was reported to contain several tetratricopeptide repeat (TPR) motifs, a degenerative 34 amino acid repeat motif reportedly involved in facilitating protein-protein interactions [64, 65]. In the convergent field of steroid hormone receptor research a 60kDa protein, later identified as a STI1 homolog, was isolated from receptor complexes [66]. P60/HOP is composed almost totally of TPR domains, nine motifs divided into three domains (TPR1 composed of 3 motifs and TPR2A and B composed of 3 motifs each). TPR domains are composed of three or more TPR motifs usually in tandem but sometimes separated or overlapping. Structural studies indicate a cradle structure of seven α-helices in which the conserved EEVD motifs of Hsp70 and Hsp90 bind by multiple electrostatic interactions. The TPR1 N-terminal domain binds Hsp70 and the TPR2A middle domain binds Hsp90 and can do so simultaneously [38, 40, 67, 68]. Additional hydrophobic interactions with residues N-terminal of the EEVD motif determine the binding specificity of each domain

for Hsp70 or Hsp90 [40]. The C-terminal EEVD motif mediates the binding of several TPR containing proteins in addition to P60HOP (see below).

The EEVD motif represents the minimal sequence for strong binding of TPR proteins. Other contact points of TPR co-chaperones have been suggested which regulate the ATPase, and therefore folding, activity of each of these proteins. P60HOP inhibits Hsp90 ATPase activity and favors binding to the open ADP-bound conformation [69]. It also favors binding to the closed ADP-bound form of Hsp70. These two conformations represent the opposite affinity states for substrate binding, and since p60HOP stimulates Hsp70 ADP exchange for ATP it is thought substrate transfer from Hsp70 to Hsp90 is stimulated as well. Hsp90 then quickly converts to an ATP-tight binding conformation, which in addition possibly causes co-factor exchange. It is important to point out that p60HOP forms homodimers that may bind homodimers of Hsp90 [69] but does not necessarily exclude the possibility of more than one TPR containing co-chaperone in complex with Hsp90 dimers forming mixed complexes.

Other TPR Co-chaperones

There are several Hsp70 and Hsp90 co-chaperones other than p60HOP that have TPR domains. Very little is known about the functions they have or impart to the chaperone complexes. The TPR proteins reviewed here are mostly Hsp90 co-horts. One family of TPR containing co-chaperones is called the high molecular weight immunophilins. In addition to containing TPR domains (composed of 3 TPR motifs), immunophilins also include a peptidylprolyl cis-trans isomerase (PPIases) domain that catalyzes the cis-trans isomerization of peptide bonds preceding proline residues.

Immunophilins are grouped into two structurally unrelated classes based on their ability to bind one of two immunosuppressive drugs that inhibit the isomerase activity. The cyclophilin (Cyp) class binds cyclosphorin A (CsA). The main member of interest for Hsp90 interaction is Cyp40 (its calculated molecular weight is 40 kDa). FKBP (FK506 Binding Proteins) proteins bind to the compounds FK506 and rapamycin, and include the Hsp90 binding members FKBP51 and FKBP52 (also identified by their calculated molecular weights) [70]. The function of these proteins in Hsp90 complexes is unknown, although all have been found in both native (substrate free) and steroid hormone bound Hsp90 complexes. One report suggests that there are two immunophilin binding sites in each Hsp90 dimer [71]. Heterocomplexes with two different immunophilin components have not been reported and in fact there are reports of competition between the different immunophilins for binding to Hsp90 [72]. Initially, a catalytic role was assumed where the immunophilin is recruited to the Hsp90/substrate complex by the TPR domain and subsequently catalyzes the slow cis-trans isomerization of peptidylprolyl bonds; however, inhibition of the PPIase activity by CsA and/or FK506 did not have an effect on Hsp90 interaction or folding of the glucocorticoid receptor [73]. Mutation of residues in the PPIase domain necessary for PPIase activity of the yeast Cyp40 (Cpr7) had no effect on GR activity when transfected into yeast. Therefore, the role of the PPIase domain in Hsp90 folding is in question, since the TPR domain and flanking regions appear to be sufficient for complex assembly and folding of the steroid receptor substrates [74].

A role in receptor attachment and trafficking has been proposed for the immunophilins [75, 76]. Cyp40 and FKBP52 both localize to the nucleus and may be the components of the Hsp90 complex that target the receptor transcription factors to the

nucleus. FKBP52 also interacts with the cytoskeletal associated motor protein dynein [77].

Another Hsp90 associated TPR containing protein is the Protein-serine/threonine Phosphatase 5 (PP5). PP5 has an N-terminal TPR domain composed of four TPR motifs and a C-terminal phosphatase domain that can catalyze the transfer of a phosphate group off of serine or threonine residues (reviewed in [78]). It is not known what role PP5 plays in the Hsp90 machinery, although an obvious possibility is to catalyze the dephosphorylation of either Hsp90 or Hsp90 associated proteins (co-hort or client). A recent report suggests this is a definite possibility for the regulation of the Hsp90 client the Heme-Regulated Inhibitor (HRI) of protein synthesis, an eIF2α kinase [79].

A final TPR containing Hsp90 associated protein is CHIP (carboxyl terminus of Hsc70-interacting protein). CHIP was originally identified as a protein that interacted with the C-terminus of Hsc70 [80]. Later it was found to also bind Hsp90 and to contain an U-box E3 ubiquitin ligase domain that could catalyze the ubiquitination of chaperone substrates. A proposed role in targeting Hsp90 and Hsp70 substrates to degradation by the proteasome has since been proposed especially in the presence of chaperone inhibiting drugs [81, 82].

Several other TPR containing Hsp90 co-horts have been identified, but defined roles in Hsp90 mediated folding of substrates have not been demonstrated. Several proposed functions have been suggested ranging from regulating Hsp90 ATPase activity to trafficking substrates to specific locations in the cell to targeting substrates for degradation. There is still much work that needs to be done to determine the functions and new protein clients and co-horts are still being identified.

Protein 23

p23 was originally identified as a novel 23-kDa acidic protein associated with the unactivated progesterone receptor (PR) complex. In addition to p23, PR complexes contained Hsp90, FKBP51 and 52, and Cyp40 [83]. p23 had no sequence homology to heat shock proteins or immunophilins or to any other protein known at that time [84]. Immune isolation of p23 from rabbit reticulocyte lysate (RRL) in the absence of receptor, also isolate Hsp90 and the immunophilins indicating p23 functions as part of the Hsp90 machinery [42]. Since then p23 has been found in association with several other Hsp90/client complexes [45, 85]. Depletion of p23 from RRL prevented the assembly of PR complexes competent to bind hormone. Addition of purified p23 restored this activity to RRL, suggesting p23 is an essential component of the Hsp90 machinery in RRL [42]. This essential function may have developed in higher organism, however, since deletion of p23 from yeast only mildly affects growth and folding of exogenous Hsp90-dependent steroid receptors or kinases [86-88].

The function of p23 in Hsp90 chaperoning is unknown. However, it is interesting to note that unlike many other Hsp90 co-horts, p23 binds only to ATP-bound Hsp90. ATP hydrolysis does not appear to be necessary for binding since non-hyrolyzable ATP analogs stabilize the substrate free Hsp90-p23 complex. In support for p23 association with the ATP-bound Hsp90, GA disrupts the p23 complex with Hsp90 and substrate. Molybdate also stabilizes the Hsp90-p23 complex and can do so when substrate is present. Formation of this complex requires the hydrolysis of ATP. In the absence of stabilizing agents the p23 association with Hsp90 and client are usually sensitive to salt

(0.5 M KCl) and heat (37 °C) [89]. In fact detection of the p23 component with PR was not seen until rapid and gentle techniques were used, and isolation of this complex is now often done in the presence of molybdate.

Even though the function of p23 in the Hsp90 machinery is unknown some reports have suggested p23 is involved in stabilizing a conformational state of Hsp90 that is necessary for folding [88]. Others propose that p23 stimulates client substrate release from Hsp90 upon ATP hydrolysis [90]. Some Hsp90 independent activities of p23 have also been identified recently, such as interacting with DNA cytosine-5 methyltransferase [91]. Also, p23 was recently identified as a cytosolic glutathione (GSH)-dependent prostaglandin E_2 synthase [92]. These activities may or may not be related to p23 function in the Hsp90 complex.

The kinase targeting p50^{cdc37} chaperone

p50^{cdc37} was originally identified in yeast as a cell division cycle (cdc) mutant that caused cell cycle arrest at Start in G1 [93]. In another field of research, a 50-kDa protein that interacted with viral transforming kinase complexes in association with Hsp90 was also identified [94]. It was not until homologs in Drosophila and mammals were identified as the 50-kDa protein associated with Hsp90 and kinases that the two fields merged. p50^{cdc37} forms complexes with Hsp90 independently and with several kinase substrates, including the Cdc28 kinase, Cdk4, Raf, members of the Src kinase family, Mps1p, HRI, and the sevenless receptor tyrosin kinase [46, 95-98]. Both Hsp90 and p50^{cdc37} bind directly to the kinase domains of these substrate kinases [44, 99, 100]. Studies on truncation mutants localize Hsp90 interaction to sites in the C-terminal half of

17

the protein and kinase interaction sites in the N-terminal half of the protein. While the ability of p50^{cdc37} to bind kinases directly is thought to be the determining factor in formation of Hsp90 complexes with kinase substrates, Hsp90 can also bind kinases independent of p50^{cdc37}. The two proteins appear to participate actively in kinase folding as indicated by increased kinase activity in response to stimulation in the presence of extra p50^{cdc37} [99, 100]. Loss of p50^{cdc37} activity resulted in loss of Hsp90 from kinase complexes and decreased half-life [99, 101]. GA treatment also disrupts the formation of salt stable Hsp90/p50^{cdc37}/kinase complex; however, it does not disrupt the native complex formed between Hsp90 and p50^{cdc37} [99]. These results suggest that each protein may regulate the others ability to form functional complexes with kinase clients.

While p50^{cdc37} ability to associate with and help fold kinases is well documented, the mechanism by which it facilitates kinase folding still remains unknown. A recent report suggesting that p50^{cdc37} regulates Hsp90 ATPase activity may provide some insight [102]. Also the identification of a new p50^{cdc37} related protein (HARC) suggests a larger family of proteins with similar function and may allow for further characterization of their functions [103].

Hsp90 clients/substrates

Proteins folded or chaperoned by Hsp90 and associated co-chaperones are called "Hsp90 clients" or "Hsp90 substrates". The protein substrates for Hsp90 are structurally and functionally diverse. Two of the groups of Hsp90 substrates have been mentioned extensively above: steroid hormone receptors and protein kinases. The steroid receptors are sometimes grouped with other transcription factor substrates. A third group of

proteins are unrelated to the first two groups or even to each other and therefore are labeled as "other". Table 1 shows a representative listing and classification of some known Hsp90 clients. Most of these substrates are regulatory proteins of some type, although, this is only a very loose generalization and does not lend itself to clear identifying structural or functional characteristics common to all. Kinase folding by Hsp90 machinery is the focus of this report, specifically folding of the Src-family member p56^{lck} (56-kDa lymphoid cell specific kinase) and to a lesser degree the Heme-Regulated Inhibitor of protein synthesis [the heme-regulated eIF2α kinase (HRI)]. Results are compared to the work on steroid receptors, since their interactions with Hsp90 machinery have been more thoroughly characterized. Pharmacological inhibition of Hsp90 and Hsp70 is also used to dissect the roles of chaperones in kinase biogenesis both *in vivo* and *in vitro*. The introduction of pharmacological intervention in the field of chaperone study, especially with the advent of the specific Hsp90 inhibitor GA, has recently and rapidly allowed dramatic growth in our understanding of Hsp90 processes.

Table 1. Examples and classification of Hsp90 substrates (adapted from [11 &12]).

Substrate Classification	Hsp90 substrate
Transcription factors	
Steroid receptors	Glucocorticoid receptor
	Progesterone receptor
	Estrogen receptor
	Androgen receptor
	Mineralcorticoid receptor
	Dioxin receptor
	Antheridiol receptor
Other transcription factors	MyoD1
	Heat shock factor
	Mutant p53
	Sim
Protein kinases	
Tyrosine	p60^{src}
	Fes
	p56^{lck}
	Hck
	ErbB2
	Wee1
	Fyn
	Sevenless receptor
Serine-threonine	Raf
	Cdk4
	HRI
	Casein Kinase II
	Akt
	Calcineurin
	MEK
Other	Telomerase
	Nitric-oxide synthase
	Cytochrome P450 2E1
	Aminoacyl-tRNA synthetase
	DNA polymerase α
	Atrial natriuretic peptide receptor
	Cystic fibrosis conductance transmembrane regulator (CFTR)
	Tubulin

CHAPTER 2

EFFECTS OF GELDANAMYCIN, AN HSP 90-BINDING AGENT, ON T CELL

FUNCTION AND THE NONRECEPTOR PROTEIN TYROSINE KINASE p56^{lck}

Introduction

The class of benzoquinone ansamycin compounds is currently under investigation

in many areas of molecular biological research. Early work with geldanamycin (GA) and

herbimycin A identified them as active antibiotic and herbicidal metabolites from

bacteria [104, 105]. Later work suggested they might be specific inhibitors of the Src-

family of protein tyrosine kinases [106, 107]. However, not all of their biological

activities could be attributed to their ability to inhibit kinases [108]. Early on these

compounds were recognized for their ability to inhibit transformed tumor cell growth and

their ability to induce differentiation of some cell lines [107, 109]. Not until relatively

recently though was their molecular target, Hsp90, and mode of action, Hsp90 inhibition,

identified [19, 110, 111].

Since the identification of Hsp90 as the molecular target of GA and Herbimycin

A the effects of treatment with these compounds on various Hsp90 clients have been the

subject of many studies. Specific effects have been reported on many Hsp90 dependent

proteins such as steroid receptors, the Raf-1 serine/theronine kinase, mutant forms of the

p53 tumor suppressor protein, both viral and cellular Src-family kinases (p60^{src} and

p56^{lck}), eIF2α kinases (HRI), ErbB-2 (HER-2/neu). Many of the Hsp90 substrates are

important for cell growth and some are found to promote unregulated growth typical of cancer cells [112-116]. One of the effects of these Hsp90 binding drugs is to inhibit the stable interactions between Hsp90 and substrate. When these complexes are disrupted often there is an associated degradation of the client usually by the proteasome [117-120]. Since many growth-promoting proteins depend on Hsp90, induction of degradation of these proteins by treatment with GA or herbimycin A often results in growth inhibition or apoptotic cell death. Other than Hsp90's ability to chaperone many growth promoting and sometimes tumor promoting proteins, Hsp90 has also been linked to resistance of some cancer cells to chemotherapy. This has been related to Hsp90's ability to stabilize activated and often mutated versions of proteins that produce the resistance phenotype [121, 122]. Along with this, Hsp90 is over-expressed in a wide variety of cancer and virally transformed cells, possibly due to a dependence that these cells have on one or more Hsp90 dependent proteins [123-125]. In order to attack multiple targets and especially target proteins involved in the multi-drug resistance of tumor cells, Hsp90 has been identified as a novel target in cancer therapy, either as a single agent or in combination with other drugs. Currently the GA derivative 17-allylaminogeldanamycin is in phase I clinical trials as a single agent and implicated for further study in combination with other drugs.

Studies of the effects of drug treatment in immune cell systems are also important. An acknowledged side effect of many cancer therapies is cytotoxicity especially to cells of the immune system [125]. For this reason some of these drugs have also been studied as potential immunosuppresants. One study has characterized the effects of GA and herbimycin A on T cell activation response via the antigen T cell receptor (TCR) and

23

CD28, which are involved in co-stimulation of TCR activated T cells. June *et al.* [126] reported that pretreatment of TCR activated peripheral mononuclear cell cultures with herbimycin A, inhibited proliferation, interleukin 2 (IL-2) and IL-2 receptor (IL-2R/CD25) production, inositol 1,4,5-triphosphate release (tested only in the Jurkat T cell line), mobilization of Ca^{2+} cellular stores (tested only in the Jurkat T cell line), and a general protein tyrosine kinase activity. T cells produce an Hsp90 dependent T cell specific protein tyrosine kinase p56^{lck} [56-kDa lymphoid cell kinase], which is necessary for signal transduction by many cell surface receptors, such as the T cell receptor (TCR), the IL-2R (CD25), and CD28, and has been the focus of research in our lab for many years. June *et al.* [126] also characterized the effects of herbimycin A on both p56^{lck} and p59^{fyn}, another protein tyrosine kinase in T cells. In these cells herbimycin A depleted the cellular levels of both proteins in overnight treatments. In order to better our understanding of the effects of these drugs and to expand on the work mentioned above, studies were conducted in both model cultured T cells and primary isolated T cells are presented here. Results from these studies indicate that different cell populations show a concentration and cell type specific sensitivity to GA both in viability and activation response. Also different populations of the Hsp90 dependent p56^{lck} kinase respond to drug treatment with variable sensitivities to degradation. Finally, a previously identified pathway for GA mediated degradation for other Hsp90 clients is challenged by results for p56^{lck}.

Materials and Methods

Materials

The E6.1 and J.CaM1.6 Jurkat human leukemia T cell lines that produce either full-length p56^{lck} or a truncated protein product, respectively, were purchased from the American Type Culture Collection (ATCC, Manassas, VA.). Splenic mononuclear cells were isolated from 7-week-old male DBA mice (Sprague Dawley, Indianapolis, IN.) All experiments on splenic mononuclear cells were provided by collaboration with Peter Yorgin (Stanford University, Palo Alto, CA.). RPMI 1640 cell culture media, penicillin, streptomycin, and sodium bicarbonate were purchased from Sigma Chemical Company (St. Louis, MO.). L-glutamax was purchased from Gibco Life Science. Fetal Bovine Serum (FBS) was purchased from Hyclone (UT.). Geldanamycin (GA) (m.w. = 560g/mol provided by the Drug Synthesis and Chemistry Branch of the Developmental Therapeutics Program, Division of Cancer Treatment, National Cancer Institute) was prepared in dimethyl sulfoxide (DMSO, Sigma Chemical Co. St. Louis, MO.). Lactacystin and clasto-lactacystin β-lactone (purchased from Calbiochem, La Jolla, CA.) were also prepared in DMSO. DMSO was used as a vehicle control in these experiments. Bafilomycin A was provided by Peter Yorgin. Anti-p56^{lck} polyclonal antibodies were prepared as ascites fluid from mice or rabbits immunized with purified recombinant histidine-tagged human p56^{lck} (provided by Dr. Paul Burn, Hoffmann-LaRoche, Nutley, N.J.) by the Hybridoma Center for the Agricultural and Biological Sciences (Oklahoma State University, Stillwater, OK.). Antibody specificity was verified by the ability to western blot and immuno-precipitate full-length radiolabeled p56^{lck} from E6.1 Jurkat T

25

cell lysates but not from J.CaM1.6 Jurkat T cell lysates. Anti-actin antibodies were provided by Peter Yorgin. Anti-ubiquitin antibodies were purchased from Sigma. Anti-mouse immunoresin was prepared by coupling goat anti-mouse IgG (Jackson-Immunologicals) to p-Nitrophenyl Chloroformate-activated agarose (Sigma). Pansorbin was purchased from Calbiochem. Nitrocellulose and polyvinyldiflouride (PVDF) were purchased from Bio-Rad (CA.) Immunoblotting blotting reagents nitro-blue tetrazolium (NBT) and bromo-chloro-indolyl-phosphate (BCIP) were purchased from Sigma Chemical Company for detection of either anti-mouse or anti-rabbit secondary antibodies conjugated with alkaline phosphatase (Jackson Immunologicals).

T cell culture

Experiments carried out on primary T cells were done in collaboration with Dr. Peter D. Yorgin, Abdul M. Fellah, Emmanuel Katsanis, Jeff M. Couchman, and Luke Whitesell in the Department of Pediatrics, Steele Memorial Children's Research Center, University of Arizona, Tuscon, AZ. 85724 as described previously [127]. Briefly, splenic mononuclear cells were isolated from 7 week-old male DBA mice (Sprague Dawley, Indianapolis, IN.) by density-gradient centrifugation of spleen homogenates in Lympholyte M (Cedar Lane Laboratories, Ontario, Canada). Isolated mononuclear cells were cultured in RPMI 1640 supplemented with FBS to 10%, 2 mM L-glutamine, 50 IU penicillin, 50 μg/ml streptomycin, 100 ng/L gentamycin, 1 mM sodium pyruvate, 1x nonessential amino acids, and 50 μM mercaptoethanol. Activated T cells were prepared by stimulation of isolated splenic mononuclear cell cultures with 100 U/ml IL-2 (from Dr. Emmanuel Akporiaye, University of Arizona, Tuscon, AZ.), or 0.5 μg/ml Con A, or

10 U/ml IL-2 and 0.5 μg/ml Con A for 72 hours prior to addition of GA or DMSO. A

predominant T cell population results from culture of mononuclear cells with Con A for

48 hours. Results of these experiments are presented in this dissertation, as they provide

part of the context in which results from my experiments are interpreted.

Jurkat T cell lines, both E6.1 and J.CaM1.6, were cultured in RPMI 1640

supplemented with 24 mM sodium bicarbonate, 2 mM L-glutamine, 50 IU penicillin, 50

μg/ml streptomycin, and FBS to 10%, and pH was adjusted to 7.0. Cultures were

maintained in a humidified 5% CO_2 atmosphere at 37°C. Duration and cell density are

indicated for each experiment.

Jurkat T cell and splenic mononuclear cell viability, growth, and activation

Jurkat T cells were cultured for indicated times in the presence or absence of

indicated concentrations of GA. Culture growth was monitored by counting aliquots of

the culture on a hemocytometer grid (dimensions of 1x1x1mm). 5-10 replicate counts

were averaged and standard deviations calculated for each condition. Viability was

assessed by the ability of cells to exclude the vital dye trypan blue (Sigma). Percent

viability was calculated by multiplying the ratio of the average number of vital cells for a

given condition over the average total number of cells by 100. The average percent

viability and growth were calculated from the averages of 13 experiments. Percent

growth was calculated by multiplying the ratio of culture density for a given condition

over the culture culture density for the drug vehicle control (DMSO) by 100.

The two-time point GA dose curve was counted, viability was assessed and

standard deviations were calculated for 5 replicate counts, as described above, and

represents a typical experiment used to calculated the averages described above. Student's t test was used to analyze significant differences. Differences were considered significant when the p value was < 0.05 indicating a confidence level greater than 95%.

Viability of resting splenic mononuclear cells was assessed similarly to Jurkat T cells. Since resting mononuclear cells represent a mixed population in order to ensure that the viability of lymphocytes was being determined, trypan blue staining was used in conjunction with cell sorting by a flow cytometer. Two experiments with six replicates each were counted and stained with trypan blue during exposure to GA. Splenic mononuclear cells preactivated with IL-2 and Con A were treated with GA for 18 hours and viability was assessed as described above.

To determine whether late addition of GA to splenic mononuclear cells preactivated with IL-2, Con A, or both would inhibit subsequent proliferation, cells were activated as described above and growth was monitored by incorporation of [^{3}H]thymidine. After 72 hours of mitogen stimulation by Con A and/or IL-2, GA, DMSO control, or no treatment control (RPMI 1640) were added to cultures concomitantly with 1 μCi of [^{3}H]thymidine. Cells were incubated for 15 hours and harvested on glass-fiber filters and incorporation of [^{3}H]thymidine was determined by liquid scintillation counting. A stimulation index was calculated as the ratio of [^{3}H]thymidine incorporated by cells under a given condition over [^{3}H]thymidine incorporated by cells in media with no treatment. Three experiments with 6 replicates each were used for statistical analysis. Differences in viability and growth stimulation between conditions were analyzed using the Student's t test as stated above.

28

Splenic mononuclear cells were stimulated to produce IL-2 and IL-2 receptor (IL-2R/CD25) in response to treatment with anti-CD3 (TCR) and anti-CD28 antibodies resulting in receptor stimulation. Production of IL-2 and IL-2R were monitored after culture for 15 hours in the presence and absence of pretreatment with 1.7 μM GA, followed by a wash and then 18 hours stimulation with antibodies. IL-2 secretion in the media of stimulated cells was compared between treatments by determining the dilutions needed to achieve 50% of the maximum incorporation of [^{3}H]thymidine in the murine IL-2 dependent cytolytic T lymphocyte line (CTLL-2, from ATCC) [128, 129]. Culture supernatants were prepared in 96 well plates as three fold serial dilutions. 2 x 10^4 prewashed CTLL-2 cells were added per well. Plates were incubated for 15 hours under standard culture conditions and then exposed to 2 μCi [^{3}H]thymidine for 6 hours before being harvested and counted on a scintillation counter. IL-2 concentrations were determined by comparison to a standard curve for known IL-2 concentrations. IL-2R/CD25 production in response to CD3/CD28 stimulation was quantified using flow cytometry to detect FITC conjugated anti-CD25 antibody (PharMingen) binding to the cells. Assays were preformed three times for statistical analysis.

Cell lysis and p56^{lck} detection

Resting or activated splenic mononuclear cells were treated with GA for the indicated time and then lysed in PBS supplemented with 10% glycerol, 1% Tween-20, 12 mM sodium deoxycholic acid, 0.1% SDS, 1 mg/L phenyl-methyl-sulfonyl-fluoride, 200 μg/L aprotinin, and 200 μg/L leupeptin) and clarified at 14000 x g for 20 minutes at 4°C. Protein concentrations were determined relative to a standard curve for BSA using the

BCA assay kit (Pierce). Cell lysates were separated by SDS-PAGE, transferred to nitrocellulose membranes, and immunostained for p56^{lck} using the chemiluminescent horseradish peroxidase substrate, Luminol, and exposure to autoradiography film. p56^{lck} levels were quantified by scanning computer densitometry.

Similarly, suspension cultures of Jurkat T cells were treated with GA as indicated and harvested by a single 400 x g centrifugation without washing, as it was determined there was significant loss of cells due to washing GA treated cells. Whole cell lysates were prepared by lysing cells in boiling 2X SDS-PAGE sample buffer [125 mM Tris-HCl (pH 6.8), 10% SDS, 55 mg/ml dithiothreitol, 10% glycerol, 0.005% bromphenol blue] [130]. For immunoprecipitations and to analyze detergent solubility of p56^{lck}, cells were lysed by rocking in RIPA lysis buffer (10 mM sodium phosphate pH 7.4, 150 mM sodium chloride, 0.1% SDS, 2% Triton X-100, 0.76% sodium deoxycholic acid, 2.5 mM EDTA, 1 mM EGTA, 50 mM sodium fluoride, 1 mM sodium vanadate, 200 μg/L aprotinin, 17 mg/L phenyl-methyl-sulfonyl fluoride, 1 mM dithiothreitol, 2 mg/L leupeptin) for 30 minutes at 4°C. Lysates were clarified by centrifugation at 14000 x g for 5 minutes at 4°C. Supernatants were either separated by SDS-PAGE or immuno-precipitated for 1 hour at 4°C with Santa Cruz biologicals anti-p56^{lck} polyclonal or MOPC-21 non-immune antibodies (Sigma) pre-bound to anti-IgG coupled agarose. Detergent (RIPA)-insoluble pellets were monitored by boiling in SDS-PAGE sample buffer. All samples were separated by SDS-PAGE and transferred to PVDF membranes for analysis by standard colorometric immuno-detection with our Mouse 3 anti-p56^{lck} polyclonal ascites fluid as our primary antibody and alkaline phosphatase conjugated secondary antibodies. Culture density was used to determine equal loading on gels.

Pulse-chase analysis

Pulse-chase analysis of p56^{lck} in GA treated Jurkat T cells was done in collaboration with Dr. Steve Hartson (Oklahoma State University, Stillwater, OK.). Sensitivity of newly synthesized p56^{lck} in Jurkat T cells to GA was determined by pretreatment of cultures with 3.6 μM GA or DMSO (control) for 1 hour. Jurkat T cells were then starved for methionine and cysteine in the absence of GA by culturing in Met/Cys deficient RPMI 1640 media for 30 minutes at 37°C. Cellular proteins were then labeled by incubating cells in RPMI 1640 supplemented with [^{35}S] Met/Cys for 20 minutes (pulse). Pulse labeling was completed by removal of cells from media and resuspension and culture in RPMI 1640 supplemented with nonradioactive Met/Cys for the indicated chase times. Mature p56^{lck} sensitivity to GA was also determined using pulse-chase techniques. Cellular proteins in Jurkat T cells were radiolabeled for 40 minutes followed by a 3-4 hour chase in non-radioactive Met/Cys supplemented RPMI 1640 allowing [^{35}S] labeled p56^{lck} to mature. 3.6 μM GA or DMSO was then added directly to the culture and cells were incubated for the indicated chase times. To monitor [^{35}S] labeled p56^{lck} levels Jurkat T cells were lysed and clarified as described by Shaw *et al.* [131]. Protein-protein interactions in lysates were further disrupted, to increase immunoadsorption specificity, by adjusting lysates to a final concentration of 1% SDS and 10 mM DTT and boiling for 5 minutes. Lysates were cooled and diluted. To reduce the affects of nonspecific binding of proteins to the immuno-matrix, lysates were premixed with 10% Pansorbin followed by immuno-precipitation with anti-p56^{lck} antibodies pre-bound to Pansorbin. Immuno-matrix was washed four times with lysis

buffer supplemented with 0.3% SDS/3 mM DTT and eluted with SDS-PAGE sample buffer. Immuno-precipitated proteins were separated by SDS-PAGE and transferred to PVDF membranes and analyzed by autoradiography for detection of [^{35}S] labeled p56^{lck}. Levels of [^{35}S]p56^{lck} were measured by computer densitometry of bands on the autoradiogram. p56^{lck} immunoprecipitations from GA and DMSO treated Jurkat T cell lysates were also assayed for kinase activity. Activity was measured by quantification of the auto-phosphorylated [^{32}P]p56^{lck} band using computer densitometry on autoradiograms.

p56^{lck} ubiquitination analysis

Since treatment of Jurkat T cells with clasto-lactacystin β-lactone (CL) was determined to recruit p56^{lck} to a RIPA/detergent insoluble fraction, a different lysis method was used to analyze these samples. Jurkat T cells were treated with GA and/or CL for the indicated times and harvested by a single centrifugation at 400 x g followed by a 5 minute boiling lysis in TNES buffer (50 mM Tris-HCl pH 7.4, 1% NP-40, 2 mM EDTA, 100 mM NaCl, 2% SDS, 10 mM N-ethyl-maleimide (NEM), 1 mM Na$_3$VO$_4$, 20 µg/ml leupeptin, and 200 µg/L aprotinin). Cellular DNA was sheared using a 21 gauge needle and lysates were cooled and clarified twice by centrifugation. Some samples were then prepared for separation by SDS-PAGE and others were immunoprecipitated with Burn's anti-p56^{lck} IgG or nonimmune IgG antibodies prebound to prewashed fast flow protein-G Sepharose (Amersham Bioscience). Immunopellets were washed four times in a modified TNES containing 0.2% SDS. Proteins were eluted by boiling in SDS-PAGE sample buffer. Samples were separated by SDS-PAGE and electro-blotted to nitro-

cellulose membranes for immunodetection with anti- p56^{lck} and anti-ubiquitin antibodies. Anti-ubiquitin antibodies are not very efficient at western blotting and require the membranes to be autoclaved for 15 minutes supposedly to make the epitope more accessible to the antibody. After autoclaving normal western-blotting protocols were followed.

Results

GA treatment is cytotoxic and inhibits growth of Jurkat T cell cultures

Previous studies of the effects of GA and Herbimycin A on T cells have not examined the cytotoxicity or growth inhibition of these agents in any great detail. To determine the effects of GA treatment on the cultured Jurkat T cell line, cultures were treated with increasing concentrations of GA for 20 hours. Figure 2A shows the concentration dependent effect of GA on cell growth and viability after 20 hours of continuous treatment. At 900 nM GA there was only a 10 % loss of viability but growth was inhibited by almost 50 %. A 10 fold increase in GA concentration caused about a 30 % loss in culture viability with little additional effect on growth inhibition. Even the live cells, cells that excluded trypan blue, had a different morphology appearing more crinkled and less rounded suggesting that they may be undergoing apoptosis. Recovery of these cells was greatly compromised by washing so washing steps were omitted in subsequent experiments. To determine how rapidly these effects occurred an intermediate time point was included in the dose curve (figure 2B). As can be seen at 8 hours, little

33

Figure 2. Growth and Viability of GA Treated Jurkat T Cells.

(A) E6-1 Jurkat T cells were cultured in media in the presence or absence of the indicated concentrations of GA (900 and 9000 nM) or DMSO (vehicle control) for 20 hours. Cells were harvested as a pellet in an eppendorf tube by centrifugation at 400 x g for 10 minutes and counted on a mm^2 hemocytometer grid using a microscope at 10x magnification. Bars on the graph represent the average % viability (calculated as # of cells unstained by the vital dye divided by the total # of cells counted for each culture multiplied by 100) and % growth (calculated as the # of cells in a given condition divided by the # of cells for the DMSO control multiplied by 100) in 13 experiments (5 replicate counts each). Error bars are the calculated standard deviations for each condition. P values for growth and viability at both 900 and 9000 nM of GA were < 0.01. (B) Jurkat T cells were cultured in media in the presence or absence of the indicated concentrations of GA (0, DMSO, 400, 900, 4000, and 9000 nM) and for the indicated times (8 and 20 hours). Both time points are graphed together to emphasize the difference in growth between cultures over time. Cells were harvested and counted and stained as in panel A. Standard deviations were calculated from 5 replicate counts and are presented as error bars. P values for growth at 20 hours and all treatment conditions were <0.01. P values for viability at 20 hours and 400 and 900 nM of GA were <0.05 and for 4000 and 9000 nM of GA were <0.01. P values are given textually and are not displayed in panels A or B.
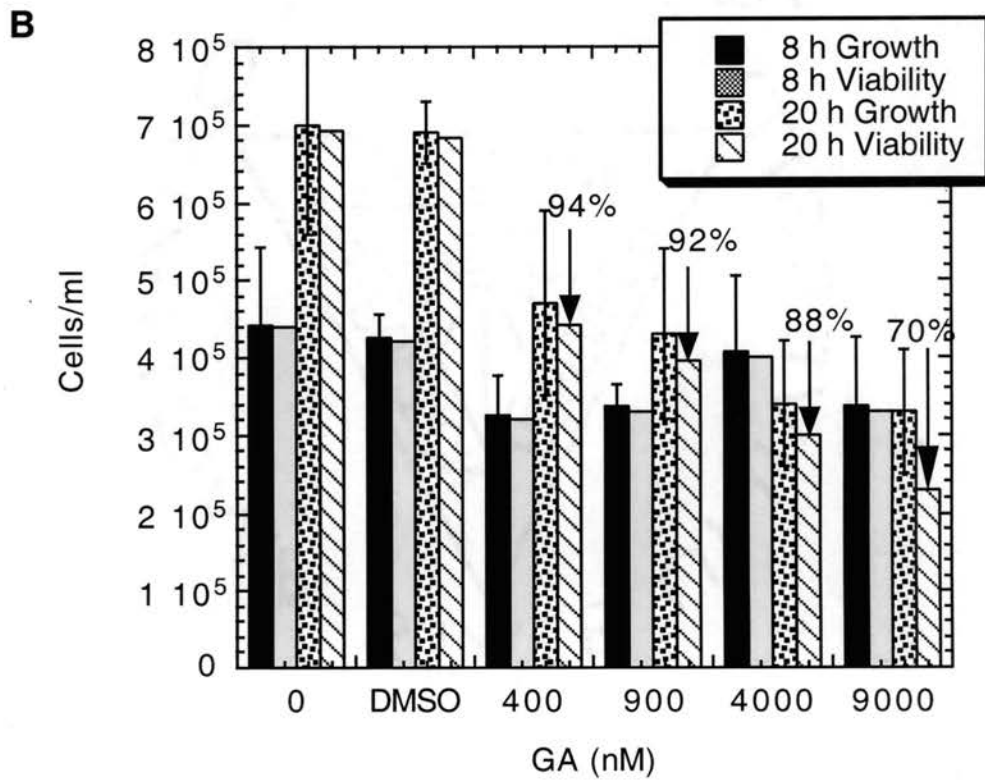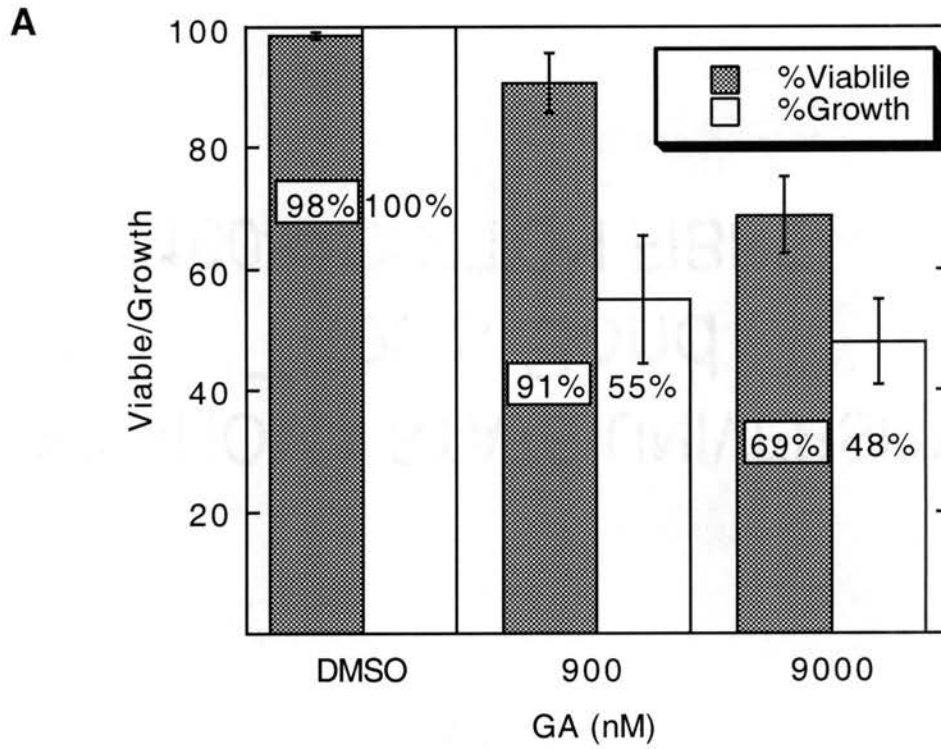
effect on culture density was observed, and no effect on viability of the cultures was apparent even at the highest concentration, 9 μM. However, when the culture time was extended to 20 hours growth was inhibited and viability was lost in a concentration dependent manner. Inhibition of growth was apparent at the lowest GA concentration tested, 400 nM, and viability of cultures was compromised by 70% at the 9000nM.

GA has different effects on the viability of resting and activated splenic T cells

Jurkat T cells are a human leukemia T cell line that is used as a T cell model system for studying T cell receptor signal transduction. They express all of the components of the TCR and are able to be activated through the TCR to produce the stimulatory cytokine IL-2 [129, 132]. However, the cultured transformed Jurkat cell line may react differently to GA treatment than do non-transformed T cells in the body. In order to determine whether Jurkat T cells respond similarly to GA, as would T cells from a primary source, mononuclear cells were isolated and cultured from the spleen of DBA mice. Mature T cells in organisms not mounting an immune response are mostly quiescent and so some of the isolated T cells were pre-activated with IL-2 and Con A, mitogens that activate T cell proliferation [133]. Cells were cultured with or without GA for 15-18 hours and then counted and assayed for viability. Splenic mononuclear cells are a primary cell that can be cultured but are not as stable in culture as transformed cell lines such as Jurkat T cells, therefore they show a higher background mortality in culture. For this reason shorter treatment times were used for these cultures. At 15 hours no significant effect on culture viability was observed for resting T cells (Figure 3A). Upon longer treatment (24-72 hours), however, a concentration dependent reduction in culture

viability was detected along with a general decrease in viability for all cultures (data not shown). Activated T cell cultures showed an enhanced mortality upon exposure to GA (Figure 3A). Geldanamycin also inhibited T cell proliferation, as measured by [^{3}H]thymidine incorporation in response to mitogen pretreatment, in a concentration dependent manner (Figure 3B). Similar work showed that pretreatment with Hsp90 inhibitors blocked both TCR-mediated phosphorylation and CD28-mediated T cell activation [126, 134]. These results indicate that Hsp90 function is necessary to initiate and maintain T cell activation in the presence of mitogens.

T cells also respond to activation through the TCR and other receptors by producing cytokines necessary to stimulate growth of other immune cells. This response was inhibited in human peripheral T cells by GA and herbimycin A, another benzoquinone ansamycin [126, 134]. When splenic T cells were pretreated with GA and then stimulated with anti-TCR antibodies (anti-CD3) IL-2 production was inhibited by 96%. Similarly, production of the IL-2 receptor in response to stimulation with anti-CD28 antibodies was inhibited by 40% when cells were pretreated with GA. These results indicate that both proliferation and cytokine production in response to T cell activation were inhibited by GA treatment. Activated T cells also appear to be more vulnerable to GA cytotoxicity.

Jurkat T cells have the ability to proliferate in culture without being activated unlike resting/quiescent T cells. Jurkats are also more vulnerable to GA cytotoxicity like the activated splenic monocytes; however, they do not produce IL-2 unless stimulated through the TCR or other cell surface receptors [129]. These results indicate that Jurkat T cells respond to GA treatment in a manner similar to mouse T cells isolated from the

Figure 3. Growth , Viability, and Stimulation of GA Treated Preactivated or Resting Splenic T Cells (Courtesy of Peter Yorgin).

(A) Splenic mononuclear cells from DBA mice were isolated and cultured in the presence (activated) or absence (resting) of 10 U/ml IL-2 and 0.5 µg/ml Con A for 72 hours. Cells were then treated with the indicated concentration of GA (0, DMSO, 17, 170, 1700nM) for 15-18 hours and then harvested for viability assessment as described for Jurkat T cells in Figure 1. Resting T cells were separated from the mixed population of isolated mononuclear cells as described in Materials and Methods using a flow cytometer. Bars represent % viability (as calculated above) and error bars represent standard deviations calculated from two experiment (6 replicates each). P values for viability of GA treated resting T cells were not significant at all concentrations when compared to untreated (0 nM) or DMSO controls. P values for activated T cells were <0.01 for all concentrations of GA when compared to untreated (0 nM) or DMSO controls. (B) Splenic mononuclear cells were isolated and cultured in the absence (resting) or presence (activated) of either 100 U/ml of IL-2, 0.5 µg/ml of Con A, or 10 U/ml of IL-2 and 0.5 µg/ml of Con A for 72 hours. Cells were then treated with the indicated concentrations of GA (0, DMSO, 17, 170, 1700 nM) concomitant with 1 µCi of [^{3}H]thymidine for 15 hour and then harvested as described in Materials and Methods by glass-filter binding. Liquid scintillation counting was used to determine the amount of [^{3}H]thymidine incorporated by cells under the indicated conditions. Incorporation is reported as the stimulation index (calculated as [^{3}H]thymidine incorporated by cells under a given condition divided by the [^{3}H]thymidine incorporated without stimulation (Resting)). Standard deviations calculated from three experiments are reported as error bars. P values for all concentrations of GA in IL-2 stimulated cells were <0.01. P values for 170 and 1700 nM GA treatement of Con A stimulated cells were <0.01, and the p value for 17 nM GA with Con A was not significant. P values for 170 and 1700 nM GA treatment of IL-2 and Con A stimulated cells were <0.01, and the p value for 17 nM GA was not significant.

A

(Bar chart)
- Y-axis: Viability (0 to 100)
- X-axis: GA (nM) — 0, DMSO, 17, 170, 1700
- Legend: Resting, IL-2 + Con A

B

(Bar chart)
- Y-axis: Stimulation (0 to 300)
- X-axis: GA (nM) — 0, DMSO, 17, 170, 1700
- Legend: IL-2+Con A, Con A, IL-2, Resting
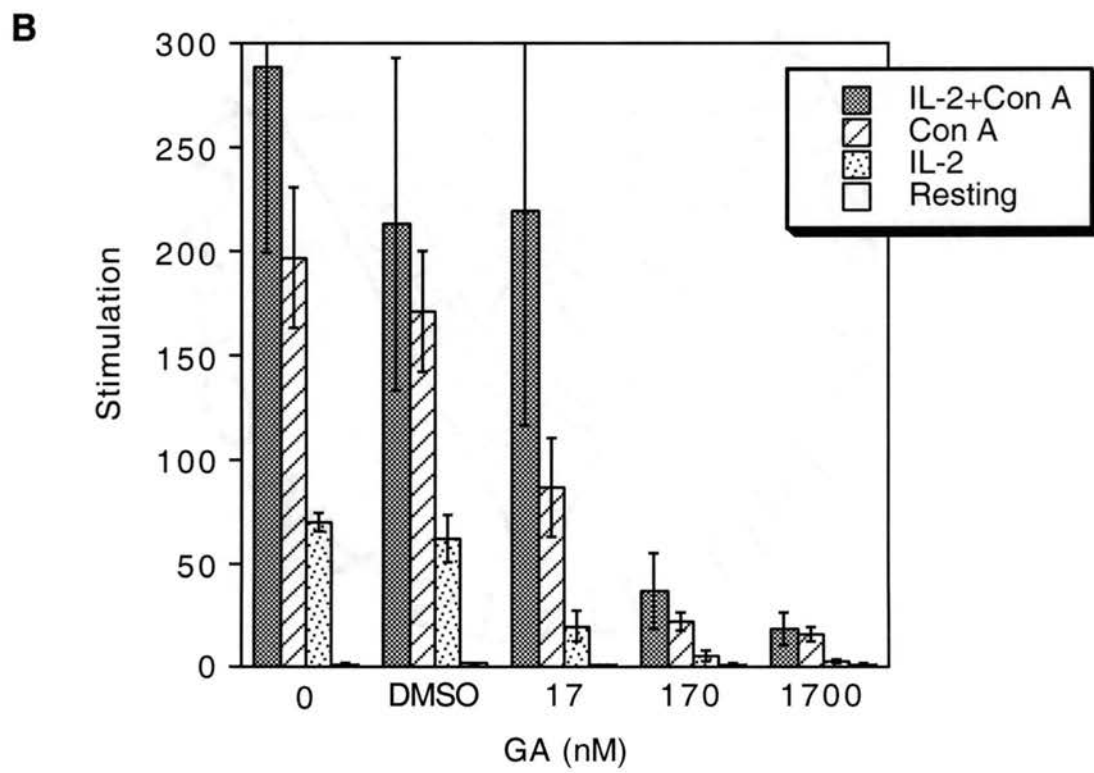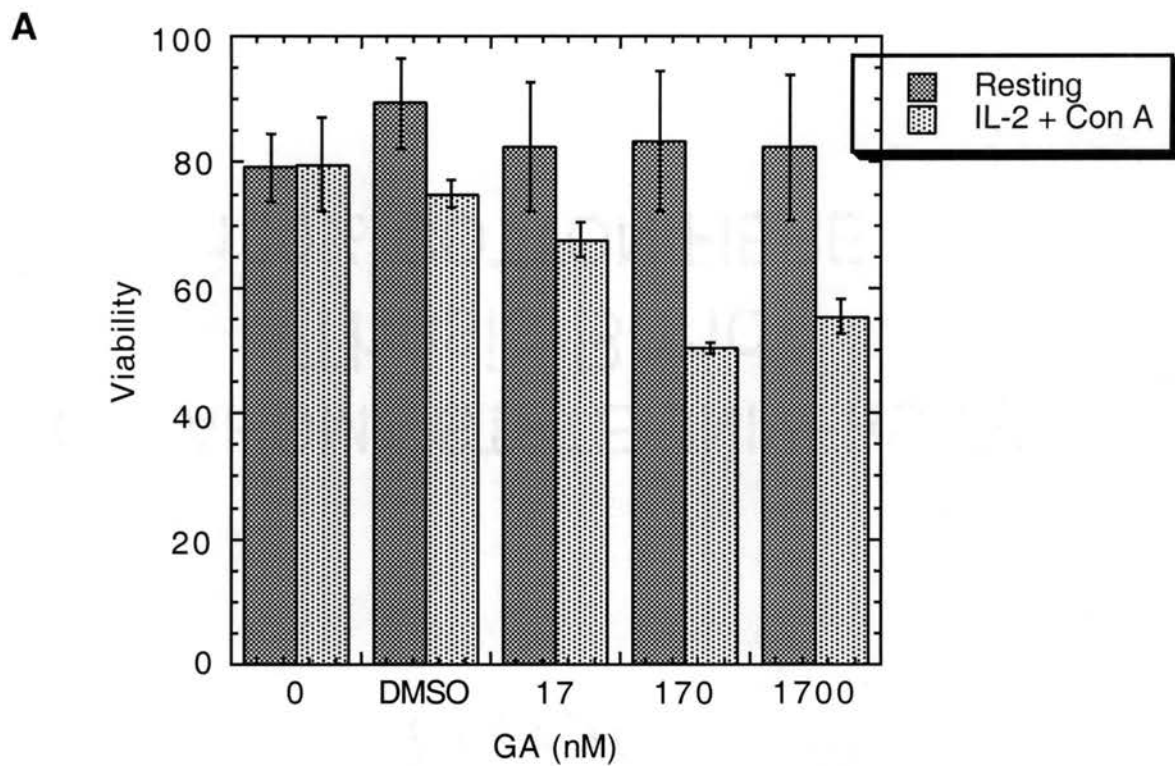
spleen and may represent an appropriate model to examine the biochemistry of GA in T cells.

p56^{lck} cellular tyrosine kinase depletion in response to GA

Stimulation through the TCR starts a signal transduction cascade that ultimately leads to T cell activation. One of the earliest events in this pathway is the activation of p56^{lck}, which in turn phosphorylates and activates other proteins necessary for signal propagation (reviewed in [135]). The importance of p56^{lck} in TCR signal transduction is well established, and therefore can be used as a marker for the effects of GA in T cell biology [136, 137]. The p56^{lck} and p59^{fyn} protein tyrosine kinases are depleted in human peripheral blood T cells pretreated with herbimycin A, correlating with a general loss in TCR-mediated tyrosine phosphorylation [126]. In order to compare the effects of GA on p56^{lck} in resting, activated, and transformed T cells, and for comparison with previous studies, p56^{lck} levels were monitored during treatment. Figure 4 shows western blots of p56^{lck} from resting and activated splenic T cells, and from transformed Jurkat T cells (Figure 4 A, B, and C respectively). In resting splenic T cells p56^{lck} levels were reduced by almost half (53.7 ± 23.1%) when treated for 24 hours with 170 nM GA (Figure 4 A, lane 2 versus 4). This level dropped to 35.3 ± 14.1% when the GA concentration was raised 10 fold (Figure 4 lane 2 versus 5). At the same concentration of GA activated splenic T cells p56^{lck} levels were reduced to background within 15 hours (Figure 4 B: lane 3 and 5 compared to lanes 2 and 4 respectively), indicating the p56^{lck} pool in these cells were more sensitive to GA treatment. In Jurkat T cells, p56^{lck} levels also dropped in response to GA treatment but it took treatment times and concentrations of GA similar to

Figure 4. Geldanamycin Mediated Depletion of Cellular p56^{lck} in Resting, Activated, and Jurkat T Cells.

(A) (Courtesy of Peter Yorgin) Splenic mononuclear cells were isolated and cultured for 24 hours in the presence or absence of indicated concentrations of GA (0, DMSO, 17, 170, or 1700 nM represented in lanes 1-5 respectively). Cells were harvested and lysed by boiling in SDS-PAGE sample buffer. Samples were loaded on to an SDS-PAGE gel and separated by electrophoresis. Proteins were transferred from the gel to nitrocellulose membranes and immunoblotted with anti-p56^{lck} antibodies (primary) and horseradish peroxidase conjugated secondary antibodies. Bands were visualized by autoradiography of chemiluminescent bands using the Luminol substrate. Detection of the actin protein in all samples was used to normalize the samples. Migration of size standards and p56^{lck} is marked and labeled on the left side of the of the panel. (B) (Courtesy of Peter Yorgin) Splenic mononuclear cells were isolated and cultured with 100 U/ml IL-2 (activated lanes 2 and 3), 0.5 mg/ml Con A (activated lanes 4 and 5), or just media (resting lane 1) for 24 hours prior to a 15 hour treatment with 1.7 μM GA (lanes 3 and 5), equal volume of DMSO (control lanes 2 and 4), or no treatment (lane 1). Samples were lysed and separated by electrophoresis as described for panel A and transferred to nitrocellulose membranes for immunoblotting with anti-p56^{lck} antibodies. Molecular weight standards and p56^{lck} migration is marked and labeled on the left side of the panel. (C) The transformed Jurkat T cell line (E6-1) as cultured in the presence (lanes 3-6 and lanes 8-11) or absence (equal volume of DMSO control-lanes 2 and 7) of GA for 8 or 20 hours. Concentrations of GA used are 400 nM (lanes 3 and 8), 900 nM (lanes 4 and 9), 4000 nM (lanes 5 and 10), and 9000 nM (lanes 6 and 11). Cells were counted, viability assayed, and harvested as a pellet at indicated times by centrifugation at 400 x g for 10 minutes. Lysis was performed using volumes of cold RIPA buffer that normalized the cell density based on previous cell counts. Cell pellets were resuspended and rocked at 4°C in cold RIPA buffer (see methods). Lysates were clarified by a 5 minute spin at 14000 x g and 4° C and supernatants were mixed with fast flow G (ffG) immunoresin prebound to Santa Cruz Biological (SCB) anti-p56^{lck} polyclonal antibodies or nonimmune IgG (nonspecific binding control lane 1) and prewashed before immunoprecipitation. Immunopellets were cleared from lysates and washed 4 times with cold RIPA buffer and eluted with SDS-PAGE sample buffer. Eluates were loaded on SDS-PAGE gels and separated by electrophoresis. Proteins were electroblotted on PVDF membranes and subjected to immunoblotting with OSU anti-Mouse 1 antibodies (primary) and alkaline phosphatase conjugated secondary anti-IgG's and visualized by colorometric staining. Migration of molecular weight markers and p56^{lck} is marked and labeled on the left side of the panel.

41

A

24 hour GA treatment

68kDa   NT   D

p56^lck –

43kDa   1   2   3   4   5

Resting

B

15 hour GA treatment

	–	+	+	–	–	IL-2
	–	–	–	+	+	Con-A
	–	+	–	+	–	DMSO
68kDa	–	–	+	–	+	GA

p56^lck –

43kDa   1   2   3   4   5

Activated

(IP p56^lck)

C

	NI	D	8 hrs				20 hrs				

66kDa –
p56^lck –
45kDa –

1   2   3   4   5   6   7   8   9   10   11

Jurkat

42
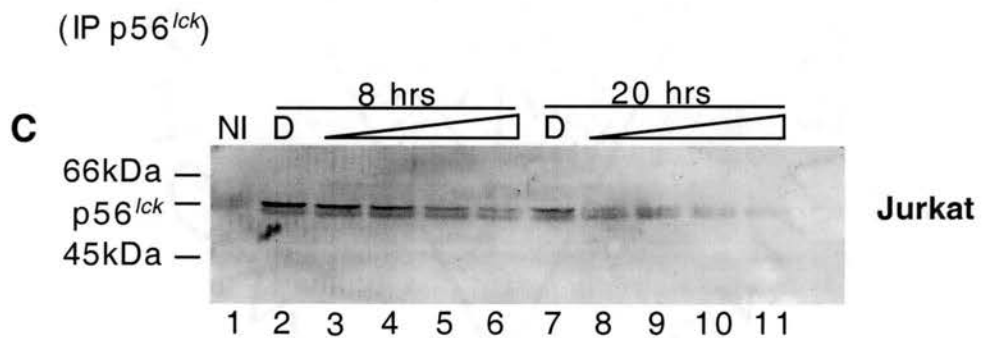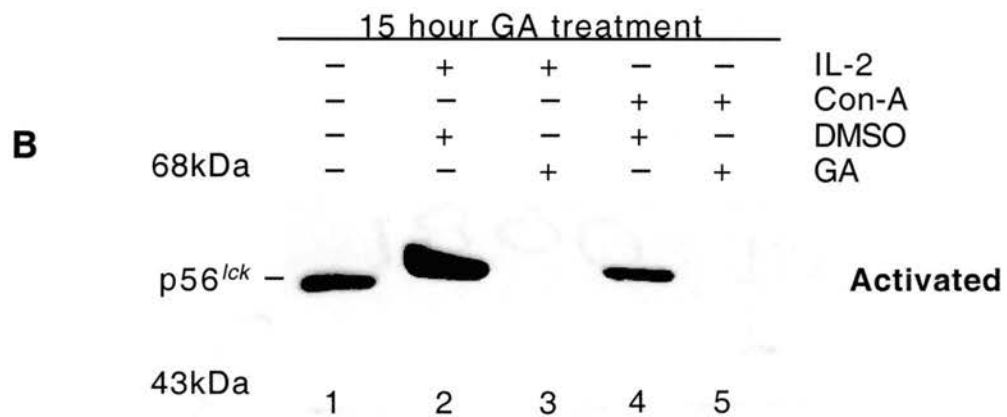
those used with resting splenic T cells to achieve the same degree of loss (Figure 4C: 900 nM GA at 8 and 20 hours; lanes 4 and 9). Once again these results indicate that Jurkat T cells respond to GA treatment in a manner similar to mouse T cells isolated from the spleen and represent an appropriate model to examine the biochemistry of GA in T cells. Since Jurkat T cells were much easier to culture and do not have the added complication of high mortality during long culture times, Jurkat T cells were used to study the biochemical mechanism by which GA induced p56^{lck} depletion.

GA has different effects on different pools of cellular p56^{lck}

GA-induced depletion of p56^{lck} could occur through more than one mechanism. First GA could affect p56^{lck} levels indirectly by affecting other Hsp90 processes that directly or indirectly affect p56^{lck}. Previous work has identified and characterized the interaction between the p56^{lck} and Hsp90 *in vitro* and *in vivo* [26, 46, 138, 139], and other Src-family kinases have been identified as Hsp90 clients [45, 140, 141], suggesting a direct effect of GA on p56^{lck} depletion. If Hsp90 is necessary to maintain mature p56^{lck} activity then inhibition of Hsp90 could generate an inactive, protease sensitive kinase. Alternatively, Hsp90 function may only be necessary for *de novo* folding and the mature p56^{lck} may be stable without Hsp90 maintenance. Depletion of cellular p56^{lck} in this scenario would result from failure of newly synthesized Hsp90 dependent kinase to replace mature Hsp90 independent p56^{lck} as it turns over by normal mechanisms. p56^{lck} depletion would occur less rapidly by the second scenario. Our results show a fairly slow turnover of p56^{lck} especially in the non-activated and Jurkat T cells, suggesting a failure to replace old kinase with new. In order to determine the mechanism of GA-mediated

depletion pulse chase analysis was used. Cells were pretreated with GA followed by pulse labeling newly synthesized p56^{lck} with [^{35}S]Met/Cys in the absence of GA and chased in the presence or absence of GA. A dramatic difference in half-life was observed (Figure 5 A). During a 120 minutes chase period (only 80 minutes are shown) little [^{35}S]Met/Cys labeled p56^{lck} was lost in the DMSO vehicle control treated culture. In the GA treated culture ~50% of the [^{35}S]Met/Cys labeled p56^{lck} was lost after 40 min of chase and was undetectable after 120 minutes of chase (data not shown).

A similar experiment was done to determine the Hsp90 dependence of mature p56^{lck} with different results. Cells were pulse labeled with [^{35}S]Met/Cys in the absence of GA and chased for 3 hours also in the absence of GA. Cultures were then supplemented with DMSO or GA and aliquots were harvested every 6 hours over a 24 hour period. As can be seen in Figure 5 B, GA increased the rate of mature p56^{lck} depletion by approximately 2 fold. In order to determine whether a loss of p56^{lck} kinase activity preceded the loss of protein in GA treated cultures p56^{lck} was immunoprecipitated and assayed for activity at 3 hours (Figure 5 C). Three hours was short enough that depletion of kinase was not significant but long enough to have inhibited cellular Hsp90 function. No significant difference in p56^{lck} kinase activity was detected in the two cultures indicating mature kinase function was not compromised by loss of Hsp90 function.

These results demonstrate that both newly synthesized and mature p56^{lck} are depleted by GA treatment, with the newly synthesized p56^{lck} apparently much more sensitive to GA than the mature. The depletion observed in previous figures is the result of both a rapid loss of newly synthesized p56^{lck} combined with a slower loss of mature p56^{lck}. Specifically, in Figure 4 C lane 5 the depletion seen at 8 hours of GA treatment is

Figure 5. Pulse-Chase Analysis of the Turnover of Newly Synthesized and Mature p56^{lck} in GA Treated Jurkat T Cells (Courtesy of Steve Hartson).

(A) Jurkat T cells were cultured for 1 hour in the presence of 3.6 µM GA or an equal volume of DMSO (vehicle control) before being transferred to media supplemented with [^{35}S]Met/Cys for pulse radiolabeling in the absence of GA. Cultures were chased in media supplemented with nonradioactive Met/Cys for the indicated times (0-80 minutes) in the absence of GA. Cells were harvested and lysed in RIPA buffer and immunoprecipitated with anti-p56^{lck} antibodies prebound to immuno-affinity matrix and prewashed. Immunopellets were washed and proteins eluted with SDS-PAGE sample buffer. Eluates were separated by SDS-PAGE and transferred to PVDF membranes and exposed to film to produce an autoradiogram. Migration of molecular weight markers is marked and labeled on the left side of the panel and mobility of p56^{lck} is marked on the right side of the panel. (B) Jurkat T cells were pulse radiolabeled with [^{35}S] Met/Cys in the absence of GA and chased (also in the absence of GA) for 3 hours in media supplemented with nonradioactive Met/Cys. Cells were cultured in the presence of 3.6 µM GA or an equal volume of DMSO for the indicated chase times (0-24 hours) after which cells were harvested, lysed, and immunoprecipitated with anti-p56^{lck} antibodies. Immunopellets were analyzed as described for samples in panel A. (C) Jurkat T cells were cultured with 3.6 µM GA or an equal volume of DMSO for 3 hours. Cells were harvested and lysed in RIPA buffer and clarified lysates were immunoprecipitated with anti-p56^{lck} antibodies. Immunopellets were washed thoroughly to remove any contaminating kinases. Equal aliquots of the immunoprecipitations were assayed *in vitro* for auto-kinase activity by incubating, for the indicated times, with kinase reaction mixtures at room temperature containing [γ-^{32}P]ATP. Kinase reaction mixtures were analyzed by SDS-PAGE and autoradiography of PVDF membranes to which [^{32}P] labeled proteins were transferred. Phosphorimaging of autophosphorylated p56^{lck} bands was used to quantitate activity at the times indicated. Graph shows that auto-kinase activity is still in the linear range.

A

97kDa –
66kDa –
45kDa –

DMSO   GA

– p56^{lck}

31kDa –

0 20 40 60 80   0 20 40 60 80
chase time (min)   chase time (min)

B

97kDa –
66kDa –
45kDa –
31kDa –

DMSO   GA

– p56^{lck}

0 6 12 18 24   0 6 12 18 24
chase time (hrs)   chase time (hrs)

C

Autophosphorylation (pixel density x mm^2)

2200
2000
1800
1600
1400
1200
1000
800
600

0 1 2 3 4 5 6
Minutes

○— DMSO
●— GA
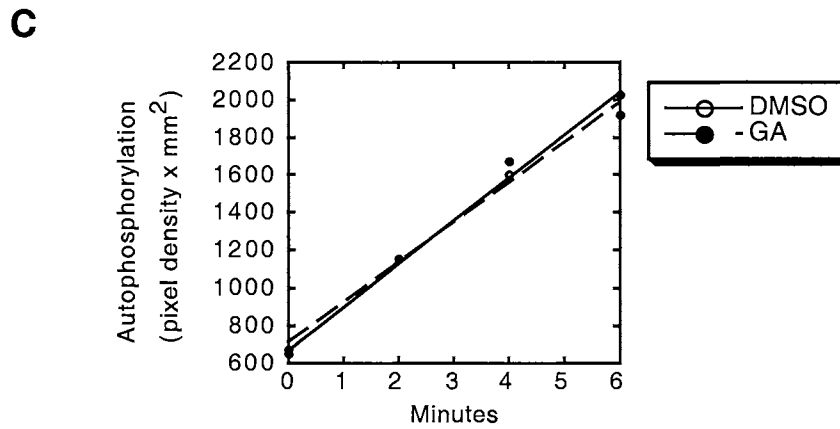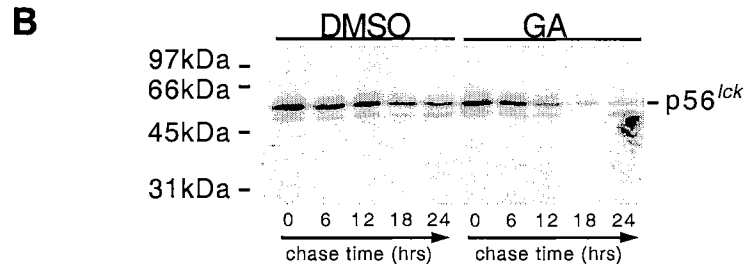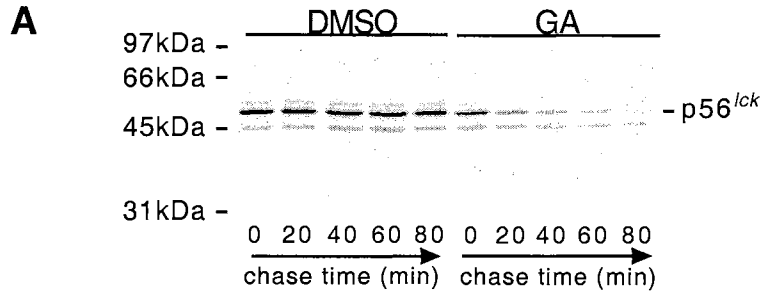
both a failure to produce nascent p56^{lck} necessary to replace old kinase combined with a more rapid turnover of mature p56^{lck}.

Proteasome inhibition and GA mediated depletion of p56^{lck}

Depletion of p56^{lck} does not necessarily mean p56^{lck} is degraded. Another possibility is that p56^{lck} is relocated to a fraction of the cell that is insoluble under the lysis conditions used; however, since we monitored total cellular protein by solubilizing pellets in SDS sample buffer, loss is probably due to degradation. The cell has many different pathways for degrading cellular proteins. The two most active are the multi-subunit proteasome protease complex, and the cellular organelle the lysosome. Due to previous reports that GA induced the degradation of some proteins by the proteasome [142] we hypothesized that the proteasome was also involved in GA mediated degradation of p56^{lck}. In order to test the hypothesis that the GA mediated depletion of p56^{lck} is through the proteasome, the highly specific proteasome inhibitors lactacystin or clasto-lactacystin β-lactone were used in conjunction with 20 hours of GA treatment of Jurkat T cells, a time at which we were sure to see significant depletion of p56^{lck}. Initially it appeared that clasto-lactacystin β-lactone provided some protection against depletion of cellular p56^{lck} (Figure 6 A lanes 3 versus 4). However, when the same experiment was repeated using a different method to lyse the cells it appeared that clasto-lactacystin β-lactone did not provide the previously seen protection against depletion of p56^{lck} (Figure 6 B lanes 3 and 4) and that clasto-lactacystin β-lactone alone caused a depletion of cellular p56^{lck} independent of GA treatment (Figure 6 B compare lanes 2 and 1). Upon analyzing the cell pellet after lysis in RIPA lysis buffer (containing SDS, Triton X-100,

and deoxycholate) a near total recruitment of $p56^{lck}$ to the detergent insoluble pellet occured upon treatment with proteasome inhibitor alone (Figure 6 C, lanes 2 and 4). The quantity of $p56^{lck}$ found in the detergent insoluble pellet was greatly increased over the normal amount of $p56^{lck}$ found in this pellet (Figure 6 C, lane 1). However GA alone did not cause a recruitment of $p56^{lck}$ to this fraction and in fact $p56^{lck}$ was mostly depleted from both fractions (Figure 6 B&C, lanes 3).

Another characteristic of proteasome degradation is the ubiquitin modification that is necessary for recognition. Ubiquitination of proteasome substrates results in an upward mobility shift of protein bands due to the increased molecular weight conferred by ubiquitin, usually represented as several slower mobility/higher molecular weight bands due to multiple ubiquitin molecules being attached. In Figure 6 C lane 4 a faint band can be seen indicating a slower mobility form of $p56^{lck}$ that may represent the ubiquitin modification.

The slower migrating band seen in Figure 6 C can be better seen in the clasto-lactacystin β-lactone treated Jurkat T cell lysate in figure 7 A lane 2 but is still represented as a minor population compared to $p56^{lck}$. Figure 7 A also shows that the upper mobility band is immuno-precipitated in a specific manner and is specific to the clasto-lactacystin β-lactone treated culture. In an attempt to detect ubiquitinated $p56^{lck}$ duplicate samples of Jurkat T cell lysates were prepared and blotted with both anti-$p56^{lck}$ and anti-ubiquitin antibodies. Figure 7 B shows that clasto-lactacystin β-lactone treatment (lane3) results in a faint slower mobility band detected by anti-$p56^{lck}$ antibodies. Interestingly, in the DMSO treated lysate (Figure 7B, lane 1) no upper band can be seen; however, in the untreated lysate (Figure 7B, lane 5) an upper band is visible and an

Figure 6. Effects of GA and Clasto-lactacystin β-Lactone Treatments on p56^{lck} from Jurkat T Cells.

(A) Jurkat T cells were cultured in the presence of 1.3 μM GA (lanes 3 and 4) and/or 10 μM clasto-lactacystin β-lactone (lanes 2 and 4) for 20 hours. DMSO was used as a vehicle control in these experiments (lanes 1). Cells were counted, harvested, and lysed either by boiling in SDS-PAGE sample buffer for 5 minutes (whole cell lysate Panel A), or by rocking in cold RIPA at 4°C for 30 minutes. Lysis volumes were normalized to give a consistent concentration of cell lysate based on cell counting. RIPA lysates were clarified by centrifugation for 10 minutes at 14000 x g at 4°C. Cell lysis supernatants where mixed with SDS-PAGE sample buffer and boiled for 5 minutes and separated by SDS-PAGE (detergent soluble Panel B). RIPA detergent insoluble pellets were resuspended/dissolved by boiling for 5 minutes in SDS-PAGE sample buffer and separated by SDS-PAGE (detergent insoluble Panel C). Gels were electro-transferred to PVDF membranes and immunoblotted with anti-p56^{lck} antibodies.
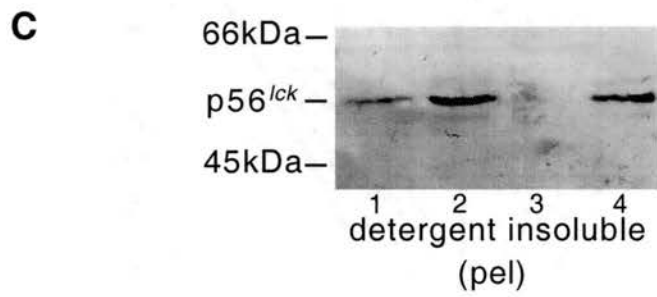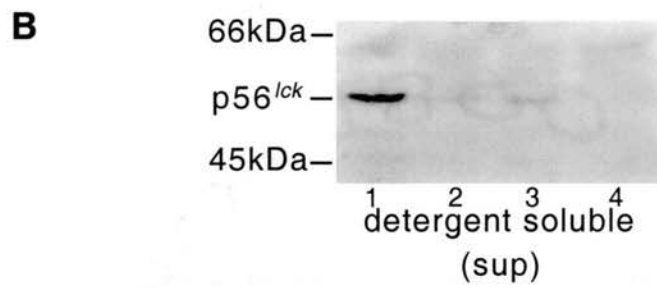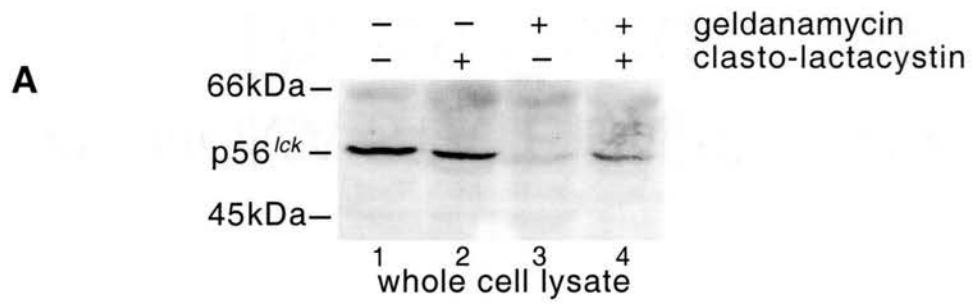
abundant lower mobility band which is very detectable by the anti-p56^{lck} antibody is also

observed. A comparison of the anti-p56^{lck} blot and the anti-ubiquitin blot shows the upper

mobility band may be ubiquitin-modified p56^{lck}; however, the prominent band detected

by anti-ubiquitin antibodies may migrate slightly slower than the upper band detected by

the anti-p56^{lck} antibodies (Figure 7B, lanes 5 and 6). The prominent band detected by

anti-ubiquitin is seen in all of the treatments (Figure 7B, lanes 6-10). One reservation is

that failure to detect the upperward mobility band by blotting with anti-p56^{lck} may reflect

epitope masking by the ubiquitin modification and therefore may not be a good indicator.

The DMSO treated sample (Figure 7B, lane 6) appears less intense indicating that DMSO

may affect the normal ubiquitination of this band. The abundant faster mobility band

detected with anti-p56^{lck} antibodies co-migrates with a band detected in the anti-ubiquitin

blot (lanes 6 and 10). This band was not seen in the previous immunoprecipitation shown

in figure 4C; however, different antibodies were used for immunoprecipitation. A

commercially available antibody from Santa Cruz Biologicals was used in figure 4C and

the rabbit anti- p56^{lck} antibody from Paul Burns [26] was used in figure 7B and C.

Differences in detection may represent differences in epitopes recognized by these

antibodies. A general increase in ubiquitin-modified proteins can be seen in the clasto-

lactacystin β-lactone treated lysates (Figure 7B, lanes 8 and 9). DMSO decreased the

background of proteins detected by anti-ubiquitin even below that seen in the untreated

lysate (Figure7B, lane 6 versus 10). Interestingly GA treatment does not appear to

increase the background of proteins detected by anti-ubiquitin antibodies (compare lanes

7 and 10). GA treatment also did not affect the intensity of the upper mobility band

detected by anti-p56^{lck} relative to the DMSO control (compare lanes 2 and 1). This

indicates that GA did not affect the quantity of this band or the abundance of the prominent band detected by anti-ubiquitin antibody or the background of ubiquitinated proteins. The identity of the upper and lower bands detected by anti-p56^{lck} antibodies are still unknown although they are probably p56^{lck} that has undergone some post-translational modification or degradation whether it is ubiquitin dependent or not.

In order to identify both the upper and lower bands detected in the anti-p56^{lck} western blot, lysates from Jurkat T cells treated with GA and/or clasto-lactacystin β-lactone were immunoprecipitated with anti-p56^{lck} antibodies (Figure 7C). A band with similar mobility as the prominent band detected by anti-ubiquitin in Figure 7B is immuno-specifically precipitated by anti-p56^{lck} antibodies (Figure 7C, lanes 1-4). The abundance of this band is unaffected by GA treatment (compare lanes 2 and 4). However, upon clasto-lactacystin β-lactone treatment the abundance of this band does not increase, only the nonspecific binding to the immunomatrix increases (Figure 7C, lanes 5 and 6). Treatment with both GA and clasto-lactacystin β-lactone reduces the nonspecific binding to an extent (Figure 7C, lane 7) but also seems to decrease the quantity in the immune lane (Figure 7C, lane 8 vs lanes 2 and 4). Anti-p56^{lck} antibodies, however, do not detect the same band detected by the anti-ubiquitin blot even though it is specific to anti-p56^{lck} immunoprecipitations. Anti-p56^{lck} antibodies do detect some faint upper mobility bands although they do not co-migrate with any of the bands detected by the anti-ubiquitin antibodies (Figure 7C lane 9). A band of similar mobility to the faster mobility band previously seen only in untreated lysates (Figure 7B lane 5) is detected in the GA/clasto-lactacystin β-lactone lane although at a reduced quantity from that seen in figure 7B, and it is not detected in the anti-ubiquitin blot, indicating it probably is not the same band.

Figure 7. Ubiquitination Analysis of p56^{lck} from GA and/or Clasto-Lactacystin β-Lactone Treated Jurkat T Cells.

(A) Jurkat T cells were treated with (lane 2) or without (lane 3) 10 μM clasto-lactacystin or equal volume of DMSO (lane 1) for 6 hours. Cells were counted and lysed by boiling in TNES (2% SDS and 10 mM NEM) buffer. Lysis volumes were normalized to give equal lysate concentration based on cell counting. DNA was sheared by passing lysates through a needle. Lysates were clarified twice by centrifugation before mixing for 3 hours with Burn's rabbit anti-p56^{lck} polyclonal antibodies, which were prebound and washed on fast flow G-sepharose. Immunopellets were washed 4 times with TNES (0.2% SDS only). Proteins were eluted by boiling immunepellets in SDS-PAGE sample buffer and loaded and separated by SDS-PAGE. Proteins were then electro-blotted from gels to PVDF membranes and immunoblotted with an OSU Mouse 1 and 3 anti-p56^{lck} polyclonal ascites cocktail. Mobility of molecular weight markers and p56^{lck} are marked on the left side of the panel. Lane 3 shows immunoprecipitation of untreated lysate with rabbit nonimmune antibodies as a control for nonspecific binding of proteins to immunomatrix. (B) Jurkat T cells were treated with 1.3 μM GA (lanes 2 and 7), 10 μM clasto-lactacystin β-lactone (lanes 3 and 8), both (lanes 4 and 9), equal volume of DMSO (lanes 1 and 6), or media (lanes 5 and 10) for 6 hours. Cells were lysed by boiling in TNES and duplicate samples were loaded on to SDS-PAGE gels for separation. Proteins were electro-blotted on to nitrocellulose membranes and immunoblotted with either anti-p56^{lck} (lanes 1-5) or anti-ubiquitin (lanes 6-10) antibodies. Membrane to be anti-ubiquitin blotted was autoclaved submerged in water for 15 minutes prior to normal immunoblotting. Mobility of molecular weight markers is labeled on the left side of the panel. Mobility of p56^{lck} is marked on the right side of the panel. (C) Jurkat T cells were treated with 1.3 μM GA (lanes 3 and 4), 10 μM clasto-lactacystin β-lactone (lanes 5 and 6), both (lanes 7-9), or equal volume of DMSO (lanes 1 and 2) for 6 hours. Cells were lysed by boiling in TNES and DNA was sheared as described for Panel A. Samples were immunoprecipitated with anti-p56^{lck} (I-immune: lanes 2, 4, 6, 8, and 9) or nonimmune antibodies (NI: lanes 1, 3, 5, and 7). Proteins eluted from immunopellets were separated by SDS-PAGE and proteins were electroblotted from gels to nitrocellulose membranes. Membranes were immunoblotted with anti-ubiquitin or anti-p56^{lck} antibodies. Duplicate samples of GA and clasto-lactacystin β-lactone treated cell lysate were loaded side by side (lanes 8 and 9) in order to facilitate lining up bands detected by either the anti-ubiquitin immunoblot (lanes 1-8) or anti-p56^{lck} immunoblot that co-migrate. Mobility of molecular weight standards is labeled on the left of the panel and mobility of p56^{lck} is labeled on the right side.

53

(IP: anti-p56^{lck})

A

B

C (IP: anti-p56^{lck})

anti-p56^{lck}

anti-ubiquitin

anti-Ubiquitin

α-p56^{lck}
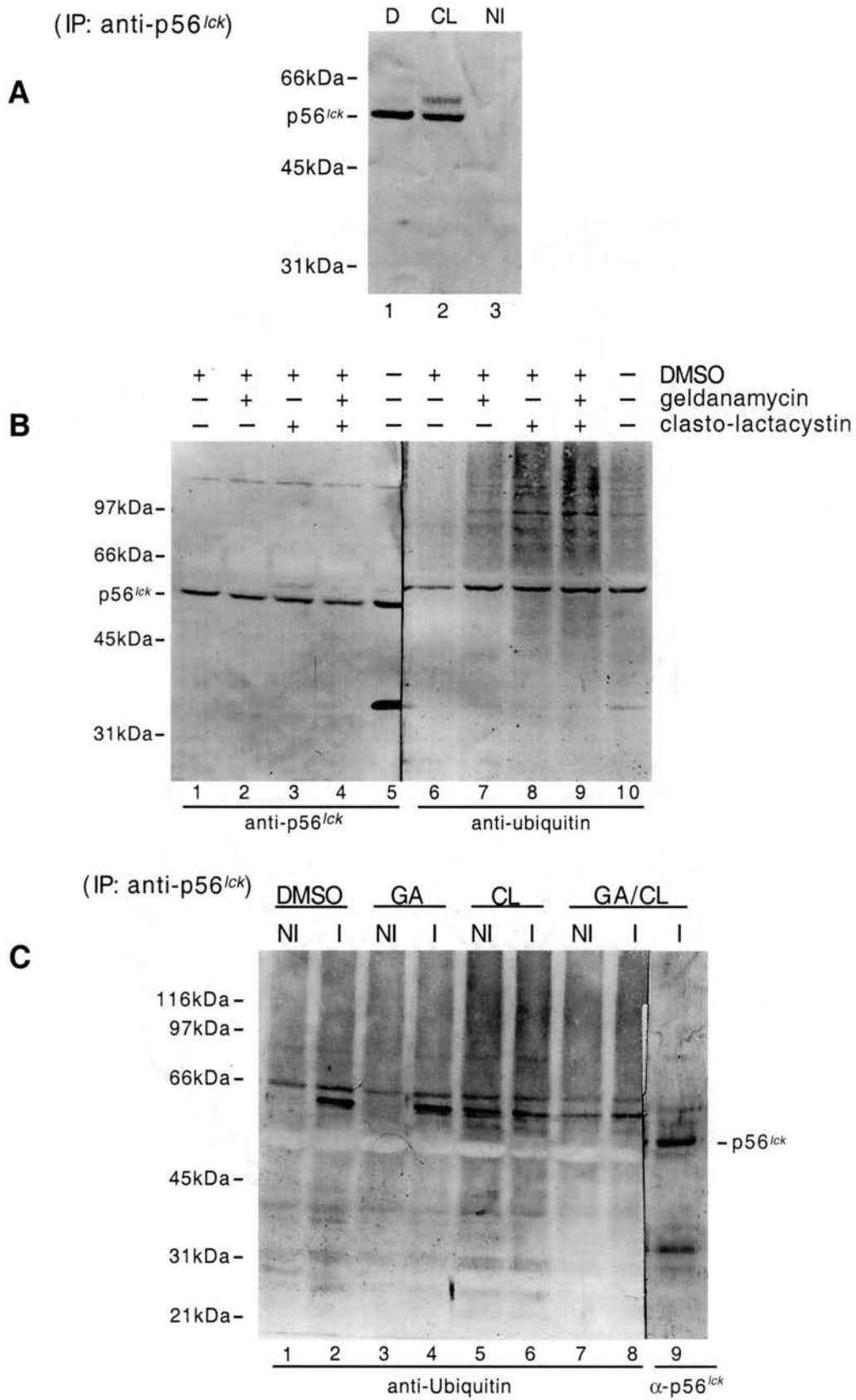
Once again GA does not increase the levels of the prominent immune-specific band detected in the anti-ubiquitin blot and in fact reduces its levels somewhat in the GA and clasto-lactacystin β-lactone treated samples. This suggests that the levels of this protein, whether ubiquitinated p56^{lck} or not, is unaffected by GA treatment. If the prominent band detected by anti-ubiquitin blotting of anti-p56^{lck} immunoprecipitates is p56^{lck} then ubiquitination of p56^{lck} is not induced by GA treatment as has been reported for other proteins [117-120]. Rather it appears that if anything p56^{lck} undergoes ubiquitination normally, which may even be in an Hsp90 dependent manner and that GA treatment alters this mechanism. Further consideration of p56^{lck} ubiquitination and degradation in the context of recent publications follows in the discussion.

Lysosomal inhibition affects GA mediated depletion of p56^{lck}

Due to the ambiguous nature of the results from experiments attempting to identify the role of the proteasome in GA mediated depletion of p56^{lck} an alternative proteolytic pathway was examined. The lysosome is a membrane bound organelle containing several proteases active at acidic pH and is involved in the degradation of cellular proteins under both normal and abnormal conditions. The lysosome and the proteasome pathways for protein degradation represent two of the major pathways for metabolism of proteins in the cell. In order to test the hypothesis that the GA mediated degradation of p56^{lck} is through the lysosome, the V-ATPase inhibitor bafilomycin A was used to rescue p56^{lck}. V-ATPases regulates the internal pH of the lysosome organelle and when inhibited the pH rises, subsequently inactivating lysosmal proteases. Figure 8 shows that bafilomycin A provided some protection against GA mediated degradation

55

Figure 8. Effect of Lactcystin and Bafilomycin A on GA Mediated Depletion of p56^{lck} in Jurkat T Cells (Courtesy of Peter Yorgin).

Jurkat T cells were cultured with media (lane 1), 2 μM bafilomycin A (lane 2) or 10 μM lactacystin (lane 3) for three hours or with media (lane 4), 1 μM bafilomycin A (lane 5), 1.7 μM GA (lane 6), 10 μM lactacystin (lane 7), 2 μM bafilomycin A and 1.7 μM GA (lane 8), or 10 μM lactacystin and 1.7 μM GA (lane 9) for 15 hours. Cells were lysed in cold RIPA buffer and separated by SDS-PAGE. Proteins were transferred to nitrocellulose membranes, which were probed with anti-p56^{lck} antibodies. Mobility of molecular weight standards is labeled on the left of the panel and p56^{lck} mobility is labeled on the right of the panel.

geldanamycin	−	−	−	−	−	+	−	+	+
bafilomycin	−	+	−	−	+	−	−	+	−
lactacystin	−	−	+	−	−	−	+	−	+

68

lck

1 2 3 4 5 6 7 8 9

43

3 hours   15 hours
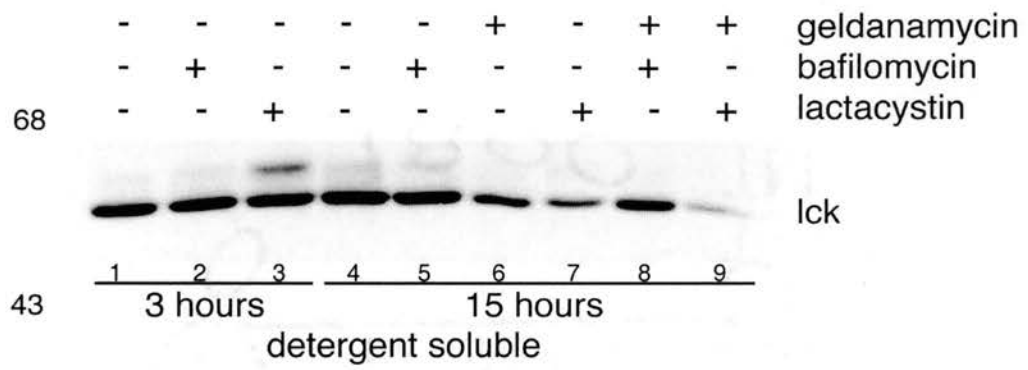
detergent soluble

and that bafilomycin A did not recruit $p56^{lck}$ to the detergent insoluble pellet (compare lanes 6 and 8). This data suggests that GA mediates $p56^{lck}$ depletion in Jurkat T cells by inducing degradation through the lysosome. The inability to detect an increase in ubiquitin-modified $p56^{lck}$ in GA treated Jurkat T cell lysates suggests that ubiquitination of $p56^{lck}$ is at least not stimulated by GA.

Discussion

The reported Hsp90 dependent substrates and their known roles in cell cycle progression, proliferation, and signal transduction have made Hsp90 a target for cancer therapy. Currently the selective cytotoxic effects of GA are being studied for use in cancer therapy (reviewed in [125]). The work presented here furthers our understanding of the effects of Hsp90 inhibition on various cell populations. Comparison of the cytostatic and cytotoxic effects of GA on the resting splenic mononuclear cells and both the activated splenic mononuclear cells and the transformed Jurkat T cell line show that the latter populations are more sensitive to GA. This suggests that proliferating cells are more sensitive to GA cytotoxicity than nonproliferating cells, although, GA is also toxic to resting splenic mononuclear cells upon longer treatment. Chemotherapeutic agents are often toxic to nontargeted cells and an unfortunate side effect of treatment is toxicity to protective proliferating immune cells. Our results also show that GA treatment inhibited the effects of T cell activation through the antigen receptor (TCR), CD28, IL-2R/CD25, and through the less specific mitogenic stimulation of Con A, thus potentially affecting the ability to mount an immune response during treatment. An account published during the preparation of this text on the effects of GA treatment on activation of peripheral T

lymphocytes through the CD28 receptor reported similar results on T cell proliferation, and IL-2 and IL-2R production [134]. These results suggest that Hsp90 function is necessary for several signal transduction pathways in T cells.

To monitor GA affects at the molecular level the known T cell specific Hsp90 substrate p56^{lck} was studied. The cytotoxic effects of GA treatment are probably only partly incurred by the effects seen on p56^{lck}; however, the effects on signal transduction through the receptors listed above are very directly related to p56^{lck} since all use p56^{lck} for signaling. Results presented here show that GA treatment of resting and activated splenic mononuclear cells, and Jurkat T cells results in a general depletion of cellular p56^{lck} levels. Interestingly, GA mediated depletion of the p56^{lck} in activated splenic mononuclear cells is more rapid than in resting splenic mononuclear cells, which correlates with the cytotoxicity. Geldanamycin mediated depletion of p56^{lck} in Jurkat T cells occurs on a time scale similar to the depletion of p56^{lck} in resting mononuclear cells; however, it can be accelerated at higher concentration of GA. Our results indicate p56^{lck} depletion has two causes: 1) a dramatic compromise and total degradation of newly synthesized p56^{lck} pools that normally replace mature p56^{lck} upon degradation, and 2) a 2-fold increase in the rate of turnover of mature p56^{lck}, with accelerated loss being most apparent at later treatment times. The first is much more rapid and probably contributes more quantitatively to the depletion seen in our studies than the second mechanism. The second mechanism is slower and does not represent a large contribution to the overall loss of p56^{lck} in GA treated cells, and may be an indirect effect of long term treatment. However, the reported effects on both pools of p56^{lck} show that both pools are dependent on Hsp90 to varying degrees. Recent reports supporting this observation and data

presented in Chapter 4 show that *in vitro* as well as *in vivo* newly synthesized p56^{lck} depends on Hsp90 to mature to a stable form which is mostly Hsp90 independent [26, 27, 138, 139]. The greater sensitivity of p56^{lck} to GA mediated depletion seen in the activated splenic mononuclear cells may be an effect of activation of the kinase. T cell activation through receptors activates the protein tyrosine kinase activity of p56^{lck}. Activated Src-family tyrosine kinases, especially the mutant transforming variety, are more reliant on Hsp90 function [27, 143], which agrees with the more rapid degradation of p56^{lck} in GA treated activated splenic mononuclear cells. The resting splenic mononuclear cells and the Jurkat T cells in which p56^{lck} has not been activated show a slower rate of GA mediated depletion. Alternatively, activated splenic mononuclear cells may turnover activated p56^{lck} more rapidly independent of GA treatment. The effect of GA treatment may be to inhibit the replenishment of p56^{lck} by increasing the degradation of newly synthesized kinase. Whether the increased rate of depletion of p56^{lck} in activated T cells is due to an increase in the rate of turnover of mature activated kinase or an inability to replenish mature active kinase stores will require further study.

Due to previous reports that Hsp90 inhibition stimulated the degradation of some Hsp90 clients via the proteasome we tested the hypothesis that GA mediated a similar degradation of p56^{lck}. Initial inquiry indicated that proteasome inhibition protected p56^{lck} from GA mediated degradation. A more thorough examination showed that the proteasome inhibitor had effects on p56^{lck} independent of GA treatment, making our initial conclusion questionable. The complex effect of the proteasome inhibitor on recruitment of p56^{lck} to a RIPA detergent insoluble fraction independent of GA treatment indicated the protective effect of the inhibitor was unrelated to GA treatment. These

results along with reports of other proteins being recruited to detergent insoluble fractions upon proteasome inhibition require careful interpretation of such experimental results [120, 144]. In order to further characterize the potential of proteasome degradation of p56^{lck} in GA treated T cells anti-ubiquitin western blots were conducted on both whole cell lysates and anti-p56^{lck} immunoprecipitations. In both samples ubiquitinated proteins were detected but it was unclear whether the protein bands detected by anti-ubiquitin antibodies were p56^{lck}. It was clear, however, that GA did not increase the quantity of the ubiquitin specific bands even when the proteasome was inhibited indicating that GA mediated degradation of p56^{lck} was not catalyzed by the proteasome, a result decidedly contrary to a mechanism in the literature that GA automatically targets client proteins to the proteasome [125, 145]. The fact that an immune-specific band precipitated by anti-p56^{lck} antibodies was detected by the anti-ubiquitin western blot suggests that p56^{lck} may be ubiquitinated and degraded by the proteasome as part of its normal turnover. Subsequent reports of a physical association and ubiquitination of p56^{lck} with both the E6AP and Cbl E3 ubiquitin ligases support this observation. In light of this new information our results suggest that the slight protection observed by treatment with clasto-lactacystin β-lactone was due to inhibition of the normal turnover of p56^{lck} and not GA mediated turnover. These reports also suggest that ubiquitin mediated degradation favored the active form of the Src family kinases, since constituitively active mutants were ubiquitinated and degraded more rapidly than the wild type kinase. Inactive kinase mutants were not ubiquitinated [146, 147]. The preferential degradation of activated p56^{lck} is consistent with the observation that activated splenic mononuclear cells show an increase in the rate of p56^{lck} depletion.

Since the ubiqutin-proteasome pathway did not appear to be involved in the observed GA mediated p56^{lck} degradation, the common lysosomal pathway of protein degradation was the next focus due to its role in normal and abnormal protein degradation and its role in receptor endocytosis and degradation, a mechanism of possible importance for the receptor associated tyrosine kinase p56^{lck}. The specific vacuolar-type H$^+$-ATPase (V-ATPase) inhibitor bafilomycin A provided protection against GA mediated degradation of p56^{lck}, a result consistent with lysosomal degradation. Bijlmakers et al. [139, 148] reported that Hsp90 activity was indirectly necessary for newly synthesized p56^{lck} to associate with ER/Golgi compartment membranes and with the co-receptor CD4. Therefore, bafilomycin A protection against GA treatment may represent an alteration in newly synthesized p56^{lck} trafficking through the ER/Golgi exocytic pathway. Bafilomycin A could also protect mature membrane associated p56^{lck} from degradation if it is endocytosed along with the TCR on way to lysosomal receptor degradation. Alternatively, GA mediated degradation of p56^{lck} could occur through more than one mechanism as reported for connexin 43 [149] and the epidermal growth factor receptor (ErbB-1). It is interesting to note that the Cbl ubiquitin ligase is reported to down regulate several signal transduction proteins, but not necessarily to the same degradation pathway. As mentioned, members of the non-receptor Src-kinase family interact with and are ubiquitinated by Cbl, and are then degraded by the proteasome. The epidermal growth factor receptor tyrosine kinase (ErbB-1), which in its nascent form is a reported Hsp90 client [150], is also ubiquitinated by Cbl. The ubiquitinated receptor is then localized in endosome compartments. Both proteasome and lysosomal inhibitors were able to inhibit the degradation of the receptor, although the proteasome inhibitor showed more

protection [151, 152]. Another ErbB family member (ErbB-2/Her2), also an Hsp90

client, is ubiquitinated, in response to GA treament, and localizes to endosomal

membrane compartments, although its degradation is prevented only by proteasome

inhibitors [153]. These results begin to suggest that degradation by the proteasome and

lysosomal pathways are not as straightforward as previously thought, and that more than

one pathway may work on one target. Finally, there is the possibility that a novel

proteolytic pathway as described for a ZAP70 tyrosine kinase mutant [154] is at work.

These results further our understanding of the effects of GA treatment on T cell

biology, by extending characterizations to different populations of cultured cells. The

enhanced sensitivity of proliferating T cells to GA cytotoxicity is shown relative to

resting T cell populations and suggests potential usefulness in cancer and

immunosuppresion therapies. Our study of the effects of GA on the $p56^{lck}$ kinase provides

insight at the molecular level, showing that the newly synthesized $p56^{lck}$ is more sensitive

to GA mediated degradation than the mature kinase. The effect on other Hsp90 clients

would vary based on their Hsp90 dependence. The mechanism of GA mediated

degradation is still unclear; however, our results do not support a GA induced ubiquitin-

mediated proteasome degradation as has been reported for other clients. These results

provide a reference for using $p56^{lck}$ as a marker of GA pharmacological activity.

Currently a derivative of GA is in Phase I clinical trials for cancer therapy and $p56^{lck}$ is

being used as a marker in these studies ([125] and personal communication). Most of

these results were published in the Journal of Immunology [127].

CHAPTER 3

CO-TRANSLATIONAL ASSOCIATION OF MOLECULAR CHAPERONES WITH

NASCENT POLYPEPTIDES CHAINS: A COMPARISON OF TWO

EXPERIMENTAL TECHNIQUES

Introduction

De novo folding of some proteins begins while the elongating polypeptide is still

bound to the ribosome. Evidence supporting co-translational folding is based on the study

of model proteins by many methods including assays of function, resistance to protease

digestion, proper disulfide bond formation, or recognition by conformation-dependent

antibodies [1, 155-159]. Ribosome bound firefly luciferase is active but only when the C-

terminus is extended such that the last 12 amino acids, which are critical for activity

[160], are no longer buried in the ribosomal tunnel [161]. Synthesis of a truncated firefly

luciferase, lacking only the stop codon, produced an inactive full-length luciferase that

remained bound to the ribosome. After release from the ribosome by puromycin,

luciferase activity immediately appeared. When compared to renatured firefly luciferase,

with a folding half-time of 14 minutes, the newly synthesized ribosome bound luciferase

had significant functional structure, and supports a mechanism whereby folding begins

co-translationally [162]. Similar experiments with C-terminally extended ribosome bound

rhodanese produced an enzymatically active protein [163]. Significant structure can be

found even in ribosome-bound polypeptides that are less than full length. Komar *et al.*

64

[164] reported that a ribosome-bound α-globin fragment as short as 86 amino acids was capable of specifically binding heme. These reports indicate a significant amount of *de novo* folding occurs during translation of these proteins, and suggests release from the ribosome is all that is necessary for completion of folding. The effect that release from the ribosome has on the overall three-dimensional structure of different proteins may depend on the importance of the C-terminal 30-40 amino acids, held in the ribosomal tunnel, to the final structure.

In the cell, newly synthesized polypeptides emerge from the ribosome into a complex crowded environment where nonproductive interactions with self, other proteins, or other biomolecules are very likely. Some initial folding events may be facilitated by the ribosome itself (reviewed in [165]). However, cells have developed a specific group of proteins called molecular chaperones that facilitate the folding of some proteins by preventing or reversing improper interactions between protein surfaces that are necessary for a functional three-dimensional structure [6]. There are many families of molecular chaperones and their role in protein folding in the cell is the focus of much current research (reviewed in [7]). Recent reports suggest that the Hsp70 and Hsp60 (chaperonin) families are the major contributors to chaperone mediated *de novo* folding [49, 50, 166]. Estimates of 15-20% of newly synthesized cytosolic polypeptides in HeLa and BHK (Baby Hampster Kidney) cells co-precipitated with Hsp70 [49, 50] and 9-15% of newly synthesized polypeptides in BHK cells co-precipitated with TRiC (the cytosolic chaperonin TCP-1 ring complex or CCT) [50]. This means an estimated 65% of newly synthesized cytosolic proteins fold without Hsp70 or TRiC assistance. Some of these

proteins may fold to a native state independently; however, other proteins may need the aid of other cytosolic chaperones.

Eggers *et al.* [49] restricted their study to translating polypeptides by using puromycin to release incomplete polypeptides from the ribosome and then immunoprecipitating with either puromycin specific or chaperone specific antibodies. Chaperone interactions were detected by western blotting proteins that co-immunoprecipitated with the puromycyl polypeptides or co-immunoprecipitation of radiolabeled puromycyl polypeptides by specific chaperone antibodies. Similar techniques have been used to look at co-translational interaction of chaperones with model proteins such as firefly luciferase, actin, and rhodanese [158, 167-169]. Most of these techniques focus on associations with the puromycin released fragments, which may represent misfolded polypeptides or folding mutants that may never achieve an independent three-dimensional structure due to incomplete folding information. The significance of results from such experimental techniques should be considered carefully [170]. An alternative technique used by Eggers *et al.* [49] to detect co-translational chaperone interactions allowed a more straightforward interpretation. Newly synthesized radiolabeled polypeptides were cross-linked to associated proteins *in vivo* prior to lysis and immunoprecipitation by chaperone specific antibodies. This confirmed the Hsp70 and Hsp60 co-translational interaction with nascent polypeptides and implicated Hsp90 as a co-translational chaperone. Hsp90 antibodies co-precipitated a distinct, but less abundant population of nascent polypeptides, which agrees with a model of Hsp90 operating on a restricted clientele [171]. Our lab has reported the co-translational interaction of Hsp90 machinery with a protein that is folded and regulated by Hsp90

activity, the heme-regulated eIF2α kinase (HRI). The significance of such interactions is underscored by studies showing the failure of newly synthesized HRI to achieve heme-regulated kinase activity in the absence of Hsp90 function [100, 172]. Here we report the co-translational chaperone interactions of three Hsp90 substrate proteins in RRL and compare techniques for detection of co-translational chaperone interactions.

Materials and Methods

Plasmids

The coding sequence for proteins to be synthesized *in vitro* were cloned into a modified pSP64T plasmid [173] as previously described [138, 172].

Polyribosome preparations

Nuclease treated rabbit reticulocyte lysate (RRL) was programmed with pSP64T luciferase, pSP64T HRI, or pSP64T Lck plasmid for coupled transcription and translation. Proteins were synthesized for 15 minutes at 30 °C as described by Hartson *et al.* [138]. Transcription was driven by the SP6 bacterial RNA polymerase promoter encoded in the pSP64T plasmid. Messenger RNA produced was translated in the presence of [^{35}S] methionine by the protein synthesis machinery endogenous to reticulocyte lysate. Protein synthesis reactions were incubated for an additional 5 minutes at 30 °C in the presence or absence of 1 mM puromycin. After puromycin treatment protein synthesis reactions were diluted with 2 volumes of ice-cold buffer containing 20 mM Tris-HCl (pH 7.5), 25 mM KCl, and 2.5 mM magnesium acetate. Diluted reactions were layered on top of 15-40% sucrose gradients containing buffer and salt

concentrations consistent with the dilution buffer. Polyribosomes were separated by centrifugation for 4.5 hours at 40,000 rpm in an AH650 Sorval rotor. The supernatant of the polyribosome pellet were removed and ribosomal pellets were dissolved in 2X SDS sample buffer (125 mM Tris-HCl (pH 6.8), 10% SDS, 55 mg/ml dithiothreitol, 10% glycerol, 0.005% bromphenol blue [130]). Proteins present in the ribosomal pellets were separated by SDS-PAGE on 10% acrylamide gels.

Immunoprecipitations

Protein synthesis reactions not separated on sucrose gradients were immunoprecipitated with primary antibodies prebound to either goat anti-mouse IgG or goat anti-mouse IgM coupled agarose. The primary antibodies used were one of the following: monoclonal mouse anti-Hsp90 IgM (8D3), monoclonal mouse anti-Hsp70 IgG (BB70), polyclonal mouse anti-p50^{cdc37} IgG, mouse non-immune IgM (8D3 control), or mouse non-immune IgG (control for BB70 and anti-p50^{cdc37}). Protein synthesis reactions were mixed with the immunoresin for 1 hour on ice. Immunoresins were washed five times with P150T (Pipes pH 7.0, 150mM NaCl, 0.5% Tween-20), and eluted by boiling in 2X SDS sample buffer for 5 minutes. Immunoprecipitated proteins were separated by SDS-PAGE on 10% acrylamide gels.

Western Blot and Immunodetection

10% SDS-PAGE gels were transferred to PVDF membrane and stained lightly with Coomassie blue to estimate the transfer efficiency. Membranes were dried and exposed to film to determine presence and pattern of radioactively labeled protein bands.

Membranes were cut according to molecular weight markers and probed with the appropriate chaperone antibodies: mouse polyclonal anti-Hsp90, mouse polyclonal anti-Hsp70 (N27 StressGen), and mouse polyclonal anti-Cdc37 [46].

Results

Hsp90 and p50^{cdc37} associate with ribosomes translating HRI mRNA

The co-translational chaperone interactions of three proteins were chosen for study based on their different dependence on chaperone function. HRI, a known Hsp90-dependent protein, was chosen as a positive control due documented co-translational interactions with Hsp90 and Hsc70 in reticulocyte lysate [100, 172]. Firefly luciferase was selected as a negative control since newly synthesized luciferase has been shown to fold independent of interactions with Hsp90. However, the Hsp90 chaperone machine interacts with and facilitates the refolding of denatured luciferase [174]. The Hsp90-dependent Src-family tyrosine kinase p56^{lck}, was chosen since its co-translational interactions with chaperones had not been characterized. These three proteins represent different types of Hsp90 substrates and a comparison of their Hsp90 and p50^{cdc37} co-translational interactions may provide insight to these differences.

In order to detect specific association of Hsp90 and p50^{cdc37} with ribosomes translating either firefly luciferase, HRI, or p56^{lck}, nuclease treated RRL was programmed with plasmid DNA containing the cDNA sequence for each protein. After a short burst of translation half of the reaction was treated with puromycin to prematurely release nascent polypeptides from the ribosome without disrupting the rest of the ribosome complex. It

was important to release only the nascent polypeptide without disrupting the ribosome complex since we wanted to detect only proteins associating with the nascent chains while being translated, and not those associated with the ribosome complex. Members of the Hsp70 family of chaperones have been reported to associate with "vacant" ribosomes in a salt-sensitive manner and may play a role in protein synthesis [175, 176]. Even under low salt conditions we achieved good release of nascent polypeptides, as monitored by loss of [^{35}S] labeled bands (Figure 9 B), with puromycin treatment. After a short puromycin treatment under protein synthesis conditions ribosomes from the protein synthesis reactions were separated by centrifugation through a sucrose gradient under conditions reported to pellet intact ribosomes (80S and greater) [100, 177-179]. The loss of nascent polypeptides in the HRI synthesis reactions (Figure 9, lanes 3 and 4) correlated with the loss of Hsp90 and p50^{cdc37} from the ribosomal pellet (Figure 9 A, lanes 3 and 4). Ribosome complexes were still intact based on three indicators: polyribosome profiles (not shown), Coomassie blue staining bands of resuspended pellets were unchanged by puromycin treatment (not shown), and the Hsp70 band on the western blot is still detected in the ribosomal pellet (Figure 9 A Hsp70 panel). The Hsp70 band in the ribosome pellet where nascent polypeptides have been released also indicates that rabbit Hsp70 interacted with vacant ribosomes as Pfund *et al.* [176] reported for yeast Ssb. Our result confirms Eggers *et al.* [49] assessment that Hsp90 interacts with some nascent polypeptides while still on the ribosome, although these interactions were not the same for all known Hsp90 clients since neither firefly luciferase nor p56^{lck} showed evidence of co-translational interaction with Hsp90 or p50^{cdc37}.

Figure 9. Chaperone Associations with Translating Ribosomes.

Nuclease treated RRL was programmed with firefly luciferase (lanes 1 and 2), HRI (lanes 3 and 4), or p56^{lck} (lanes 5 and 6) cDNAs and allowed to synthesize protein for 15 minutes at 30 °C in the presence of [^{35}S] methionine to radiolabel newly synthesized polypeptides. Protein synthesis reactions were then either treated (even lanes) or not treated (odd lanes) with 1 mM puromycin for 5 minutes at 30 °C to release nascent polypeptides from the translating ribosomes. Polyribosome complexes were separated from other RRL protein complexes by centrifugation through a 15 to 40% sucrose gradient as described in "Materials and methods". Components of the polyribosome complex were further separated by 10% SDS-PAGE and blotted to a PVDF membrane. The membrane was analyzed by (A) immunodetection with antibodies against Hsp70 (N27), Hsp90 (polyclonal OSU), p50^{cdc37} (polyclonal OSU) and (B) exposure to film for detection of [^{35}S] labeled nascent polypeptide. 2 µl of RRL (lane 7) were used as a standard for immunodetection.

72
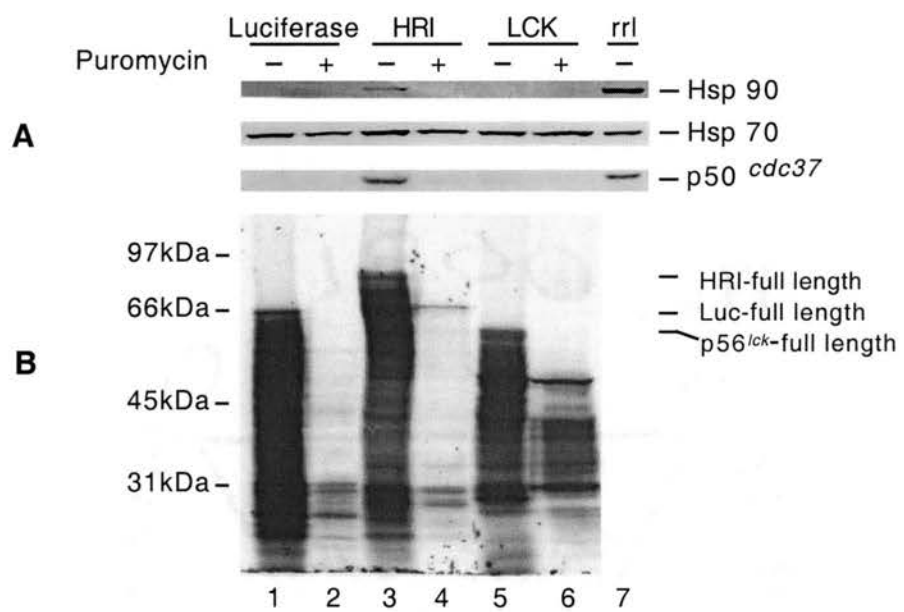
Co-precipitation of prematurely released nascent polypeptides by anti-Hsp90 antibodies

An alternative technique used to detect co-translational interactions is immunoprecipitation or co-precipitation of prematurely released (by puromycin) nascent polypeptides using antibodies either for puromycin (to bring down the nascent polypeptides) or for specific chaperones of interest [49, 166, 167, 180]. Figure 10 is the autoradiogram of [^{35}S] labeled nascent (puromycin released) polypeptides that co-immunoprecipitated with Hsp90. Hsp90 co-immunoprecipitated specific bands, smaller than the full-length protein, for all three proteins, as seen in the immune lanes (Figure 10, lanes 2, 5, and 8). The 8D3 antibody co-precipitated a broad-range of HRI polypeptides (lane 5 vs 6). However, for p56^{lck} the larger polypeptides seemed to be more highly represented in the co-immunoprecipitate (Figure 10, lanes 7-9). A select few luciferase polypeptides co-immunoprecipitated above background, although the background was especially high (Figure 10, lanes 1-3). Analysis of the autoradiogram indicated interaction of Hsp90 with some of the ribosome free incomplete products of each protein. Only the co-translational interaction of Hsp90 with HRI was detected by the ribosomal pellet technique (Figure 9). A comparison of the different techniques and reasons for the different results can be found in the "Discussion" section.

Co-precipitation of prematurely released nascent polypeptides by anti-Hsp70 and anti-p50^{cdc37} antibodies

Figure 11 is the autoradiogram of [^{35}S] labeled nascent polypeptides that co-immunoprecipitated with Hsp70 and p50^{cdc37}. Each protein had immune-specific bands, smaller than full-length, that co-precipitated with Hsp70 above background (Figure 11,

Figure 10. Co-Immunoprecipitation of Nascent Polypeptides with Monoclonal Anti-Hsp90 Antibodies.

Nuclease treated RRL was programmed with firefly luciferase (lanes 1-3), HRI (lanes 4-6), or p56^{lck} (lanes 7-9) cDNAs and allowed to synthesize protein for 15 minutes at 30 °C in the presence of [^{35}S] methionine to radiolabel newly synthesized polypeptides. Protein synthesis reactions were then treated with 1 mM puromycin for 5 minutes at 30 °C to release nascent polypeptides from the translating ribosomes. Equal aliquots of the protein synthesis reactions were mixed (as described in "Materials and methods") with goat anti-mouse IgM coupled agarose, which had been prebound with either anti-Hsp90 monoclonal IgM (I) or a non-immune IgM (NI) as a control. 2 μl of each protein synthesis reaction were loaded (UF) to show the mixed population of polypeptides input in each immunoprecipitation.

luciferase | HRI | LCK
NI I UF | NI I UF | NI I UF

66kDa–
45kDa–
31kDa–
21kDa–
14kDa–

– HRI-full length
– Luc-full length
p56^{lck}-full length

1 2 3 4 5 6 7 8 9

75
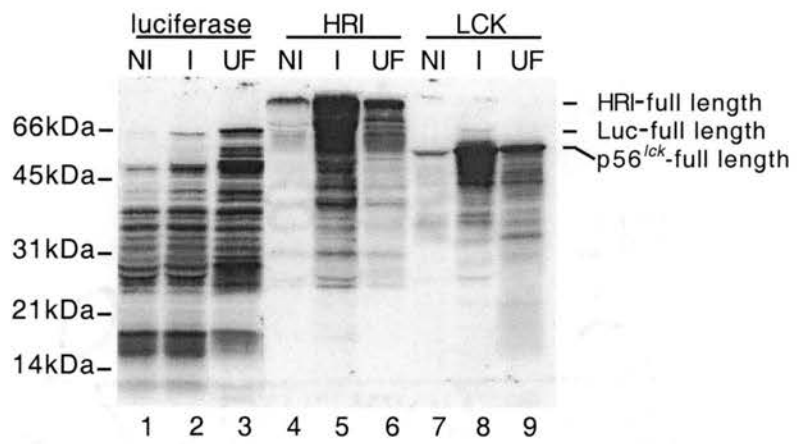
Figure 11. Co-Immunoprecipitation of Nascent Polypeptides with Anti-Hsp70 and Anti-p50^{cdc37} Antibodies.

Nuclease treated RRL was programmed with firefly luciferase (lanes 1-4), HRI (lanes 5-8), or p56^{lck} (lanes 9-12) cDNAs and allowed to synthesize protein for 15 minutes at 30 °C in the presence of [^{35}S] methionine to radiolabel newly synthesized polypeptides. Protein synthesis reactions were then treated with 1 mM puromycin for 5 minutes at 30 °C to release nascent polypeptides from the translating ribosomes. Equal aliquots of the protein synthesis reactions were mixed (as described in "Materials and methods") with goat anti-mouse IgG coupled agarose, which had been prebound with anti-Hsp70 monoclonal IgG (lanes 2, 6, and 10), anti-p50^{cdc37} IgG (lanes 3, 7, and 11) or a non-immune IgG (lanes 1, 5, and 9) as a control. 2 μl of each protein synthesis reaction were loaded (lanes 4, 8, and 12) to show the mixed population of polypeptides input in each immunoprecipitation.
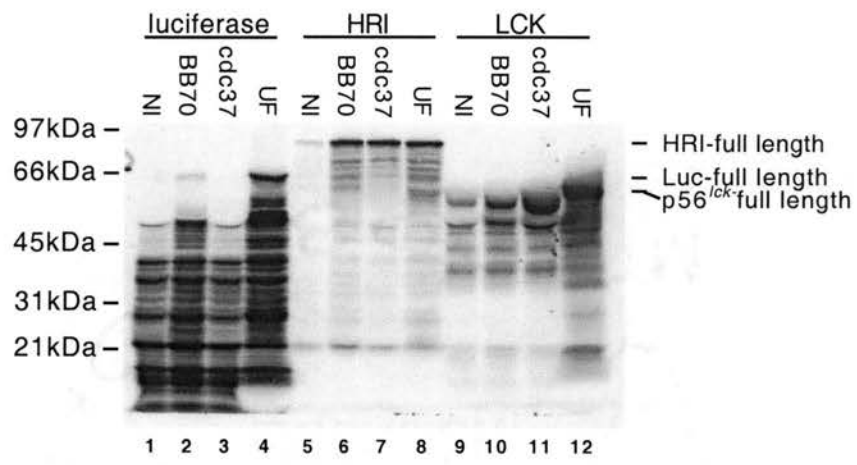
lanes 2, 6, and 10). HRI and p56^{lck} also had some nascent polypeptides that co-precipitated with p50^{cdc37} (Figure 11, lanes 7 and 11); however, none of the luciferase nascent polypeptides co-precipitated with p50^{cdc37} above background (Figure 11, lanes 1 and 3). As mentioned above for the Hsp90 immunoprecipitations, most of the co-precipitating nascent polypeptides were the larger species. The p50^{cdc37} co-precipitation of p56^{lck} and HRI mostly brought down polypeptides close to full length or full-length kinases (Figure 11, lanes 7 and 11), suggesting that p50^{cdc37} interaction requires more sequence or even a specific sequence or structure found close to the C-terminus of the protein.

Chaperone/Domain interactions

Since the two kinases being studied also showed differences in their co-translational chaperone interactions possible reasons for the differences were sought. Previous work done in our laboratory suggested that p56^{lck} interacted with Hsp90 and p50^{cdc37} primarily through the kinase domain (Figure 12, lane 3 and [27]). However, HRI has multiple domains that interact with Hsp90 and Hsp70 (Figure 13, lane2 and 4). The domain organization of the proteins and the location of their interacting domains in relation to emergence from the ribosome might resolve these differences. The kinase domain of p56^{lck} is at the C-terminus and is the last domain to emerge from the ribosome and therefore may not allow interaction until released from the ribosome. The heme binding domain (HBD; Figure 13, lane 4) is located at the N-terminus of HRI and would be exposed early allowing it to possibly interact with Hsp90, although there is no p50^{cdc37} present. Also the two lobes of the HRI kinase domain are separated by a long insertion

Figure 12. Hsp90 and p50^{cdc37} Co-Immunoprecipitate with the Kinase Domain of p56^{lck}.

Nuclease treated RRL was programmed with histidine tagged full length p56^{lck} (lane 2) or the histidine tagged protein tyrosine kinase catalytic domain (lane 3) cDNAs and allowed to synthesize protein for 20 minutes at 37 °C in the presence of [^{35}S] methionine to radiolabel proteins. Protein synthesis reactions were then clarified and mixed with goat anti-mouse IgG coupled agarose, which had been prebound with anti-His monoclonal IgG (lanes 1-3). RRL with out template DNA was also immunoprecipitated with anti-His bound IgG coupled agarose as a control to determine the level of nonspecific binding of chaperones to the immunoresin (lane 1).

(IP anti-His)

H_6-p56^{lck}

NT   FL Cat

116kDa —
97kDa —   —Hsp90

45kDa —   —p50^{cdc37}

66kDa —

—[^{35}S]H_6-FL-p56^{lck}

45kDa —

31kDa —   —[^{35}S]H_6-Cat
21kDa —

1   2   3

80
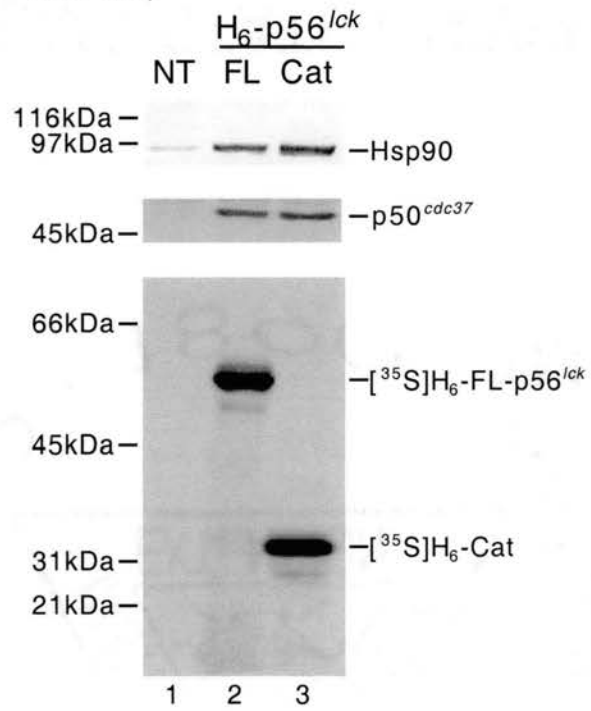
Figure 13. Hsp90 and p50^{cdc37} Co-Immunoprecipitate with the N-lobe of the HRI Kinase Domain (Courtesy of Jieya Shao).

Nuclease treated RRL was programmed with the histidine tagged N-lobe of the HRI kinase domain (lanes 1 and 2) or the histidine tagged Heme-binding domain (HBD, lanes 3 and 4) cDNAs and allowed to synthesize protein for 20 minutes at 30 °C in the presence of [^{35}S] methionine to radiolabel proteins. Protein synthesis reactions were then clarified and mixed with goat anti-mouse IgG coupled agarose, which had been prebound with anti-His monoclonal IgG (lane 2 and 4) or with a control non-immune antibody (lanes 1 and 3).

sequence and may allow the N-terminal lobe (N-lobe Figure 13, lane 2) to protrude from the ribosome and interact Hsp90 and p50^{cdc37} before release. More consideration is given in the discussion.

Discussion

The co-translational interaction of Hsp90 and p50^{cdc37} with the ribosome bound HRI kinase (Figure 9) indicates that Hsp90 and p50^{cdc37} play a role in folding some nascent polypeptides while still on the ribosome. This early interaction with Hsp90 and p50^{cdc37} supports the possibility that the Hsp90 chaperone cycle is taking place while the kinase is still being translated. In the traditional Hsp90 cycle model for steroid hormone receptors proteins are initially recognized and folded by Hsp70, and cofactors, then passed to Hsp90, and cofactors, via the dual interacting protein p60^{HOP} (Hsp70/Hsp90 Organizing Protein). The Hsp70-Hop-Hsp90 complex is referred to as the "intermediate" complex. Once Hsp70 and Hop dissociate, Hsp90 and various cofactors form what is called the "mature" or "late" complex (reviewed in [11]). p50^{cdc37} is one of the Hsp90 cofactors that is traditionally reported in "mature" complexes ([46]). Since Hsp70 is also found in the ribosome pellets all of the components are at least present, therefore the Hsp70 may be passing the partially folded kinase to the Hsp90 machinery. Alternatively, the Hsp70 and Hsp90 chaperone machines may represent two alternative independent pathways. Either way this work indicates that Hsp90 folding is not restricted to post-translational events.

The differences these substrates displayed toward Hsp90 machinery interaction (Figure 9) may be attributable to the concept of modular folding. This concept suggests that a protein's sequence is composed of modules that can fold and retain structure and function independently, in a manner similar to how they behave in the context of the full length protein. These modules have most of the same characteristics attributed to protein domains, although the definition of a protein domain has many uses that are not necessarily restricted by structural or functional considerations. For the purpose of folding they are referred to as independent folding units. Large proteins may have many domains each of which is thought to fold largely independent of other domains, although the interaction between domains is very important often representing strategies of regulation of function or complex formation. A comparison of the domain structure of these clients may help explain the differences in interactions. Hartson *et al.* [27] reported that the different domains of the p56^{lck} kinase showed differences in dependence on Hsp90 activity to achieve function. When Hsp90 activity was inhibited during synthesis the SH2 domain, in the context of the full-length protein, folded to a functional structure capable of binding phosphotyrosine peptide. The kinase domain, however, was not active under the same conditions. This dependence is corroborated/supported by the interaction studies of the independently synthesized domains. The kinase domain of both HRI and p56^{lck} is enough to co-immunoprecipitate Hsp90 and p50^{cdc37} (figures 12 and 13). In both proteins, the kinase domain is at the C-terminus representing the last complete domain to emerge from the ribosome, although both have their own unique C-terminal "tail" sequence. Hsp90 interaction with the kinase domain may be sterically hindered by the ribosome complex and may require release from the ribosome. The ribosome complex

can cover as many as 80 amino acids during polypeptide synthesis (reviewed in [165]).

HRI, however, has additional modules reported to interact with Hsp90 machinery. The N-terminal Heme Binding Domain (HBD) interacts with Hsp90 machinery (Figure 13), and is the first domain to emerge from the ribosome and could explain why Hsp90 pellets specifically with the HRI-ribosome complex. HRI also has an extended sequence (called the insertion sequence) that separates the N-terminal and C-terminal lobes of its kinase domain. This sequence has some Hsp70 interacting ability (unpublished observation), and may allow more of the kinase domain to be exposed for Hsp90 binding. Finally HRI also has a longer C-terminal tail following its kinase domain than $p56^{lck}$, which might function as described for the insertion sequence. One or more of these additional modules may allow Hsp90 machinery to bind HRI while still on the ribosome, whereas $p56^{lck}$ appears to interact with Hsp90 machinery mostly through its C-terminal kinase domain.

When results from the ribosome pellet technique (Figure 9) are compared with results from the co-immunoprecipitation technique (Figure 10 and 11) some differences stand out. Figure 10 shows that Hsp90 antibodies are able to co-precipitate nascent chains of firefly luciferase and $p56^{lck}$ even though Hsp90 is not detectable in the ribosome pellets. One explanation is the difference in sensitivity of the two techniques. Figure 9 detection is based on the western blotting of a ribosomal pellet, which is less sensitive than detection of radioactive nascent polypeptides in the chaperone immunoprecipitations of Figures 10 and 11. The amounts of nascent polypeptides co-precipitated by Hsp90 antibodies in the HRI and $p56^{lck}$ reactions are comparable, but Hsp90 is not detected in the ribosomal pellet of $p56^{lck}$. The amount of co-precipitated luciferase nascent polypeptides is considerably less so Hsp90 and $p50^{cdc37}$ may not be detectable in the

luciferase ribosomal pellet. Previous work in our lab indicates that luciferase does not require Hsp90 activity for *de novo* folding in RRL to become an active enzyme, but favors an Hsp90 pathway for refolding after being denatured [174].

Another possibility is that the co-immunoprecipitation of nascent incompletely synthesized luciferase and p56[lck] by the Hsp90 antibodies may be an artifact induced by the premature release of polypeptides from the ribosome. These polypeptides would be in various stages of folding, whether chaperone assisted or not, and represent various folding intermediates. Interactions with molecular chaperones would be expected since chaperones by nature of their cellular function have an affinity for unfolded polypeptides. A specific example of this is the role Hsp90 plays in re-folding denatured firefly luciferase. This is also supported by the observation that puromycin treatment of cultured chicken embryo cells stimulated a stress response inducing synthesis of Hsp70 among other stress proteins [166, 181] probably due to the release of mis-folded polypeptide chains. These interactions would not represent the true *in vivo* folding pathway of the *de novo* polypeptides emerging from the ribosomes. The interpretation of the co-translational interaction between Hsp90 and luciferase is complicated further by the identification of more than one pathway for luciferase renaturation in RRL, although the Hsp90 dependent pathway is kinetically favored [182].

HRI is the only protein we can confidently say interacts with Hsp90 co-translationaly since it is confirmed by both techniques, and since the interactions detected by the traditional co-immunoprecipitation method are questionable due to the known affinities of chaperones for unfolded potentially aggregating pools of proteins. However, HRI is the first example of a specific co-translational Hsp90 client indicating the

86

possibility of others as suggested by Eggers *et al.* [49] and the need to study other Hsp90 co-translational interactions. Initial indications are that simply being an Hsp90 client does not qualify a protein for co-translational interactions. There is also the possibility that other proteins may be identified as Hsp90 clients while on the ribosome but not after co-translational vectorial folding.

The co-translation interaction of all three proteins with Hsp 70 is easier to interpret, and agrees with previous reports that Hsp70 interacts with ribosomes and many nascent polypeptides co-translationally [49, 158, 166, 167, 176]. Based on what is known about the Hsp70 recognition motif a co-translational interaction with all three is not surprising. Rudiger *et al.* [56] characterized the substrate-binding motif of the *E. coli* Hsp70 homologue DnaK by scanning peptide libraries generated from 37 biologically relevant proteins and found an Hsp70 binding motif every 36 to 84 amino acids by scanning. Most of these motifs would normally be buried in the hydrophobic core of the folded protein and not accessible; however, in the case of protein synthesis these sites would be exposed and available for Hsp70 binding and folding. The consensus substrate motif is better characterized for Hsp70 than for Hsp90. Our understanding of the Hsp90 substrate-binding motif is very limited so no predictions about the prevalence of Hsp90 binding sites can be made. However, Nathan *et al.* [171] reported little effect on total cellular protein *de novo* synthesis and folding upon of loss of Hsp90 function in yeast, but the effect on folding of specific known Hsp90 substrates was critical, indicating Hsp90 does not play a critical role in folding of most cellular proteins.

CHAPTER4

CHAPERONE INTERACTIONS WITH THE IMMATURE PROTEIN TYROSINE

KINASE p56^{lck} IN THE RRL MODEL SYSTEM

Introduction

Hsp90 machinery associates with and provides essential functions for several

regulatory proteins including steroid hormone receptors and protein kinases (reviewed in

chapter 1). Of these, the steroid receptor assembly pathway has been the most thoroughly

characterized, and has generated the chaperone cycle model described in chapter 1. This

work indicates that Hsp90 machinery provides essential reiterative maintenance folding

for these receptor transcription factors, keeping them in a conformation capable of

binding hormone. Hsp90 maintains prolonged, although dynamic, associations with these

receptor complexes in the absence of hormone. For this reason receptor complexes can be

isolated an characterized with less consideration for time than other complexes formed

with proteins that only interact during *de novo* folding, such as p56^{lck}. Some of the Hsp90

client kinases also have prolonged maintenance interactions dependent on regulatory

stimuli. In this way both steroid hormone receptors and client kinases such as HRI are

similar. Prior to maintenance these substrates also depend on Hsp90 for *de novo* folding,

which is defined in different ways. For HRI, early folding intermediates interacting with

Hsp90 machinery are not active and cannot be activated by normal stimuli (NEM and

heme deficiency). Upon longer incubation of the complex, and inferred folding, Hsp90-

associated HRI matures into a conformation that can be stimulated to become an active kinase [172].

Other Hsp90 clients appear to interact only during maturational *de novo* folding. Hsp90 associates with certain immature kinases, and the importance of this native association is implied from the effects of GA on stability of the immature protein's structure and activity [101, 117, 127, 139, 183]. A specific example of this is the p56^{lck} kinase. Immature inactive p56^{lck} synthesized *in vitro* interacts with Hsp90,and p56^{lck}/Hsp90 hetrocomplexes are stable in the presence of high salt. However, in the presence of GA, p56^{lck}/Hsp90 heterocomplexes are salt labile and the kinase is more sensitive to protease [27]. This also agrees with the results in chapter 2 showing a rapid degradation of newly synthesized p56^{lck} in T cells treated with GA.

A third group of Hsp90 clients can be defined by their dependence on Hsp90 as well. This group includes retrovirus-encoded oncogene products, such as v-src, v-fps, v-yes, and v-fes, which were some of the earliest identified Hsp90 substrates [94]. Later these kinases were identified as mutant forms of cellular kinases, such as p60^{c-src}. Initially it was not clear whether the cellular kinases interacted with Hsp90. It is now being realized that the mutant kinases have a prolonged interaction with and continued maintenance dependence on Hsp90, in comparison to their cellular counter-parts [27, 139]. This makes the Hsp90 interaction more readily detectable and may explain the initial confusion over Hsp90's role in the cellular "wild-type" kinase folding.

As stated, the conditional maintenance folding of steroid receptors has been the most thoroughly characterized of Hsp90 clients; however, the *de novo* maturation of newly synthesized proteins, and how it relates to conditional and continued maintenance

is still poorly understood. One difference identified between two such Hsp90 clients is shown in chapter 3: the co-translational interactions of Hsp70, Hsp90, and p50^{cdc37} with HRI, but not with p56^{lck}. This work was done in RRL, which was also used for many of the characterization studies on steroid receptor assembly [31, 184-186]. Interactions with Hsp70, p60^{HOP}, p48^{HIP}, Hsp90, FKBP51 and 52, Cyp40, and p23 were reported. The same components were associated with the recombinant Fes kinase and the Heat-shock transcription factor [45]. In order to study *de novo* maturational folding, a system for specifically generating nearly uniform pools of substrate protein in the presence of the chaperone machinery was needed. Since we also wanted to compare the results to the work done on steroid receptors in RRL, the *in vitro* coupled transcription-translation system of nuclease treated RRL was chosen. In addition *in vitro* translation allowed us to label our client with radioactive amino acids enabling very sensitive detection of client p56^{lck}. Here we report the interactions of several chaperones and their co-chaperone partners specific to immature p56^{lck} kinase.

Materials and Methods

Materials

All cDNAs to be transcribed *in vitro* were cloned in to a modified pSP64T plasmid with an SP6 RNA polymerase promoter [173] as previously described [138]. Cloned cDNAs were: wild type p56^{lck}; mutant p56^{lck} in which the codon for the regulatory 505 tyrosine was replaced with the codon for phenylalanine (F505); mutant p56^{lck} in

90

which the codon for the active site 273 lysine was replaced with the codon for arginine (R273); catalytic domain in which only the sequence for the catalytic domain (Cat) of p56^{lck} (residues 238-509); N-lobe containing only the sequence corresponding to the N-terminal lobe of the catalytic domain of p56^{lck} (residues 238-323); C-lobe containing only the sequence corresponding to the C-terminal lobe of the catalytic domain of p56^{lck} (residues 316-509); HRI N-lobe containing only the sequence corresponding to the N-terminal lobe of the catalytic domain of HRI (residues 154-231); and heme-binding domain (HBD) containing the sequence corresponding to the heme-binding domain of HRI (residues 1-153).

L-[^{35}S]-methionine and [γ-^{32}P]ATP were purchased from DuPont-NEN. Geldanamycin (GA) was provided by the Drug Synthesis and Chemistry Branch, Developmental Theraputics Program, Division of Cancer Treatment, National Cancer Institute and was prepared in DMSO (Sigma). Clofibric acid (ClA) was purchased from Sigma Chemical Co. (St. Louis, MO.) and was prepared in H$_2$O by adjusting the pH with 1 M KOH until only a little ClA was left undissolved. Sodium molybdate (Na$_2$(MoO$_4$)) was purchased from Sigma and was prepared as a 1 M stock in H$_2$O. Bovine serum albumin (BSA) and reduced carboxy-methylated-BSA (RCM-BSA) were purchased from Sigma and prepared in H$_2$O. Peptide-φ (pep-φ FYQLALT) was synthesized by the Sarkey's Biotechnology Research Laboratory (OSU) and purified by reverse-phase chromatography on a C18 column at the Molecular Biology Resource Facility (University of Oklahoma Health Sciences Center, UOHSC). Purity and concentration was analyzed by MALDI-mass spectroscopy and by quantitative amino acid analysis using β-(thienyl)-DL-alanine as an internal standard. Purity was determined to be > 98%. Anti-

penta His monoclonal antibodies were purchased from Qiagen. Antibodies for Hsp90, p50^{cdc37}, and p56^{lck} were prepared by the Hybridoma Center for the Agricultural and Biological Sciences (OSU) as ascites fluid from mice immunized with recombinantly purified H$_6$p50^{cdc37} and H$_6$p56^{lck}, or with Hsp90 purified from RRL [46, 187]. Other antibodies used include: non-immune control mouse IgG from the MOPC-21 hybridoma (Sigma); N27 anti-Hsp70 mouse monoclonal IgG was purchased from StressGen; EC1 anti-FKBP52 mouse monoclonal IgG was provided by Dr. Lee Faber [188]; anti-cyp40 rabbit polyclonal antibody against the C-terminus was purchased from Affinity BioReagents (PA3-O22); JJ3 and JJ5 anti-p23 mouse monoclonal antibodies were provided by Dr. David Toft [84]; goat anti-mouse IgG (for making immunoresin) and alkaline phosphatase conjugated goat anti-mouse and anti-rabbit IgG (secondary antibodies for western-blotting) were purchased from Jackson Immunoresearch Laboratories. Nitro blue tetrazolium (NBT), 5-bromo-4-chloro-3-indolyl phosphate (BCIP), and p-nitrophenyl-chloro-formamide activated agarose were purchased from Sigma Chemical Co. (St. Louis MO.). Goat anti-mouse IgG was coupled to agarose as previously described [189]. Enolase for p56^{lck} kinase assays was purchased from Sigma and prepared as described by Cooper *et al.* [190] in enolase denaturation buffer (EDB-50mM NaOAc/HOAc pH 3.3) and denatured at 30 °C for 5 minutes prior to mixing with kinase assay components.

In vitro coupled transcription/translation in rabbit reticulocyte lysate

pSP64T plasmids containing the indicated cDNAs were transcribed and translated in coupled reactions containing ~70% (v/v) micrococcal nuclease treated rabbit

reticulocyte lysate (prepared as described in [191]). Other components and final concentrations are as follows: 7.8% (v/v) deionized distilled H_2O, 19.17% (v/v) TnT buffer [0.052 M creatine phosphate (Sigma), 0.0052 M dithiothreitol (BioWorld), 0.0157 M $Mg(OAc)_2$, 0.574 M KOAc (Sigma), 0.1 mM amino acid pool (-methionine), 4.177 mM γ-NTP pool (Boehringer Mannheim), 2.79 mM Tris-HCl (Sigma) to adjust pH to 7.3]; 0.04 μg/μl pSP64T plasmid cDNA; 0.02% (v/v) SP6 RNA polymerase (Promega); and 0.1 μCi [^{35}S] methionine. Reactions were mixed either by pipeting up and down and stirring with the pipet tip or by gently vortexing with a variable speed vortex so as not to introduce bubbles. After reactions were assembled on ice they were transferred to either 30 or 37 °C water baths (as indicated) for the indicated times. For reactions where re-initiation of protein synthesis was stopped, 60 μM aurintricarboxylic acid (ATA) was added and mixed by pipeting up and down and stirring with the pipet tip. Geldanamycin treatment was performed, when possible, concurrently with coupled transcription/translation reactions since treatment does not affect protein synthesis in this system. However, when clofibric acid, pepϕ, BSA, RCM-BSA, or heat shock (HS) was used, treatments were restricted to after re-initiation was inhibited and polyribosomes were allowed to run off, since most of these inhibit protein synthesis if initiated before synthesis was completed. Drugs, peptides, or proteins were added directly to protein synthesis reactions; however, heat shock treatment was conducted by transferring the tube to a water bath at 42 °C for the indicated time.

Immunoadsorptions

Antibodies against p56^{lck}, penta-His epitope tags, FKBP52 (EC1), or p23 (JJ3 and JJ5) were prebound to 15 μl (packed volume) of agarose resin conjugated with goat anti-mouse IgG antibodies, and washed once with 10 mM PIPES (pH 7.0), 50 mM NaCl, once with 10 mM PIPES (pH7.0), 500 mM NaCl, and twice with 10 mM PIPES (pH 7.0), 50 mM NaCl. Washed immunoresins were mixed on ice for 1-2 hours with 30-50 μl protein synthesis reactions (as indicated) which had been chilled and clarified by a 5 minute spin at 10000-14000 x g at 4 °C. After mixing, immunoresins were washed 5 times with 10 mM PIPES (pH 7.0), 0.05-0.5% Tween-20, and the indicated concentrations of NaCl and/ or sodium molybdate. Absorbed materials were eluted by boiling for 5 minutes in SDS-PAGE sample buffer and separated by SDS-PAGE. Protein bands were transferred from the gel to PVDF membranes and analyzed by autoradiography or immunoblotting as indicated.

p56^{lck} kinase assays

Mature or nascent [^{35}S] labeled p56^{lck} was immunoprecipitated as stated above and washed 3-4 times with IP wash buffer [50 mM HEPES pH 7.4, 2% (v/v) Triton X-100, 120 mM NaCl, 1 mM sodium vanadate] and 2 times with kinase wash buffer (100 mM PIPES pH 7.0, 10 mM MnCl$_2$). Washed immunoresins were then mixed with kinase assay mix (100 mM PIPES pH 7.0, 10 mM MnCl$_2$, 100 μg denatured enolase (2 μg/μl) 10-50 μM nonradioactive ATP, and 10-15 μCi [γ-^{32}P]ATP) in a room temperature H$_2$O bath for 6 minutes. Kinase reactions were stopped by addition of boiling SDS-PAGE

sample buffer. Samples were separated by SDS-PAGE, transferred to PVDF membranes, and analyzed by autoradiography.

Results

Chaperone interactions with immature p56^{lck} kinase client.

Previous work done with the progesterone receptor (PR) ([31, 45, 192] and reviewed in chapter 1) found PR to initially form a complex with Hsp70 and Hsp40, and proceed through a dynamic cycle of chaperone interactions necessary to keep the receptor in a state competent to bind hormone. In similar fashion, many of the same components were found complexed with the estrogen receptor, the aryl hydrocarbon receptor, and the Fes tyrosine kinase [45]. In order to compare p56^{lck} interactions with those reported for the steroid hormone receptors and the Fes kinase as well as extend those characterizations, we modeled p56^{lck} folding in nuclease treated RRL.

Rabbit reticulocyte lysate is a cell free system of mammalian origin in which controlled protein synthesis can be conducted. Rabbit reticulocyte lysate is also rich in chaperones and can generate active folded proteins of many types. The previous chapter reported the different co-translational interactions of three different protein substrates with chaperones. Here we further characterized post-translational interactions between the kinase p56^{lck} and molecular chaperones. In order to determine whether p56^{lck} interacted with chaperones after translation, protein synthesis in RRL was performed in the absence of puromycin. Protein synthesis generally shuts off in RRL after 15-20 minutes at 37 °C as shown in Figure 14. Incorporation of [^{35}S] methionine plateaued after

Figure 14. Protein Synthesis in RRL at 37 °C.

Nuclease treated RRL was programmed with (•) or without (○) p56^{lck} cDNA and incubated in a 37 °C water bath for 30 minutes in the presence of [^{35}S] methionine to radiolabel newly synthesized p56^{lck}. 1 μl of RRL was spotted on to filter paper at the indicated times and precipitated in 10% TCA. Filter papers were washed, bleached with 15% hydrogen peroxide, and submerged in liquid scintillation cocktail for counting
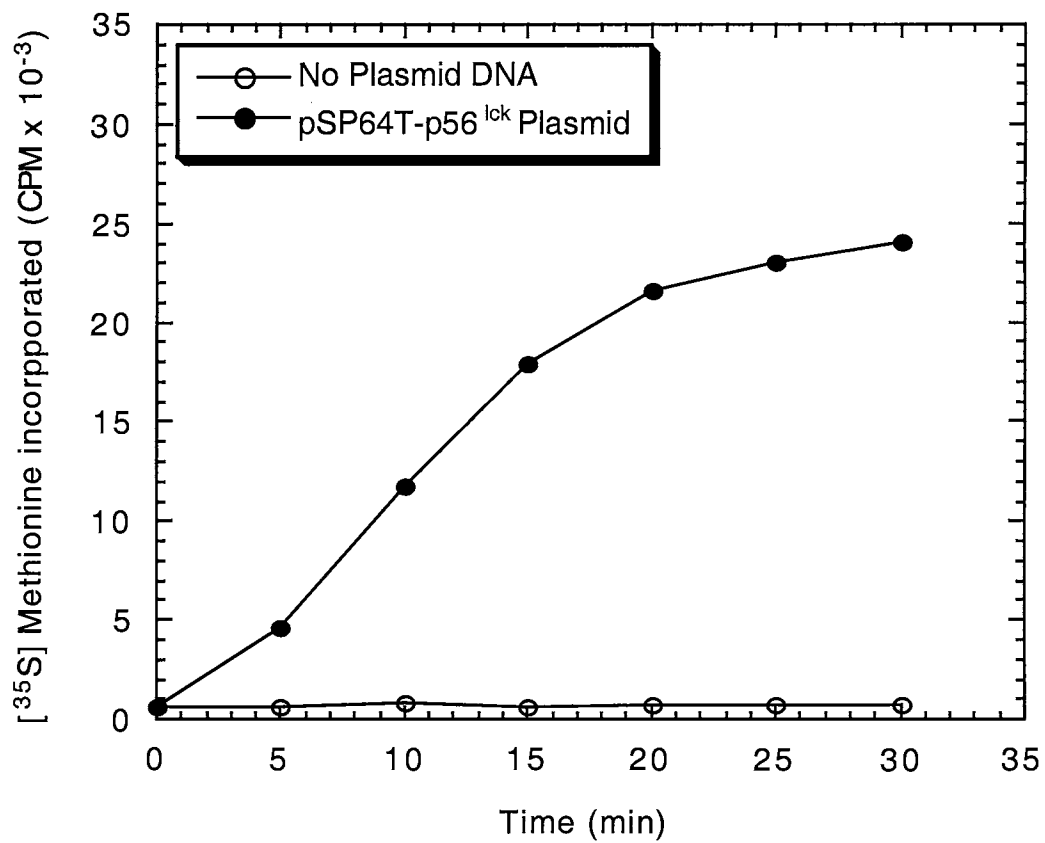
20 minutes of synthesis at 37 °C. To detect very early post-translational interactions with p56^{lck}, nuclease treated RRL was programmed with plasmid DNA containing cDNA encoding full-length p56^{lck}. Synthesis was conducted for 20 minutes at 37 °C and an aliquot of the synthesis reaction was immediately immunoprecipitated with anti-p56^{lck} antibodies (Figure 15, lanes 1 and 2). The remainder of the protein synthesis reaction was incubated for 1 hour at 37 °C and then immunoprecipitated (Figure 15, lanes 3 and 4). As can be seen in the autoradiogram (bottom panel labeled [^{35}S] p56^{lck}) only full-length p56^{lck} was captured. Chaperones that co-absorbed with p56^{lck} were eluted and separated by SDS-PAGE. Hsp90, Hsp70, and p50^{cdc37} all co-immunoprecipitate with p56^{lck} after 20 minutes of synthesis, and after an hour incubation at 37 °C the quantity of these chaperones dramatically dropped (Figure 15, lane 2 versus lane 4 and Figure 16, lanes 3 and 4 versus lanes7 and 8). The temporal chase of Hsp90 has been reported for p56^{lck} [174]; however, the interactions of Src family kinases with Hsp70 have not been well characterized. The importance of Hsp90 function for temporally immature p56^{lck} during biogenesis is also shown by GA inhibition of p56^{lck} kinase activity ([27]; and Figures 19 and 20, lane 5 in both). Hsp90 chaperone complexes with substrates and co-chaperones are often stabilized by addition of molybdate during immunoprecipitation. Molybdate stabilizes the Hsp90 complexes to high ionic strength [24, 25]; however, the kinase complex shown in Figure 15 is stable to washes in high ionic strength (0.5 M NaCl) buffers even in the absence of stabilizing agents (Figure 16, lane 4). These results indicate that Hsp90 and p50^{cdc37} form a complex with newly synthesized p56^{lck} that is stable in 0.5 M salt, but not with mature p56^{lck} (Figure 16, lanes 7 and 8). This complex

Figure 15. Time Course of Chaperone Interactions with Wild Type p56^{lck} Kinase.

Nuclease treated RRL was programmed with (+, lanes 2 and 4) or without (-, lanes 1 and 3) p56^{lck} cDNA and allowed to synthesize protein for 15 minutes at 37 °C in the presence of [^{35}S] methionine to radiolabel newly synthesized p56^{lck}. Aliquots of the protein synthesis reactions were immediately clarified and mixed with goat anti-mouse IgG coupled agarose, which was prebound with mouse anti-p56^{lck} (lanes 1 and 2). The remainder of the protein synthesis reactions was incubated for 1 hour at 37 °C and then immunoprecipitated as described above (lanes 3 and 4). Proteins bound to the immunopellets were eluted with sample buffer and separated by SDS-PAGE. Gels were electro-transferred to PVDF membranes and immunoblotted with the indicated antibodies [anti-Hsp90 (OSU mouse ascites fluid), anti-Hsp70 (N27), or anti-p50^{cdc37} (OSU mouse ascites fluid) as indicated on the right side of the panel]. [^{35}S]p56^{lck} was detected by autoradiography (see bottom panel labeled [^{35}S]p56^{lck} on the right side of the panel). The location of the molecular weight standards is marked on the left side of the panel.

(IP p56*lck*)

	0 min	60 min
p56*lck*	− +	− +

97kDa— ——Hsp90

66kDa— ——Hsp70

—p50*cdc37*

—[³⁵S]p56*lck*

1 2 3 4
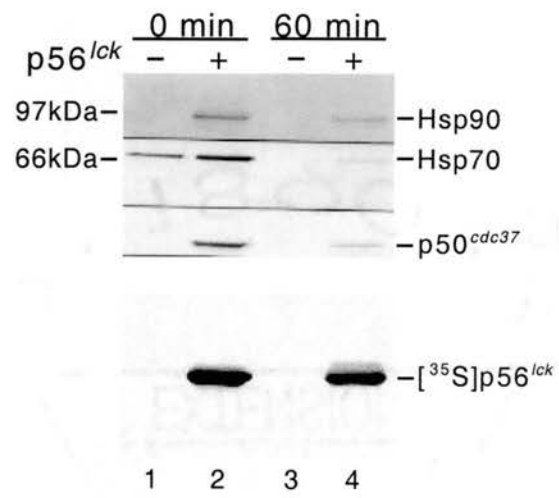
Figure 16. Salt-stable Association of Hsp90 and p50^{cdc37} with p56^{lck} Maturation Intermediates.

Nuclease treated RRL translation reactions were (lanes 3, 4, 7, and 8), or were not (lanes 1, 2, 5, and 6) programmed with p56^{lck} cDNA. After 25 minutes of synthesis in the presence of [^{35}S] methionine, reinitiation was inhibited with ATA (60 μM) and reactions were either immediately immunoabsorbed with anti-p56^{lck} antibodies (lanes 1-4) or incubated further (chase) for 60 minutes (lanes 5-8) prior to immunoabsorption. Immunopellets were washed with buffers containing 0.5 M NaCl (labeled H even-numbered lanes) or without (labeled L, odd-numbered lanes). [^{35}S]p56^{lck} was detected by autoradiography (see middle panel, labeled [^{35}S]p56^{lck} on the left side of the panel). Hsp90 and p50^{cdc37} were detected by immunoblotting with anti-Hsp90 or anti-p50^{cdc37} antibodies (see left side of the panels). First lane (rrl std), naïve lysate loaded as a standard for detection of chaperones.

(IP p56^lck)

	rrl std	1	2	3	4	5	6	7	8
hsp90 –									
[35S]p56^lck –									
p50^cdc37 –									
lck template		–	–	+	+	–	–	+	+
salt wash		L	H	L	H	L	H	L	H
chase time				0 min				60 min	
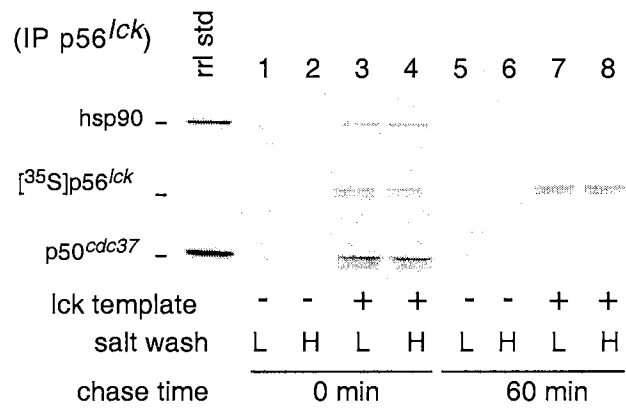
with p56^{lck} kinase is different than the salt labile complex Hsp90 and p50^{cdc37} form in the absence of substrate kinases [46].

We were interested in determining the effects of chaperone binding drugs on substrate kinase chaperone complexes. As stated in Chapter 1, GA binds to Hsp90 in the ADP bound conformation and as shown in Chapter 2, GA treatment depletes cellular levels of p56^{lck} from T cells and disrupts the salt stable interaction of Hsp90 with newly synthesized p56^{lck} synthesized in RRL [26]. To extend the characterization of the effects of GA treatment to the Hsp90 co-chaperone p50^{cdc37} and the fellow chaperone Hsp 70, we treated RRL's translating p56^{lck} with GA. The salt stable chaperone complex formed with p56^{lck} was destabilized in the presence of high salt (Figure 17, lane 6 versus lane 8). Interestingly, even when the complex was washed with low salt buffer (0 M) the p50^{cdc37} component was lost and the amount of Hsp90 captured was reduced (Figure 17, lane 4). However, when p50^{cdc37} was captured out of GA treated RRL in the absence of kinase the complex with Hsp90 was not affected; although, it is important to emphasize that this complex is much more salt labile in the absence of kinase [46].

Hsp70 has a functional interaction with newly synthesized p56^{lck}.

The Hsp70 component of the kinase complex was examined similarly with the treatment of chaperone binding drugs. Geldanamycin was used again and the Hsp70 binding drug clofibric acid (ClA) was included in the study. Clofibric acid has been reported to disrupt Hsp70 interactions with HRI affecting its regulation of HRI kinase activity [179]. A loss of p50^{cdc37} can be seen with GA treatment (Figure 18, lane 4-control versus lane 8) and a little loss of Hsp90, since this was done at 150 mM salt. In contrast

Figure 17. Kinase-Chaperone Heterocomplexes Formed in the Presence of Geldanamycin.

Nuclease treated RRL was programmed with (+, even-numbered lanes) or without (- odd-numbered lanes) H_6-p56^{lck} cDNA and allowed to synthesize protein with [^{35}S] methionine briefly in the presence (+, lanes 3, 4, 7, and 8) or absence (-, lanes 1, 2, 5, and 6) of geldanamycin. After synthesis RRLs were immunoadsorbed with antibodies against the penta-His peptide and washed with (lanes 5-8) or without (lanes 1-4) 0.5 M NaCl. Immunocomplexes were analyzed by western blotting to detect Hsp90, p50^{cdc37} (marked on the left side of the panel), or autoradiography to detect [^{35}S] labeled H_6-p56^{lck} (bottom panel marked [^{35}S]H_6-p56^{lck} on the left side of the panel). The location of the molecular weight standards (kDa) is marked on the right side of the panels. Antibody heavy chains were eluted from the immunoresins as well and are also marked on the left side of the panels (ab hc).

(IP anti-His)

Hsp90 —   - 97
                                           - 66
ab hc —
p50 *cdc37* —   - 45

[^{35}S]H$_6$p56^{lck} —

p56^{lck} template   - + - +   - + - +
geldanamycin   - - + +   - - + +
                      _____   _____
                        low salt   high salt
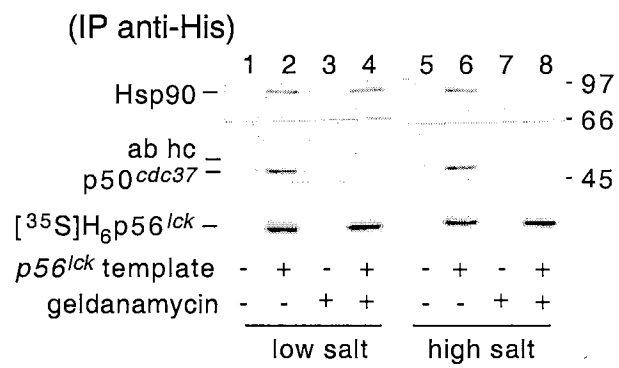
Figure 18. Drug Effects On Chaperone Interactions with p56^{lck} Kinase.

Nuclease treated RRL was programmed with (+, lanes 2, 4, 6, 8, and 10) or without (-, lanes 1, 3, 5, 7, and 9) p56^{lck} cDNA and allowed to synthesize protein for 8 minutes at 37 °C in the presence of [^{35}S] methionine to radiolabel newly synthesized p56^{lck}. Initiation of protein synthesis was inhibited with ATA (60 μM) and synthesis of initiated messages was completed by a 5 minute incubation at 37 °C. RRLs were separated into equal aliquots and treated without (lanes 1 and 2) or with DMSO (control lanes 3 and 4), H$_2$O (control, lanes 5 and 6), geldanamycin (GA lanes 7 and 8), or clofibric acid (ClA, lanes 9 and 10). Immunoprecipitations were washed, eluted with sample buffer, and separated by SDS-PAGE. Proteins were electroblotted on PVDF and immunoblotted with the indicated antibodies [marked on the right side of the panel: anti-Hsp90 (OSU mouse ascites fluid), anti Hsp70 (N27), or anti-p50^{cdc37} (OSU mouse ascites fluid)]. [^{35}S] labeled p56^{lck} was detected by autoradiography (marked on the right side of the panel). The location of the molecular weight standards is marked on the left side of the panel.

(IP anti-His)

	NT		DMSO		H₂O		GA		CIA	

97kDa– ...... −Hsp90
66kDa– ...... −Hsp70
...... −HC
45kDa– ...... −p50^{cdc37}

−[^{35}S]H$_6$p56^{lck}

1   2   3   4   5   6   7   8   9   10
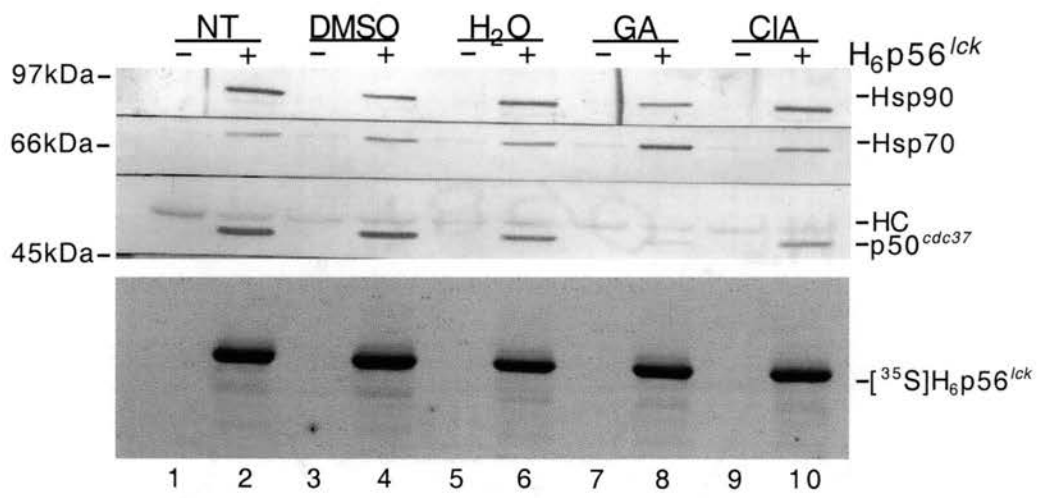
the amount of Hsp70 increased by 3 fold (Figure 18, lane 4-control versus lane 8). The levels of chaperones binding p56^{lck} upon ClA treatment were not affected (Figure 18, lane 6-control versus lane 10). It is thought that blocking the function of Hsp90, as done with GA treatment, causes an accumulation of Hsp70 on substrate due to an inability to pass from Hsp70 to Hsp90 during its normal chaperone mediated folding pathway. This is supported by our observation that more Hsp70 co-adsorbs with p56^{lck} in GA treated lysate. Our inability to inhibit Hsp70 binding to p56^{lck} could be due a difference in our observed interaction and that reported for HRI. It could also indicate that Hsp70 interacts with newly synthesized p56^{lck} in a nonspecific manner and does not represent an important functional component of the complex.

In order to test whether Hsp70 was a functional chaperone component of p56^{lck} biogenesis, the kinase was synthesized in RRL and treated with ClA. As shown for the interaction of p56^{lck} and Hsp70, the mature kinase does not interact with Hsp70 (Figure 15, lane 4) suggesting that the mature kinase does not need Hsp70. Treatment of p56^{lck} with either ClA or GA (a positive control) resulted in a 78% or 54% decrease in kinase activity (Figure 19, lanes 4 and 5 respectively), as measured by phosphorylation of the exogenous substrate denatured enolase. Autokinase activity measured by phosphorylation of p56^{lck} itself resulted in similar inhibition (Figure 20). A comparison of inhibition of nascent versus mature p56^{lck} kinase activity showed the mature kinase only lost 16% of its activity when treated with ClA (Figure 19, lane 2 versus 6) and 6% of its activity when treated with GA (Figure 19, lane 3 versus 7). This correlates with the interaction data and suggests that the mature p56^{lck} kinase is much less dependent on Hsp70 and Hsp90 for function. Clofibric acid has other actions in addition to binding Hsp70, such as binding to
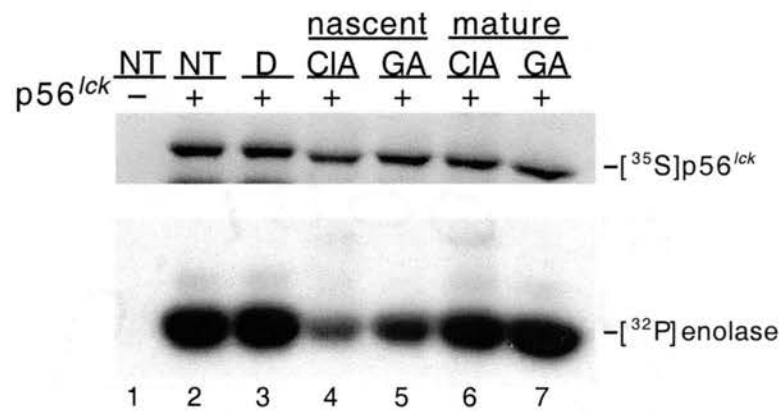
Figure 19. Drug Effects on p56^{lck} Kinase Activity.

Nuclease treated RRL was programmed with (+ lanes 2-7) or without (- lane 1) p56^{lck} cDNA and allowed to synthesize protein for 12 minutes in the presence of [^{35}S] methionine to radiolabel newly synthesized p56^{lck}. Initiation of protein synthesis was inhibited with ATA (60 μM) and ribosomes were allowed to run off for 5 minutes at 37 °C. Protein synthesis reactions were separated into "nascent" and "mature" fractions. Nascent fractions were treated without (lanes 1 and 2) or with 1% DMSO (lane 3), 15 mM clofibric acid (ClA, lane 4), or 89 μM geldanamycin (GA, lane 5) for 30 minutes at 37 °C. Mature fractions were incubated for 30 minutes followed by a 10 minute treatment with either 15 mM ClA (lane 6) or 89 μM GA (lane 7). Fractions were then clarified and mixed with anti-IgG coupled agarose prebound with anti-p56^{lck} antibodies for 1 hour on ice. Immunoprecipitations were washed and kinase activity assayed with [γ-^{32}P]ATP and enolase as described in material and methods. Phosphorylated proteins were eluted and separated by SDS-PAGE and transferred to PVDF. Membranes were dried and exposed to autoradiography film. The location of the [^{35}S]p56^{lck} band is marked on the right side of the upper panel and the location of the [^{32}P]enolase band is marked on the right side of the upper panel.

109

(IP p56*lck*)

NT NT D CIA GA CIA GA

nascent   mature

p56*lck* − + + + + + +

−[³⁵S]p56*lck*

−[³²P]enolase

1 2 3 4 5 6 7

the Peroxisome Proliferator-Activator Receptor α (PPAR-α) [193-199], therefore other

Hsp70 modulating agents and conditions were tested for effects on p56^{lck} kinase activity.

First, the specific Hsp70 binding peptide termed peptide φ (pepφ), based on high affinity

binding peptides identified by phage display libraries [200] and closely resembling the

motif Hsp70 recognizes in substrates [201]. Second, reduced carboxy-methylated bovine

serum albumin (RCM-BSA) imitates the structure and chemistry of denatured proteins

recognized by Hsp70 during stress condition such as heat shock. Lastly, heat shock itself

was also induced in the RRL system by incubating the lysate at 42 °C for 10 minutes.

Pepφ provided the most inhibition of all the conditions that modulate Hsp70 function,

inhibiting 75% of the autokinase activity and 59% of the enolase phosphorylating activity

(Figure 20, lane 2 versus 6). Only GA treatment provided more inhibition, 77% and 65%

inhibition of the autokinase and enolase phosphorylating activitiy (Figure 20, lane 4

versus 5). Both RCM-BSA and heat shock (HS) inhibited p56^{lck} auto-kinase activity by

37% and 72% respectively (Figure 20, lanes 8 and 9). These results further support the

importance of Hsp70 in folding and biogenesis of an active p56^{lck} kinase.

Previous work presented by our laboratory has shown that the constitutively

active transforming mutant kinase p56^{lck}F505, in which the regulatory tyrosine at position

505 is mutated to a phenylalanine, has a prolonged and greater dependence on Hsp90

function at 37 °C than does the wild type p56^{lck} kinase. In order to test whether this

dependence of the mutant p56^{lck}F505 kinase on Hsp90 for maintenance of kinase activity

at physiological temperatures corresponded with a greater dependence on Hsp70 we

assayed kinase activity in the presence and absence of drugs. The mature wild type p56^{lck}

kinase showed no disactivation of its enolase phosphorylating activity in the presence of

111

Figure 20. Effects of Hsp70 Modulators on p56^{lck} Kinase Activity.

Nuclease treated RRL was programmed with (+ lanes 2-10) or without (- lane 1) p56^{lck} cDNA and allowed to synthesize protein for 10 minutes at 37 °C in the presence of [^{35}S] methionine to radiolabel newly synthesized p56^{lck}. Initiation of protein synthesis was inhibited with ATA and ribosomes were allowed to run off for 4 minutes at 37 °C. Protein synthesis reactions were separated into equal aliquots and matured in the presence of H$_2$O (Con, lane 2), 15 mM clofibric acid (ClA, lane3), 1% DMSO (lane 4), 89 μM geldanamycin (GA, lane 5), 0.5 mM peptide ϕ (pepϕ lane 6), 1.5 mg/ml bovine serum albumin (BSA, lane 7), 1.5 mg/ml reduced carboxy methylated-BSA (RCM-BSA, lane 8), or in RRL at the heat shock temperature of 42 °C (HS, lane 9). Fractions were then clarified and mixed with anti-IgG coupled agarose prebound with anti-p56^{lck} antibodies and assayed for kinase activity as described above. A fraction of the untreated p56^{lck} was treated with 15 mM ClA during the kinase assay as a control (lane 10). The location of [^{35}S]p56^{lck} is labeled on the right side of the top panel. The location of [^{32}P]p56^{lck} is marked on the right side of the middle panel. The location of [^{32}P]enolase (exogenous substrate) is marked on the right side of the bottom panel.
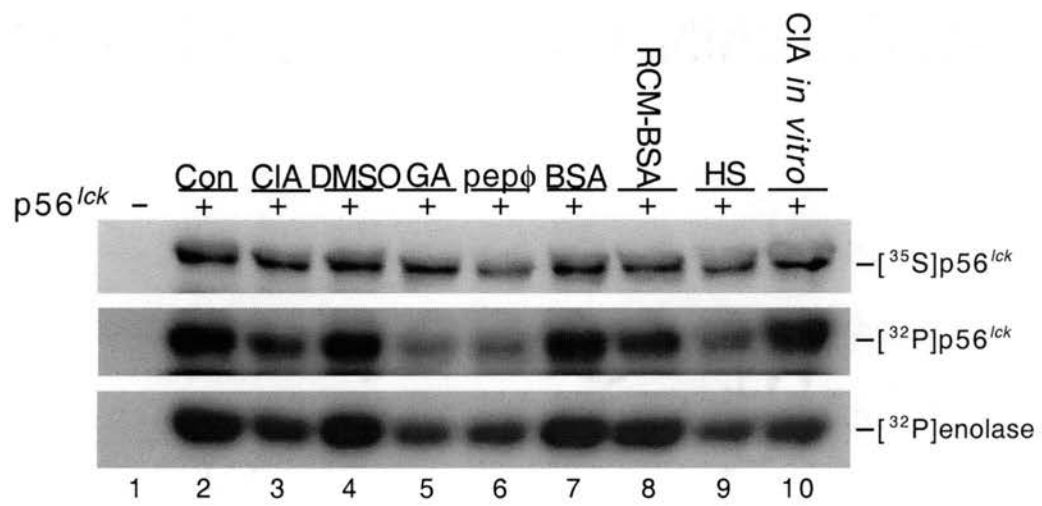
ClA or GA (Figure 21A, bottom band lanes 2-5). A little (21%) of the wild type p56^{lck}

autokinase activity was inhibited by ClA but not by GA treatment (Figure 21A, top band

lane 3 versus 4 and lane 2 versus 5). In contrast to their effects on wild type p56^{lck}, both

ClA and GA treatment decreased the ability of the p56^{lck}F505 mutant to phosphorylate

enolase by 97% and 56% respectively (Figure 21A, lane 7 versus 8 and lane 6 versus 9).

This result indicates that the p56^{lck}F505 mutant kinase depends on both Hsp70 and Hsp90

to maintain kinase activity at physiological temperatures.

Kinase activity is not essential for chaperone interactions.

Figure 21 showed that the chaperone dependence of a constitutively active kinase

mutant was greater than that of the regulated wild type kinase. Two possible reasons for

this greater dependence on chaperones Hsp70 and Hsp90 are addressed here. One is that

the active kinase may be the preferred conformation recognized by the chaperone

machinery, probably due to instability in the structure. Alternatively, the regulatory

phosphorylation site in the C-terminal tail may inactivate the kinase and thereby add

stability to the kinase allowing it to mature to an Hsp90 independent state. The first

reason would predict that an inactive kinase should not interact with chaperones and the

second reason would predict an inactive kinase should not mature to an Hsp90

independent state. In order to test these predictions another p56^{lck} kinase mutant was used

in which the active site lysine (K) 273 was conservatively mutated to an arginine (R).

This mutant is inactive as a tyrosine kinase (reviewed in [202]). A time course

experiment as described for Figures 15 and 16 was conducted and the presence of Hsp90

and p50^{cdc37} in immature and mature kinase complexes was examined by western blotting.

Figure 21. Disactivation of Wild Type and F505 p56^{lck} Kinase by Clofibric Acid and GA.

(A) Nuclease treated RRL was programmed without (- lane 1) or with wild type (wt lanes 2-5) or F505 (lanes 6-9) p56^{lck} cDNA and allowed to synthesize protein for 20 minutes at 37 °C in the presence of [^{35}S] methionine to radiolabel newly synthesized p56^{lck}. Initiation of protein synthesis was inhibited with ATA, ribosomes were allowed to run off, and wild type or mutant kinase was matured for 1 hour at 37 °C. Protein synthesis reactions were separated into equal aliquots and treated with 1% DMSO (lanes 2 and 6), H$_2$O (lanes 3 and 7), 15 mM ClA (lanes 4 and 8), or 89 μM GA (lanes 5 and 9) for 1 hour at 37 °C. Aliquots were then mixed with anti-IgG coupled agarose prebound with anti-p56^{lck} antibodies and assayed for kinase activity as described above. The location of the [^{32}P]p56^{lck} band and the [^{32}P]enolase band are marked on the right side of the panel. (B) A fraction of the immunopellet that was used for each kinase assay was separated on another gel to show equal amounts of [^{35}S] kinase were used in the kinase assay. Lanes 1, 3, 5, and 7 show [^{35}S] wt p56^{lck} and lanes 2, 4, 6, and 8 show [^{35}S] F505 mutant kinase input into the different kinase assays. (The [^{35}S]p56^{lck} band or bands are marked on the right side of the panel.) The different drug treatments for each immunopellet are labeled above the lanes: DMSO (lanes 1 and 2), H$_2$O (lanes 3 and 4), ClA (lanes 5 and 6), and GA (lanes 7 and 8).

116
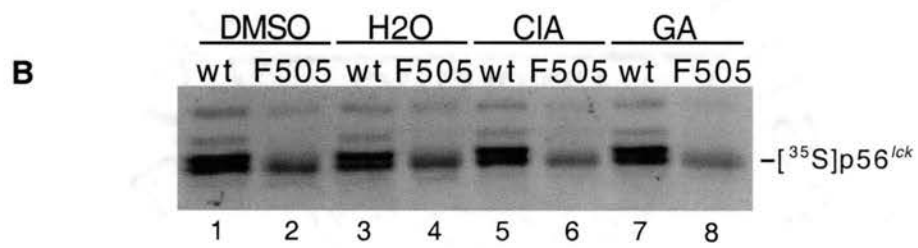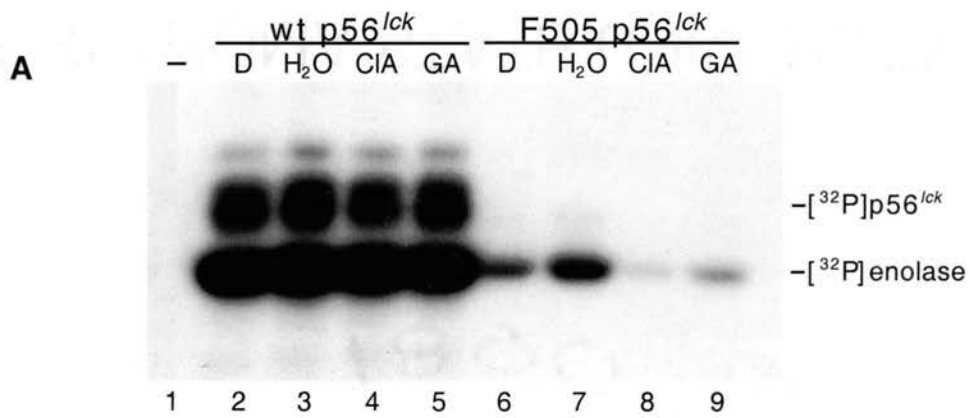
Both Hsp90 and p50^{cdc37} formed a complex with the immature kinase (Figure 22 lane 2) and chased off the mature kinase within 60 minutes, as shown for wild type p56^{lck} (Figure 22 lane 4). This indicates that kinase activity is not the sole requirement for chaperone interactions.

Other componenets of the immature p56^{lck} kinase chaperone complex.

We have identified Hsp70, Hsp90, and p50^{cdc37} as dynamic functional components necessary for the biogenesis of an active p56^{lck} kinase. Other components of the Hsp90 chaperone machinery reported to interact with steroid receptors and some protein kinases (p60^{v-src}, Raf, and Fes) include FKBP52, Cyp40, and p23 [45, 95, 203]. However, there is some disagreement as to whether the TPR containing immunophilins are part of the kinase chaperone complex [43, 44]. To determine whether the p56^{lck} chaperone complexes contain these components histidine tagged p56^{lck} was synthesized in RRL and immunoadsorbed using an anti-pentaHis antibody. It was found that adding the sequence for a six residue histidine tag to the 5'-end of the p56^{lck} cDNA increased the translation efficiency and allowed for the generation of more kinase, and therefore better detection of co-adsorbing proteins. The mechanism of the increase in translation efficiency is unknown. Figure 23 shows the autoradiogram and the immunostained membrane of the samples eluted from the immunoprecipitation of H$_6$- p56^{lck}. Both low salt (no salt: Figure 23, lanes 7-12) and high salt (0.5 M: Figure 23, lanes 1-6) washes were done and both GA (Figure 23: lanes 3, 4, 9, and 10) and MoO$_4$ (Figure 23, lanes 5, 6, 11, and 12) were included in the characterization. As shown in the low salt samples, the immunophilins Cyp 40 and FKBP52 were brought down in the complex (Figure 23, lane 8); however,

Figure 22. Time Course of Chaperone Interactions with Kinase Inactive R273 p56^{lck} Mutant.

Nuclease treated RRLs were programmed with (+, lanes 2 and 4) or without (-, lanes 1 and 3) p56^{lck}-R273 cDNA and allowed to synthesize protein for 20 minutes at 37 °C in the presence of [^{35}S] methionine to radiolabel newly synthesized mutant p56^{lck}. Aliquots of protein synthesis reactions were immediately clarified and mixed with immunoresins (0 min, lanes 1 and 2). In the remainder of the protein synthesis reactions initiation of protein synthesis was inhibited with ATA and mutant p56^{lck} was matured for 60 minutes at 37 °C before immunoprecipitation as described above and in materials and methods (60 min, lanes 3 and 4). R273[^{35}S]p56^{lck} was detected by autoradiography (labeled [^{35}S]p56^{lck}-R273 on the right-hand side of the bottom panel). Hsp90 and p50^{cdc37} were detected by immunoblotting with the appropriate antibodies and are labeled on the right-hand side of the top panel. The antibody heavy chain (HC, location marked on the right side of the top panel) also eluted from the immunoresin, and was detected by the secondary antibody. The location of molecular weight standards is marked on the left side of the top panel.

119
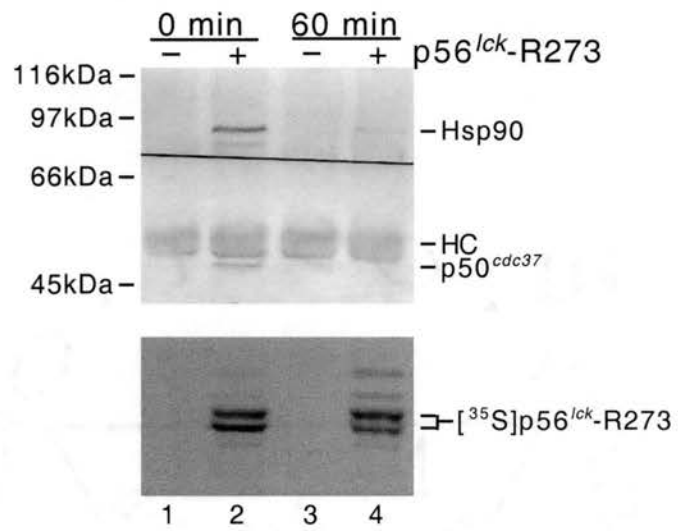
Figure 23. Effects of Drugs on p56^{lck} Interactions with Chaperones and Co-chaperones.

Nuclease treated RRLs were programmed with (+, lanes 2, 4, 6, 8, 10, and 12) or without (-, lanes 1, 3, 5, 7, 9, and 11) p56^{lck} cDNA and allowed to synthesize protein for 20 minutes at 37 °C in the presence of [^{35}S] methionine. Protein synthesis reactions were treated with indicated drugs [1% DMSO (lanes 1, 2, 7, and 8), 89 μM GA (lanes 3, 4, 9, and 10), and 20 mM Na$_2$(MoO$_4$) (lanes 5, 6, 11, and 12)] and mixed with immunoresins prebound with anti-His antibodies. Two sets of immunoprecipitations were prepared and subjected to different wash conditions. Lanes 1-6 were washed with a "High Salt" wash buffer (0.5 M NaCl). Lanes 7-12 were washed with a "Low Salt" wash buffer (0 mM NaCl). For both sets 20 mM Na$_2$(MoO$_4$) was included in the wash buffers for samples treated with molybdate (lanes 5, 6, 11, and 12). Immunoabsorbed proteins were eluted with SDS-PAGE sample buffer and separated by SDS-PAGE. Protein bands were electroblotted to PVDF membrane and subjected to autoradiography (bottom panel, labeled [^{35}S]H$_6$p56^{lck} on the right side of the panel) and immunostaining with indicated antibodies (top panel, labeled on the right side of the panel: Hsp90 OSU mouse ascites fluid, Hsp70 N27, FKBP52 EC1, p50^{cdc37} OSU mouse ascites fluid, polyclonal Cyp40 from Affinity BioReagents). The location of the molecular weight standards is marked on the right side of the top panel.

(IP anti-His)

High Salt | Low Salt

DMSO   GA   MoO$_4$ DMSO   GA   MoO$_4$ H$_6$p56^{lck}
− +   − +   − +   − +   − +   − +

97kDa− .... −Hsp90

66kDa− .... −Hsp70

−FKBP52

−p50^{cdc37}

45kDa− .... −Cyp40

−[^{35}S]H$_6$p56^{lck}

1   2   3   4   5   6   7   8   9   10   11   12
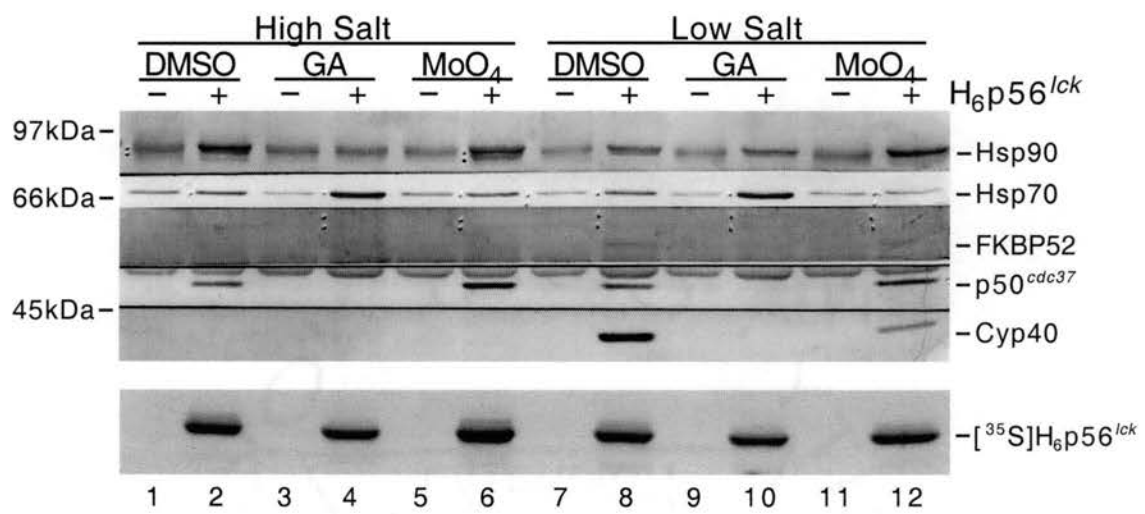
GA treatment disrupted this interaction much like the disruption seen for p50^{cdc37} (Figure 23, lane 10). Molybdate did not stabilize this complex and in fact less Cyp 40 and FKBP52 were recovered, although, it did enhance the interaction of both Hsp90 and p50^{cdc37} with the kinase (Figure 23, lane 12). Interestingly the immunophilin interactions, unlike p50^{cdc37}, were not stabile in high salt (Figure 23, lanes 1-6). Unsuccessful attempts were made to detect p23 by immuno-staining.

The poor detection of FKBP52 by the EC1 antibody and the lack of detection of p23 in Figure 23 made identification of these interacting partners uncertain. Most experiments done by immunoprecipitating p56^{lck} failed to detect FKBP52 and all failed to detect p23. Detection of FKBP52 was only possible when high quantities of p56^{lck} kinase were synthesized. The FKBP52 and p23 antibodies are reported to be much better at immunoprecipitating than immuno-blotting. For this reason immunoprecipitations of FKBP52 and p23 were conducted and the [^{35}S]p56lck kinase was detected by autoradiography.

Immunoprecipitation of FKBP52 also enabled us to determine whether both FKBP52 and p50^{cdc37} were components of the same complex on the kinase or if they interacted with the kinase in independent complexes. This is an important issue since previous reports have suggested that p50^{cdc37} and TPR containing proteins, such as FKBP52 and Cyp40 compete for the same or topologically adjacent sites on Hsp90. Silverstein *et al.* [44] concluded that p50^{cdc37} and TPR containing proteins are mutually exclusive components of the Hsp90 machinery that sterically hindered the binding of the other due to the close proximity of their binding sites on Hsp90. Figure 24 shows the immunoprecipitation of FKBP52 with the monoclonal EC1 antibody. In contrast to the

results of Silverstein and co-workers, our lab has shown that $p50^{cdc37}$ forms a significant, but salt labile component, of the native (substrate-free) FKBP52 complex [46]. To further our characterization, we show that anti-FKBP52 antibodies co-adsorbed $p56^{lck}$ in an immune specific fashion (Figure 24: lane 4 versus 5, and lane 8 versus 9), and the complex was stable to washes at 150 mM NaCl. A comparison of the amount of Hsp90 co-absorbed with FKBP52 in the presence and absence of kinase (Figure 24: lane 2 versus 4, and lane 6 versus 8) show more Hsp90 complexed with FKBP52 in the presence of $p56^{lck}$. The same analysis was done for $p50^{cdc37}$. Some $p50^{cdc37}$ associated with FKBP52 without kinase (Figure 24, lanes 2 and 6), but when $p56^{lck}$ was included (Figure 24, lanes 4 and 8) there was a significant increase in the amount of $p50^{cdc37}$ associated with FKBP52. In addition, the Hsp90 complex stabilizing agent molybdate failed to stabilize this complex as indicated by the loss of some $p56^{lck}$ and $p50^{cdc37}$ upon addition of 20 mM $Na_2(MoO_4)$ (Figure 24, lanes 6-9). To further this characterization a time course, as described for Figures 15, 16, and 22, was conducted to determine whether $p56^{lck}$ chased off of the FKBP52 complex. Immediately after synthesis $p56^{lck}$ interacted with FKBP52 along with Hsp90 and $p50^{cdc37}$ (Figure 25, lane 4). After 60 minutes neither $p56^{lck}$ kinase nor $p50^{cdc37}$ associated with FKBP52, although Hsp90 and Hsp70 were still associated (Figure 25, lane 8). These results suggest that $p56^{lck}$ dramatically increases the association of $p50^{cdc37}$ with the FKBP52 complex.

Figure 26 shows the co-immunoprecipitation of $p56^{lck}$ with p23 (lane 1). Hsp90 and $p50^{cdc37}$ also interacted with p23. Treatment with molybdate did not stabilize the interaction of p23 with $p56^{lck}$ or $p50^{cdc37}$, but did slightly increase the amount of Hsp90 associated with p23 (Figure 26, lane 3). Treatment with GA disrupted the association of

Figure 24. Molybdate Destabilization of Chaperone and p56^{lck} Complexes.

Nuclease treated RRL was programmed with (+: lanes 4, 5, 8, and 9) or without (-
: lanes 2, 3, 6, and 7) p56^{lck} cDNAs, and allowed to synthesize protein for 25
minutes at 30 °C in the presence of [^{35}S] methionine. Protein synthesis reactions
were aliquoted and either treated with [20 mM Na$_2$(MoO$_4$) (lanes 6-9)] or without
[(0 mM Na$_2$(MoO$_4$) lanes 2-5)] molybdate. RRL was separated into equal aliquots
and were then immunoprecipitated with the immune monoclonal antibody EC1 (I:
lanes 2, 4, 6, and 8) or with the non-immune antibody (NI: lanes 3, 5, 7, and 9)
and analyzed as described above. [^{35}S]H$_6$p56^{lck} was detected by autoradiography
(bottom panel) and is labeled on the right-hand side of the panel. Hsp90, p50^{cdc37},
and Cyp40 were detected by immunostaining and are labeled on the right-hand
side of the top panel. The location of the molecular weight standards is marked on
the left side of the top panel.
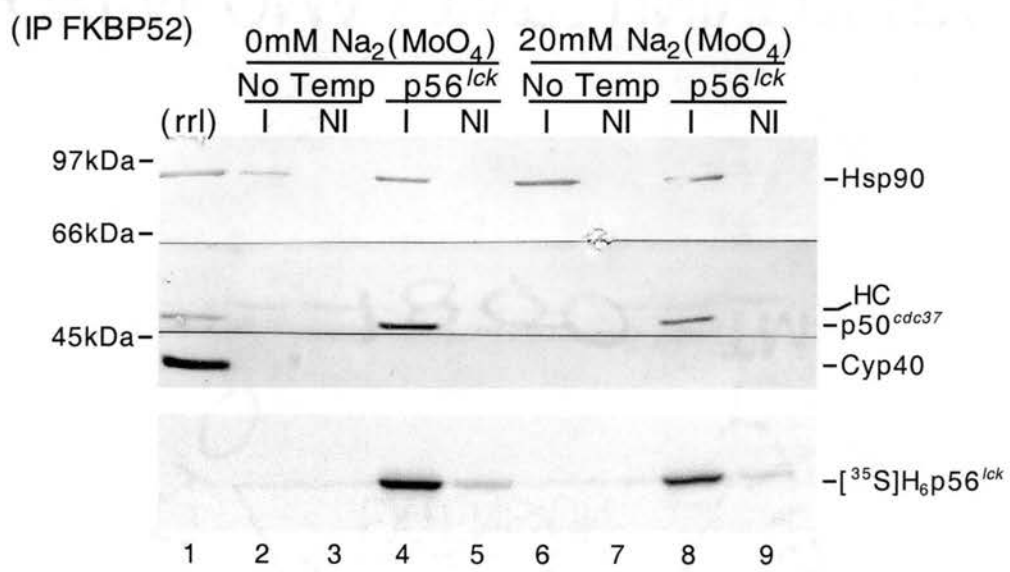
Figure 25. Time Course of FKBP52 Interaction with p56^{lck} Kinase.

Nuclease treated RRL was programmed with (+: lanes 3, 4, 7, and 8) or without (-: lanes 1, 2, 5, and 6) p56^{lck} cDNAs and allowed to synthesize protein for 20 minutes at 37 °C in the presence of [^{35}S] methionine. Aliquots of protein synthesis reactions were immediately mixed with immunoresins prebound with the immune monoclonal antibody EC1 (I: lanes 2 and 4) or with the non-immune antibody (NI: lanes 1 and 3) for 1 hour on ice, washed, and eluted with SDS-PAGE sample buffer. The remainder of the protein synthesis reactions was treated with ATA to inhibit initiation, and p56^{lck} was matured for 60 minutes at 37 °C. Matured p56^{lck} was immunoprecipitated and eluted as decribed above. Eluant was separated by SDS-PAGE, electroblotted and analyzed by autoradiography and immunostaining as described above. [^{35}S]H$_6$p56^{lck} was detected by autoradiography (bottom panel) and is labeled on the side. Hsp90, Hsp70, FKBP52, p50^{cdc37} were detected by immunostaining and are marked on the right side of the top panel. The location of the molecular weight standards is marked on the left side of the top panel.

126

(IP FKBP52)

	0 min				60 min			
	No Temp		p56*lck*		No Temp		p56*lck*	
	NI	I	NI	I	NI	I	NI	I

97kDa —

—Hsp90

66kDa —

—Hsp70

⊐—FKBP52

—HC

—p50*cdc37*

45kDa —

⊐—[³⁵S]H₆p56*lck*

1   2   3   4   5   6   7   8

127

Figure 26. Interaction of p23 with p56^{lck} Kinase and Disruption by GA.

Nuclease treated RRL was programmed with p56^{lck} cDNAs and allowed to synthesize protein for 20 minutes at 37 °C in the presence of [^{35}S] methionine. After synthesis reactions were treated with 20 mM Na$_2$MoO$_4$ (lanes 3 and 4), 89 μM GA (lanes 5 and 6), or nothing (lanes 1 and 2). Samples were immediately clarified and mixed with immunoresins prebound with the immune antibody JJ3 (monoclonal p23 antibody labeled "I" odd-numbered lanes) or the non-immune antibody ("NI " even-numbered lanes) for 1 hour on ice. Non-treated and GA treated immunopellets (lanes 1, 2, 5, and 6) were washed with 150 mM NaCl and MoO$_4$ treated immunopellets (lanes 3 and 4) were washed with 100 mM NaCl and 20 mM Na$_2$MoO$_4$. [^{35}S]p56^{lck} was detected by autoradiography (bottom panel, labeled on the right side). Hsp90, p50^{cdc37}, and p23 were detected by immunoblotting and are labeled on the right side of the upper panels. The location of the molecular weight standards is marked on the left side of the upper panels.
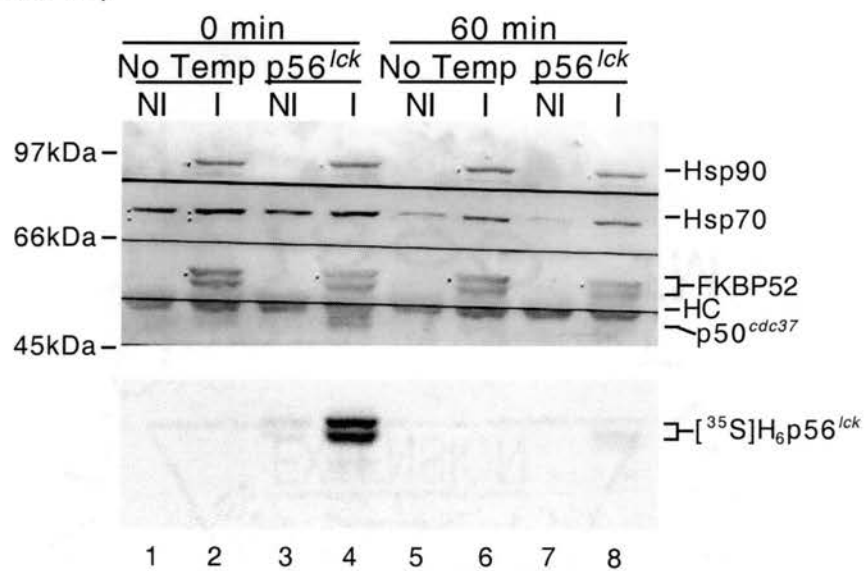
(IP p23)

97kDa—

66kDa—

45kDa—

31kDa—

| | | MoO₄ | | GA | |
| I | NI | I | NI | I | NI |

—Hsp90

—HC
—p50ᶜᵈᶜ³⁷

—LC
—p23

—[³⁵S]p56ˡᶜᵏ

1   2   3   4   5   6

(IP p23)

MoO_4 GA

| I | NI | I | NI | I | NI |

97kDa—

66kDa—   —Hsp90

45kDa—   —HC
                             —$p50^{cdc37}$

31kDa—   —LC
                             —p23

                             —$[^{35}S]p56^{lck}$

1   2   3   4   5   6
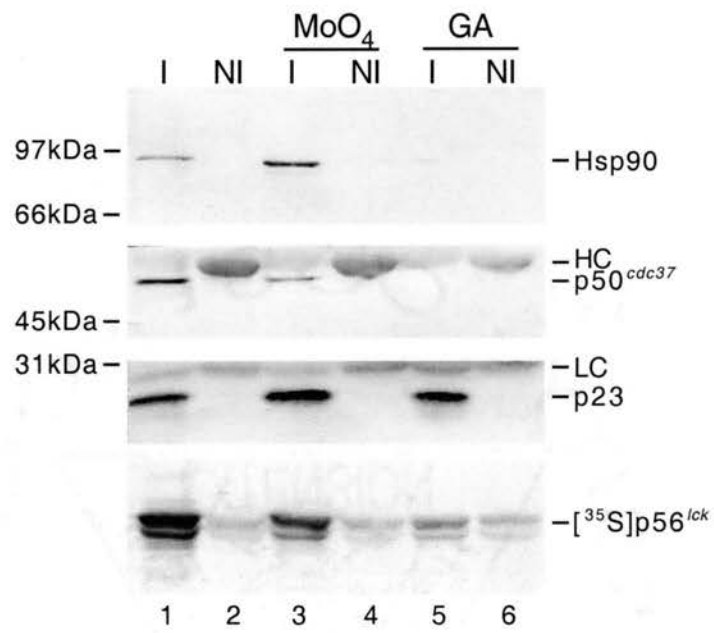
Hsp90, p50^{cdc37}, and p56^{lck} with p23 (Figure 26, lane 5), suggesting Hsp90 mediates the interaction of p56^{lck} and p50^{cdc37} with p23.

p56^{lck} kinase domain interactions with chaperone components.

Early work characterizing the interactions between the viral p60^{v-src} kinase and Hsp90 and p50^{cdc37} localized the interactions to the kinase domain (reviewed in [94]). Hsp90 and p50^{cdc37} interact with the kinase domains of other protein kinases as well [44, 45, 95]. Figures 12 and 13 in the chapter 3 also localize the interactions of Hsp90 and p50^{cdc37} with the kinase domains of p56^{lck} and HRI. Here we try to further define the part or parts of the kinase domain that are necessary for chaperone interactions. The structure of the kinase domains of most eukaryotic protein kinases are very similar and can be separated into two subdomains, or lobes: the N-terminal lobe (N-lobe) and the C-terminal lobe (C-lobe). Clones of each lobe were made with a His-tag and translated in RRL as described before. Figure 27 shows the immunoprecipitation of each of the lobes in comparison with both full-length p56^{lck} and the kinase catalytic domain (Figure 27: lanes 2 and 3, respectively). Hsp90 and p50^{cdc37} both co-immunoprecipitated with the full-length kinase, the catalytic domain, and the N-terminal lobe of the catalytic domain, but not with the C-terminal lobe of the catalytic domain (Figure 27: lanes 2, 3, 4, and 5 respectively). Interestingly, the Cyp40 interaction favored the catalytic domain as shown by the increase in the amount binding, and it was greater than the amount for either the full-length p56^{lck} or the N-lobe, even when normalized for the amount of Hsp90 and p50^{cdc37}. Immunoprecipitations with both FKBP52 and p23 antibodies (Figures 28 and 29 respectively) indicate that these co-chaperones interact specifically with the N-terminal

Figure 27. p56^{lck} Kinase Lobe Interactions with Hsp90 and p50^{cdc37}.

Nuclease treated RRL was programmed with full-length (FL, lane 2) H$_6$-p56^{lck}, His-tagged catalytic domain (Cat, lane 3), His-tagged N-terminal lobe (NL, lane 4), or His-tagged C-terminal lobe (CL, lane 5) cDNAs or without template (NT, lane 1). After protein synthesis at 37 °C for 20 minutes in the presence of [^{35}S] methionine reactions were adjusted to 20 mM Na$_2$MoO$_4$ and immediately clarified and mixed with immunoresins preabsorbed with antibodies against the penta-His antigen for 1 hour on ice. Immunoresins were washed, eluted with SDS-PAGE sample buffer, and separated by SDS-PAGE. [^{35}S] labeled p56^{lck} constructs were detected by autoradiography (bottom panel, labeled on the right side). Hsp90, p50^{cdc37}, and Cyp40 were detected by immunostaining and are labeled on the right-hand side of the top panels. The location of the molecular weight standards is marked on the left side of the top panels.

131
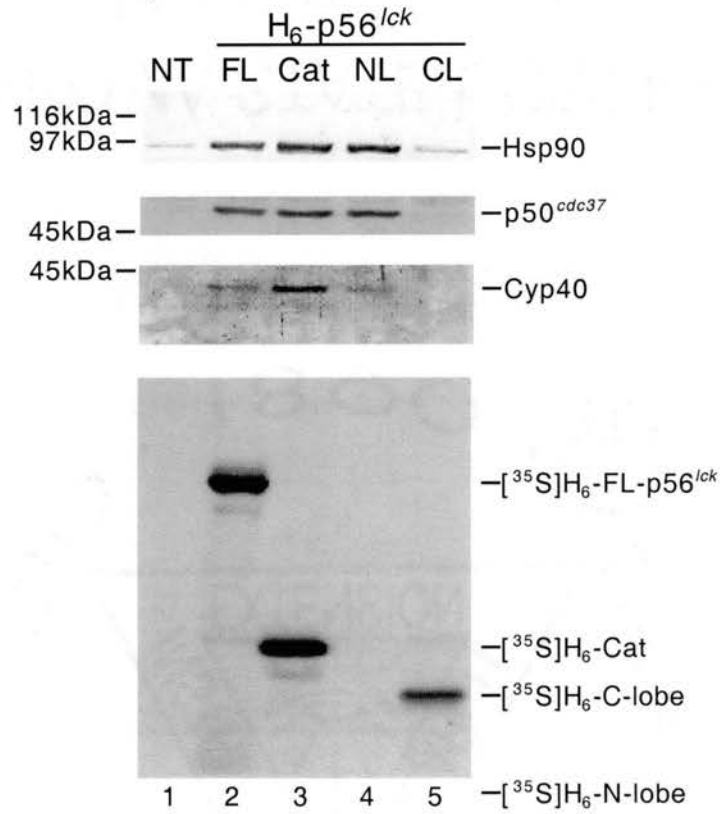
Figure 28. Interaction of p56^{lck} Fragments with FKBP52.

Nuclease treated RRL was programmed with the H$_6$-p56^{lck} catalytic domain (Cat, lanes 3 and 4), H$_6$-N-terminal lobe (N-lobe, lanes 5 and 6), H$_6$-C-terminal lobe (C-lobe, lanes 7 and 8) cDNAs or without (No Temp, lanes 1 and 2) template. After protein synthesis in the presence of [^{35}S] methionine for 20 minutes at 37 °C, reactions were adjusted to 20 mM Na$_2$MoO$_4$ and immediately clarified and mixed with immunoresins preabsorbed with the immune monoclonal antibody EC1 ("I" even-numbered lanes), or the nonimmune antibody ("NI" odd-numbered lanes). Immunoresins were washed, eluted, and separated by SDS-PAGE. [^{35}S] labeled p56^{lck} constructs were detected by autoradiography (top panel) and labeled on the right-hand side. Hsp90 and p50^{cdc37} were detected by immunostaining and are labeled on the right-hand side (bottom panels). The location of the molecular weight standards is marked on the left side of the top panel.

(IP anti-FKBP52)

31kDa—

21kDa—

—[³⁵S]H₆-Cat

—[³⁵S]H₆-C-lobe

—[³⁵S]H₆-N-lobe

—Hsp90

HC
p50^cdc37

1 2 3 4 5 6 7 8
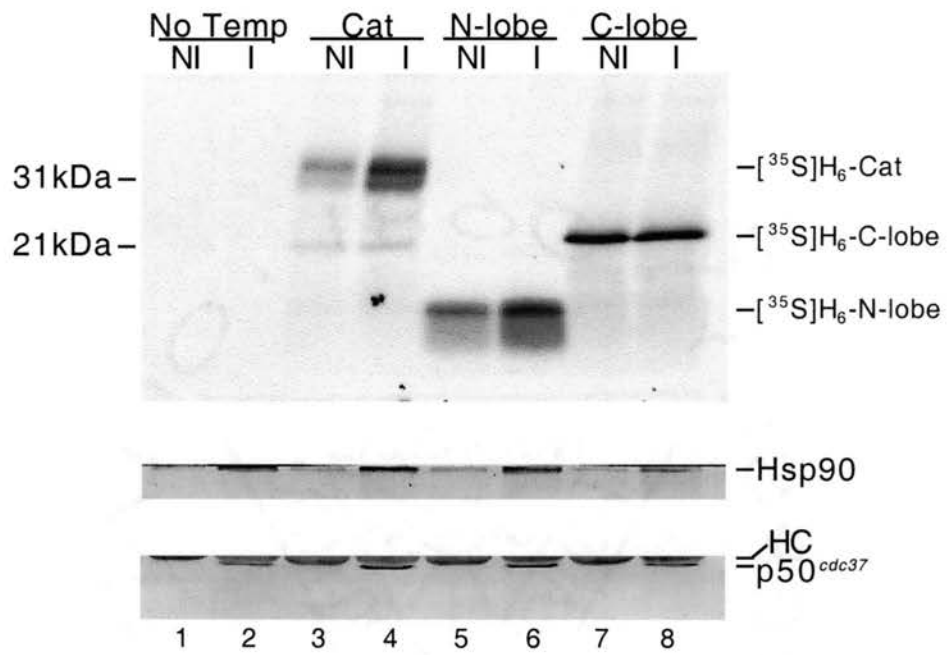
Figure 29. Interaction of p56*lck* Fragments with p23.

Nuclease treated RRL was programmed with the H_6-p56*lck* full-length (FL, lanes 3 and 4), H_6-p56*lck* catalytic domain (Cat, lanes 5 and 6), H_6-N-terminal lobe (N-lobe, lanes 7 and 8), H_6-C-terminal lobe (C-lobe, lanes 9 and 10) cDNAs or without (No Temp, lanes 1 and 2) template. After protein synthesis in the presence of [^{35}S] methionine for 20 minutes at 37 °C reactions were adjusted to 20 mM Na_2MoO_4 and immediately clarified and mixed with immunoresins preabsorbed with the immune monoclonal antibody JJ3 ("I" even-numbered lanes), or the nonimmune antibody ("NI" odd-numbered lanes). Immunoresins were washed, eluted, and separated by SDS-PAGE. [^{35}S] labeled p56*lck* constructs were detected by autoradiography (top panel) and labeled on the right-hand side. Hsp90 and p50*cdc37* were detected by immunostaining and are labeled on the right-hand side (bottom panel). The location of the molecular weight standards is marked on the left-hand side of the both panels.

(IP anti-p23)

	No Temp		FL		Cat		N-lobe		C-lobe	
	NI	I	NI	I	NI	I	NI	I	NI	I

66kDa—

45kDa—

31kDa—

21kDa—
14kDa—

—[^{35}S]H$_6$-FL-p56^{lck}

—[^{35}S]H$_6$-Cat

—[^{35}S]H$_6$-C-lobe

—[^{35}S]H$_6$-N-lobe

97kDa—

66kDa—

45kDa—

31kDa—

—Hsp90

—p50^{cdc37}

1   2   3   4   5   6   7   8   9   10

136
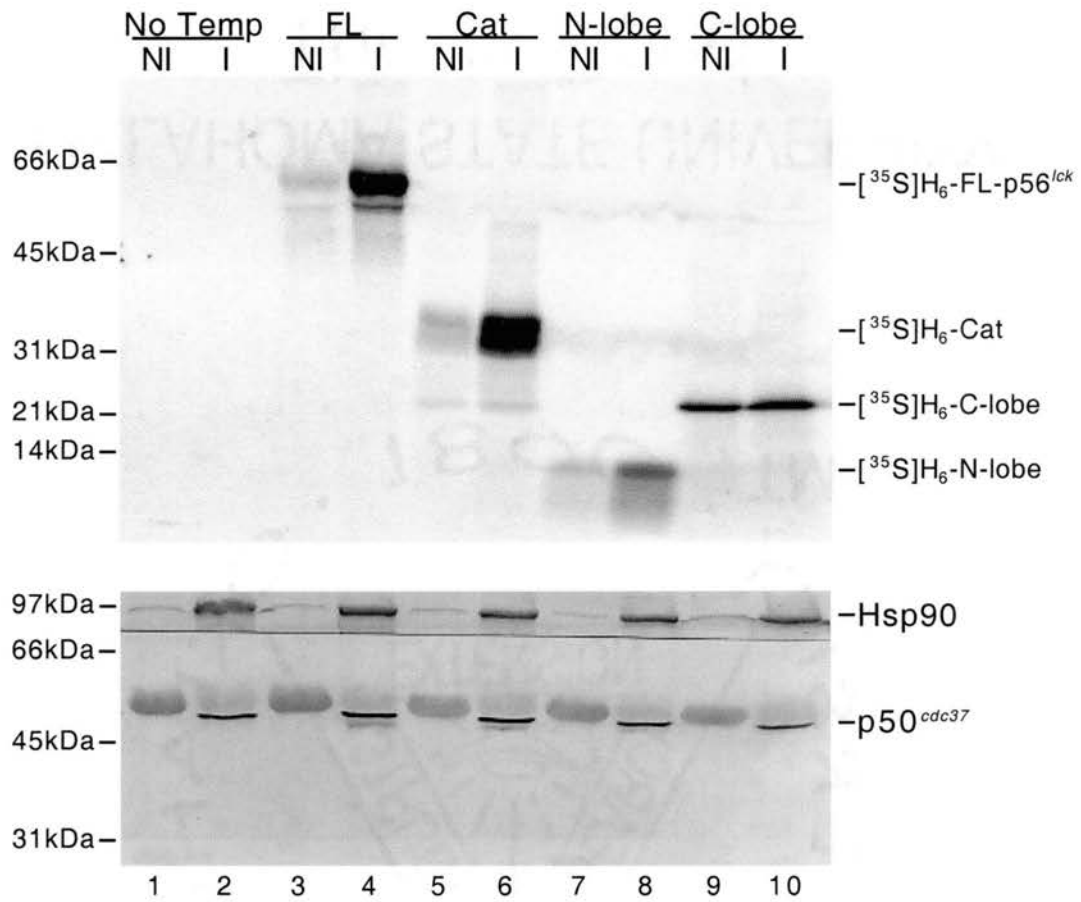
lobe of the catalytic domain (Figure 28, lanes 5 and 6; Figure 29, lanes 7 and 8). The nonspecific binding of the C-terminal lobe in these experiments was so high that it was not possible to determine specificity of binding (Figure 28, lanes 7 and 8; Figure 29 lanes 9 and 10); however, since Hsp90 and p50^{cdc37} did not interact with the C-terminal lobe FKBP52 and p23 probably do not either.

Discussion

Several subtle and more obvious conclusions can be drawn from the results presented here. Figures 15-18 and 23-26 document the chaperone and co-chaperone interactions with immature p56^{lck}. Immature p56^{lck} interacts with Hsp70, Hsp90, and p23, many of the same components reported to interact with many of the steroid hormone receptors (ER-[45], GR-[32], PR-[31], and AR-[47, 204]) and other protein kinases (Raf-[95], HRI-[205], Fes-[45]). We also characterized the interaction of p50^{cdc37}, the "protein kinase-targeting subunit of Hsp90" which is thought to be specific to Hsp90/kinase substrate complexes [101]. The p50^{cdc37} interaction with p56^{lck}, like the Hsp90 interaction, was stable to salt washes up to 0.5 M. We did not attempt higher salt concentrations. This argues against an electrostatic interaction between chaperones and client kinase and agrees with the idea that Hsp90 recognizes hydrophobic patches in its clientele. The fact that Hsp90 interaction with p50^{cdc37} in the absence of substrate is more salt labile, a 30% loss at 150 mM NaCl [46], suggests this interaction may be more electrostatic in nature. These observations together indicate that p50^{cdc37} interacts with the p56^{lck} bound Hsp90 complex more than passively through Hsp90. The same cannot be said for the

immunophilin or p23 interactions since they do not show an increased stability to high salt in the presence of p56^{lck}. p50^{cdc37} is an active member of the Hsp90 machinery as suggested by the functional dependence some kinases have for p50^{cdc37} [99-101].

Our study of the immunophilin components of the p56^{lck}-chaperone complex goes against one of the current models of Hsp90 function. Owen-Grillo *et. al.* [43] proposed that steroid receptors associate with immunophilin containing Hsp90 complexes and kinases associate with p50^{cdc37} containing Hsp90 complexes [43, 95, 206]. In contradiction to this model, we show FKBP52 and Cyp40 associated with p56^{lck}, a finding consistent with other reports of immunophilin interactions with kinases [45, 205, 207]. As an extension of this model Siverstein *et al.* [44] proposed that p50^{cdc37} and TPR containing cohorts, such as FKBP52 and Cyp40 compete for the same or topologically adjacent sites on Hsp90. Surprisingly, p50^{cdc37} associated with the FKBP52 complex and was significantly increased when p56^{lck} was present. This finding suggests that the presence of p56^{lck} enhanced this interaction, and that p50^{cdc37} and FKBP52 are not mutually exclusive on Hsp90 complexes.

Our observation that both FKBP52 and Cyp40 associate with p56^{lck} raised the possibility that both were in the same Hsp90 complex. Both FKBP52 and Cyp40 associated with p56^{lck} when the immature kinase was immunoprecipitated; however, when FKBP52 immunoprecipitations were blotted for Cyp40, no Cyp40 was detected. This finding suggests that the proteins are in different Hsp90 complexes, a possibility supported by a report that the immunophilin components compete for binding to Hsp90 [72]. However, identification of a 1:1 stoichiometry for TPR containing proteins and

Hsp90 monomers again raises the possibility of mixed hetero-immunophilin containing Hsp90 dimers.

GA treatment of these complexes with immature p56^{lck} rendered them much more salt labile. p50^{cdc37}, FKBP52, Cyp 40, and p23 all washed off the p56^{lck} complex at 0 M salt in the presence of GA, and Hsp90 washed off at 0.5 M in the presence of GA. These results suggest the co-chaperone interactions are mediated by Hsp90. p50^{cdc37} is the only Hsp90 cohort known to directly interact with kinase clients [101], but even this interaction was disrupted by GA. Only Hsp70 retained a salt stable interaction with p56^{lck} in the presence of GA. Hsp70 interacted with p56^{lck} independent of Hsp90 and in the absence of Hsp90 it appeared to increase its association. It has been proposed that GA treatment may cause Hsp90 substrates to accumulate in an Hsp70 bound reiterative cycle unable to pass to Hsp90 due to this inhibition. All of the chaperone components also chased off of the mature p56^{lck} within an hour incubation at 37 °C. However, the p56^{lck}F505 mutant, which is reported to have a prolonged conditional dependence on Hsp90, showed a prolonged dependence on Hsp70 function for kinase activity at 37 °C [27].

Other Hsp90 substrates, such as the steroid receptors and the serine/threonine kinase HRI, however, are reported to have prolonged maintenance interactions with these chaperones until some maturational event occurs allowing them to become chaperone independent. These interactions are dynamic, however, and do not represent static holding complex awaiting a stabilizing event, rather the substrates in this model go through cycles of binding, folding, and release until they achieve a state stable and independent of the need for chaperone folding. For the steroid receptors this event is

ligand binding and for HRI it is phosphorylations associated with heme-deficiency [33, 172, 179]. It is assumed that p56^{lck} also undergoes some maturational event or events, which allow it to gain chaperone independence, an event that occurs fairly rapidly in RRL. One possibility is phosphorylation of the regulatory 505 tyrosine. Hartson *et. al.* [27] proposed this due to the instability of mature p56^{lck} kinase which had the 505 tyrosine mutated to phenylalanine. Mature p56^{lck}F505 lost activity upon treatment with GA, the Hsp90 inhibitory drug [27]. Here we show a similar loss of activity upon treatment with ClA, an Hsp70 inhibitory drug, indicating that both Hsp70 and Hsp90 are necessary for nascent folding of both kinases but, are required for the continued maintenance of only the mutant kinase. Other results from our laboratory demonstrate that a similar mutation in the Hck Src-family kinase, also has a requirment for continued maintenance by Hsp90 at 37 °C [143]. The F505 mutation or F527 mutation in p60^{src} is the main alteration associated with converting p60^{src} and p56^{lck} into oncogenic kinases [208]. Oncogenic transformation by these kinases can be reverted by treatment with GA [26, 110]. Phosphorylation of the 505 tyrosine represses the kinase activity by inducing the binding of the SH2 domain, the phosphotyrosine-binding domain of Src family kinases, to p56^{lck}'s C-terminus. This binding appears to force the two lobes of the kinase domain closer together [209, 210]. Reppressed Src family kinases form another intermolecular interaction. The linker region between the SH2 domain and the kinase domain adopts a polyproline type-II helix (PP-II) that is bound by the SH3 domain, the polyproline-binding domain of Src family kinases. Both intermolecular interactions are thought to give the kinase more stability and may be events necessary to gain chaperone independence. This hypothesis predicts that oncogenic mutations that prevent the stable

inhibitory interaction of the SH3 and SH2 domains with the catalytic domain of Src-family kinases would also show a requirement for conditional maintenance by Hsp90.

The chaperone components are not interacting with the tyrosine 505 directly since the C-terminal lobe of the kinase domain, which includes the tyrosine 505, did not interact with any of the chaperone components. The N-terminal lobe was able to either immunoprecipitate with or co-immunoprecipitate with all of the chaperone components. What Hsp90 and its co-chaperones recognize in client proteins is still unknown although here we have localized the interaction site within a subdomain of the kinase catalytic domain. Currently clones are being made in our lab based on the molecular weight of bands identified from figures 10 and 11 of chapter 3. While these bands may only represent artifacts induced by treatment with puromycin and early release from the ribosome they may be useful for identifying high affinity binding motifs in known client kinases.

The results presented here, as stated, was modeled in RRL and so any interactions identified here need to be confirmed in T cells, the normal site of $p56^{lck}$ expression. This confirmation, however, will need to overcome technical barriers and so may never be feasible. One is the population of $p56^{lck}$ known to interact with Hsp90 machinery. Only immature $p56^{lck}$ appears to interact and depend on Hsp90 machinery for folding. This represents a very small pool of the overall $p56^{lck}$ in T cells. The pool of co-chaperones interacting with $p56^{lck}$ also is very small and the antibodies for most of these co-chaperones are not very sensitive. A specific example of the short-comings in identifing these interactions using current methods and reagents is that a cell line that expresses $p56^{lck}$ at 30 times the normal levels (LSTRA) had to be used in order to detect its

interaction with just Hsp90, which is one of the most highly expressed proteins in the cell (1-2% of total cytosolic protein). Even using LSTRA cell extracts detection of the interaction between p56^{lck} and Hsp90 required large quantities of cells to be cultured. RRL allows for the specific and controlled synthesis of a single radioactively labeled immature uniform population of protein product in a chaperone rich environment[26]. Nonetheless, the RRL model system is limited and sure to miss important protein interactions specific to certain tissues and cells.

CHAPTER 5

SUMMARY

The body of work presented here begins by showing an *in vivo* dependence of a

kinase for chaperone function. The chaperone interactions with this kinase are then

monitored and modeled from very early, during translation, to a mature active stable

state, independent of chaperone interaction and function.

GA affects immature p56^{lck} and overall T cell biology

The effects of the specific Hsp90 inhibitor, GA, on T cell biology and specifically

on cellular p56^{lck} showed that activated and proliferating T cells are more sensitive to GA

toxicity, a result common to many chemotherapeutic drugs. The depletion of cellular

p56^{lck} suggests Hsp90 dependence in vivo, especially for the newly synthesized p56^{lck}. A

lysosomal degradation pathway induced by GA is implicated. The effects of GA on p56^{lck}

in T cells agree with a concurrent study using transfected p56^{lck}. However, we utilized the

Jurkat T cell line, which endogenously expresses p56^{lck}, and allows for characterization in

a more natural setting.

Co-translational interactions

The work focused on early interactions of p56^{lck} with chaperones, due to the more

pronounced dependence on Hsp90 shown by the newly synthesized p56^{lck} in T cells.

Using the RRL system to extend our study of p56^{lck} interaction with chaperones we

143

compared the co-translational interactions of three different proteins. Only HRI showed

interactions with Hsp90 and p50^{cdc37} while still on the ribosome. This may indicate a very

early need of HRI for chaperone intervention. HRI activity is also very closely regulated

since it regulates the very important process of protein translation initiation.

Immature p56^{lck} chaperone interactions in RRL

The post-translational interactions of newly synthesized p56^{lck}, as modeled in

RRL, show that most of the same components necessary to reconstitue activatable steroid

receptor complexes are also involved in early folding of p56^{lck}. These interactions are

necessary for biogenesis of active kinase, but are not necessary to maintain mature kinase

activity. However, mutant kinases appear to be more dependent on Hsps for activity.

These results show that very minor changes can make a dramatic difference in protein

stability.

Concluding remarks

Until recently protein folding by molecular chaperones, such as Hsp70 and Hsp90

were thought to be restricted to stress related events. However, a better appreciation of

the crowded environment of the cell and the potential pitfalls newly synthesized proteins

encounter during *de novo* folding indicate Hsp70, Hsp90, and other chaperones play a

more significant role in general protein folding than previously thought. It is also realized

that chaperones are not merely involved in folding, but can also regulate the function of

some substrates such as HRI, and steroid receptors, making it a target for

pharmacological intervention. The central role of Hsp90 in many processes of

morphological evolutionary changes and a potential role in cancer cell evolution were recently suggested by Rutherford and Lindquist [211].

BIBLIOGRAPHY

1.   Fedorov, A.N. and T.O. Baldwin, *Cotranslational protein folding*. J. Biol. Chem., 1997. **272**: p. 32715-32718.

2.   Carrell, R.W. and D.A. Lomas, *Conformational disease*. Lancet, 1997. **350**: p. 134-138.

3.   Beissinger, M. and J. Buchner, *How chaperones fold proteins*. Biol. Chem., 1998. **379**: p. 245-259.

4.   Anfinsen, C.B., *Principles that govern the folding of protein chains*. Science, Wash., 1973. **181**: p. 223-230.

5.   Minton, A.P., *The influence of macromolecular crowding and macromolecular confinement on biochemical reactions in physiological media*. J. Biol. Chem., 2001. **276**: p. 10577-10580.

6.   Ellis, R.J. and S.M. van der Vies, *Molecular chaperones*. Annu. Rev. Biochem., 1991. **60**: p. 321-347.

7.   Gething, M.-J. and J. Sambrook, *Protein folding in the cell*. Nature, 1992. **355**: p. 33-45.

8.   Ruddon, R.W. and E. Bedows, *Assisted protein folding*. J. Biol. Chem., 1997. **272**: p. 3125-3128.

9.   Smith, D.F., L. Whitesell, and E. Katsanis, *Molecular chaperones: biology and prospects for pharmacological intervention*. Pharmacol. Rev., 1998. **50**: p. 493-514.

10.   Borkovich, K.A., et al., *hsp82 is an essential protein that is required in higher concentrations for growth of cells at higher temperatures*. Mol. Cell. Biol., 1989. **9**: p. 3919-3930.

11.   Buchner, J., *Hsp90 & Co.-a holding for folding*. Trends Biol. Sci., 1999. **24**: p. 136-141.

12.   Richter, K. and J. Buchner, *Hsp90: chaperoning signal transduction*. J. Cell. Physiol., 2001. **188**: p. 281-290.

13.   Csermely, P., et al., *The 90-kDa molecular chaperone family: structure, function, and clinical applications. A comprehensive review*. Pharmacol. Ther., 1998. **79**: p. 129-168.

14.   Young, J.C., I. Moarefi, and F.U. Hartl, *Hsp90: a specialized but essential protein-folding tool*. J. Cell. Biol., 2001. **154**: p. 267-273.

15.   Argon, Y. and B.B. Simen, *GRP94, an ER chaperone with protein and peptide binding properties*. Semin. Cell. Dev. Biol., 1999. **10**: p. 495-505.

16.   Felts, S.J., et al., *The Hsp90-related protein TRAP1 is a mitochondrial protein with distinct functional properties*. J. Biol. Chem., 2000. **275**: p. 3305-3312.

17.   Nemoto, T., et al., *Mechanism of dimer formation of the 90-kDa heat-shock protein*. Eur. J. Biochem., 1995. **233**: p. 1-8.

18. Stebbins, C.E., et al., *Crystal structure of an Hsp90-geldanamycin complex: Targeting of a protein chaperone by an antitumor agent.* Cell, 1997. **89**: p. 239-250.

19. Roe, S.M., et al., *Structural basis for inhibition of the Hsp90 molecular chaperone by the antitumor antibiotics radicicol and geldanamycin.* J. Med. Chem., 1999. **42**: p. 260-266.

20. Dutta, R. and M. Inouye, *GHKL, an emergent ATPase/kinase superfamily.* Trends Biochem. Sci., 2000. **25**: p. 24-28.

21. Prodromou, C., et al., *Identification and structural characterization of the ATP/ADP-binding site in the Hsp90 molecular chaperone.* Cell, 1997. **90**: p. 65-75.

22. Richter, K., et al., *Coordinated ATP hydrolysis by the Hsp90 dimer.* J. Biol. Chem., 2001. **276**: p. 33689-33696.

23. Prodromou, C., et al., *The ATPase cycle of Hsp90 drives a molecular 'clamp' via transient dimerization of the N-terminal domains.* Embo J., 2000. **19**: p. 4383-4392.

24. Sullivan, W., et al., *Nucleotides and two functional states of hsp90.* J. Biol. Chem., 1997. **272**: p. 8007-8012.

25. Grenert, J.P., et al., *The amino-terminal domain of heat shock protein 90 (hsp90) that binds geldanamycin is an ATP-ADP switch that regulates hsp90 conformation.* J. Biol. Chem., 1997. **272**: p. 23843-23850.

26. Hartson, S.D., et al., *Hsp90-mediated folding of the lymphoid cell kinase p56lck.* Biochemistry, 1996. **35**: p. 13451-13459.

27. Hartson, S.D., et al., *Modular folding and evidence for phosphorylation-induced stabilization of an hsp90-dependent kinase.* J. Biol. Chem., 1998. **273**: p. 8475-8482.

28. Louvion, J.F., R. Warth, and D. Picard, *Two eukaryote-specific regions of Hsp82 are dispensable for its viability and signal transduction functions in yeast.* Proc. Natl. Acad. Sci. U.S.A., 1996. **93**: p. 13937-13942.

29. Scheibel, T., et al., *The charged region of Hsp90 modulates the function of the N-terminal domain.* Proc. Natl. Acad. Sci. U.S.A., 1999. **96**: p. 1297-1302.

30. Scheibel, T., T. Weikl, and J. Buchner, *Two chaperone sites in Hsp90 differing in substrate specificity and ATP dependence.* Proc. Natl. Acad. Sci. U.S.A., 1998. **95**: p. 1495-1499.

31. Smith, D., *Dynamics of heat shock protein 90-progesterone receptor binding and the disactivation loop model for steroid receptor complexes.* Mol. Endocrinol., 1993. **7**: p. 1418-1429.

32. Dittmar, K.D., et al., *Folding of the glucocorticoid receptor by the heat shock protein (hsp) 90-based chaperone machinery.* J. Biol. Chem., 1997. **272**: p. 21213-21220.

33. Pratt, W.B. and D.O. Toft, *Steroid receptor interactions with heat shock protein and immunophilin chaperones.* Endocrine. Rev., 1997. **18**: p. 306-360.

34. Morishima, Y., et al., *Stepwise assembly of a glucocorticoid receptor.hsp90 heterocomplex resolves two sequential ATP-dependent events involving first hsp70 and then hsp90 in opening of the steroid binding pocket.* J. Biol. Chem., 2000. **275**: p. 18054-18060.

147

35. Hutchison, K.A., et al., *Proof that hsp70 is required for the assembly of the glucocorticoid receptor into a heterocomplex with hsp90.* J. Biol. Chem., 1994. **269**: p. 5043-5049.

36. Dittmar, K.D., et al., *The role of DnaJ-like proteins in glucocorticoid receptor/hsp90 heterocomplex assembly by the reconstituted hsp90/p60/hsp70 foldosome complex.* J. Biol. Chem., 1998. **273**: p. 7358-7366.

37. Fliss, A.E., et al., *Domain requirements of DnaJ-like (Hsp40) molecular chaperones in the activation of a steroid hormone receptor.* J. Biol. Chem., 1999. **274**: p. 34045-34052.

38. Chen, S., et al., *Interactions of p60, a mediator of progesterone receptor assembly, with heat shock proteins hsp90 and hsp70.* Molecular Endocrinology, 1996. **10**: p. 682-693.

39. Johnson, B.D., et al., *Hop modulates hsp70/hsp90 interactions in protein folding.* J. Biol. Chem., 1998. **273**: p. 3679-3686.

40. Scheufler, C., et al., *Structure of TPR domain-peptide complexes: critical elements in the assembly of the Hsp70-Hsp90 multichaperone machine.* Cell, 2000. **101**: p. 199-210.

41. Smith, D.F., et al., *Two FKBP-related Proteins Are Associated with Progesterone Receptor Complexes.* J. Biol. Chem., 1993. **268**: p. 18365-18371.

42. Johnson, J.L. and D.O. Toft, *A novel chaperone complex for steroid hormone receptors involving heat shock proteins, immunophilins and p23.* J. Biol. Chem., 1994. **269**: p. 24989-24993.

43. Owens-Grillo, J.K., et al., *A model of protein targeting mediated by immunophilins and other proteins that bind to hsp90 via tetratricopeptide repeat domains.* J. Biol. Chem., 1996. **271**: p. 13468-13475.

44. Silverstein, A.M., et al., *p50cdc37 binds directly to the catalytic domain of Raf as well as to a site on hsp90 that is topologically adjacent to the tetratricopeptide repeat binding site.* J. Biol. Chem., 1998. **273**: p. 20090-20095.

45. Nair, S.C., et al., *A pathway of multi-chaperone interactions common to diverse regulatory proteins: estrogen receptor, Fes tyrosine kinase, heat shock transcription factor Hsf1, and the aryl hydrocarbon receptor.* Cell Stress and Chaperones, 1996. **1**: p. 237-250.

46. Hartson, S.D., et al., *p50^{cdc37} as a non-exclusive Hsp90 cohort which participates in Hsp90-mediated folding of immature kinase molecules.* Biochemistry, 2000. **39**: p. 7631-7644.

47. Rao, J., et al., *Functional interaction of human Cdc37 with the androgen receptor but not with the glucocorticoid receptor.* J. Biol. Chem., 2001. **276**: p. 5814-5820.

48. Rassow, J., et al., *Mitochondrial protein import: biochemical and genetic evidence for interaction of matrix hsp70 and the inner membrane protein MIM44.* J. Cell. Biol., 1994. **127**: p. 1547-1556.

49. Eggers, D.K., W.J. Welch, and W.J. Hansen, *Complexes between nascent polypeptides and their molecular chaperones in the cytosol of mammalian-cells.* Mol. Biol. Cell, 1997. **8**: p. 1559-1573.

50. Thulasiraman, V., C.-F. Yang, and J. Frydman, *In vivo newly translated polypeptides are sequestered in a protected folding environment.* EMBO J., 1999. **18**: p. 85-95.

51. Welch, W.J., *The mammalian stress response: cell physiology and biochemistry of stress proteins.*, in *Stress proteins in biology and medicine.*, C. Georgopolous, Editor. 1990, Cold Spring Harbor Laboratory: Cold Spring Harbor, N.Y. p. 223-278.

52. Schmid, D., et al., *Kinetics of molecular chaperone action.* Science, 1994. **263**: p. 971-973.

53. Zhu, X., et al., *Structural analysis of substrate binding by the molecular chaperone DnaK.* Science, 1996. **272**: p. 1606-1614.

54. Takenaka, I.M., et al., *Hsc70-binding peptides selected from a phage display peptide library that resemble organellar targeting sequences.* J. Biol. Chem., 1995. **270**: p. 19839-19844.

55. Rudiger, S., A. Buchberger, and B. Bukau, *Interaction of Hsp70 chaperones with substrates.* Nat. Struct. Biol., 1997. **4**: p. 342-349.

56. Rudiger, S., et al., *Substrate specificity of the DnaK chaperone determined by screening cellulose-bound peptide libraries.* Embo J., 1997. **16**: p. 1501-1507.

57. Deuerling, E., et al., *Trigger factor and DnaK cooperate in folding of newly synthesized proteins.* Nature, 1999. **400**: p. 693-696.

58. Mayer, M.P. and B. Bakua, *Hsp70 chaperone systems: diversity of cellular functions and mechanism of action.* Biol. Chem., 1998. **379**: p. 261-268.

59. Hainaut, P. and J. Milner, *Interaction of heat-shock protein 70 with p53 translated in vitro: evidence for interaction with dimeric p53 and for a role in the regulation of p53 conformation.* EMBO J., 1992. **11**: p. 3513-3520.

60. Sugito, K., et al., *Interaction between hsp70 and hsp40, eukaryotic homologues of DnaK and DnaJ, in human cells expressing mutant-type p53.* FEBS Lett., 1995. **358**: p. 161-164.

61. Schumacher, R.J., et al., *Cooperative action of hsp70, hsp90, and DnaJ proeins in protein renaturation.* Biochemistry, 1996. **35**: p. 14889-14898.

62. Caplan, A.J., et al., *Hormone-dependent transactivation by the human androgen receptor is regulated by a dnaJ protein.* J. Biol. Chem., 1995. **270**: p. 5251-5257.

63. Nicolet, C.M. and E.A. Craig, *Isolation and characterization of STI1, a stress-inducible gene from Saccharomyces cerevisiae.* Mol. Cell. Biol., 1989. **9**: p. 3638-3646.

64. Honore, B., et al., *Molecular cloning and expression of a transformation-sensitive human protein containing the TPR motif and sharing identity to the stress-inducible yeast protein STI1.* J. Biol. Chem., 1992. **267**: p. 8485-8491.

65. Blatch, G.L. and M. Lassle, *The tetratricopeptide repeat: a structural motif mediating protein-protein interactions.* Bioessays, 1999. **21**: p. 932-939.

66. Smith, D.F., et al., *Identification of a 60-kilodalton stress-related protein, p60, which interacts with hsp90 and hsp70.* Mol. Cell. Biol., 1993. **13**: p. 869-876.

67. Lassle, M., et al., *Stress-inducible, murine protein mSTI1. Characterization of binding domains for heat shock proteins and in vitro phosphorylation by different kinases.* J. Biol. Chem., 1997. **272**: p. 1876-1884.

68. Demand, J., J. Luders, and J. Hohfeld, *The carboxy-terminal domain of hsc70 provides binding sites for a distinct set of chaperones.* Mol. Cell. Biol., 1998. **18**: p. 2023-2028.

69. Prodromou, C., et al., *Regulation of hsp90 ATPase activity by tetratricopeptide repeat (TPR)-domain co-chaperones*. EMBO J., 1999. **18**: p. 754-762.

70. Young, J.C., W.M. Obermann, and F.U. Hartl, *Specific binding of tetratricopeptide repeat proteins to the C-terminal 12-kDa domain of hsp90*. J. Biol. Chem., 1998. **273**: p. 18007-18010.

71. Pirkl, F. and J. Buchner, *Functional analysis of the Hsp90-associated human peptidyl prolyl cis/trans isomerases FKBP51, FKBP52 and Cyp40*. J. Mol. Biol., 2001. **308**: p. 795-806.

72. Ratajczak, T. and A. Carrello, *Cyclophilin 40 (CyP-40), mapping of its hsp90 binding domain and evidence that FKBP52 competes with CyP-40 for hsp90 binding*. J. Biol. Chem., 1996. **271**: p. 2961-2965.

73. Owens-Grillo, J.K., et al., *The cyclosporin A-binding immunophilin CyP-40 and the FK506-binding immunophilin hsp56 bind to a common site on hsp90 and exist in independent cytosolic heterocomplexes with the untransformed glucocorticoid receptor*. J. Biol. Chem., 1995. **270**: p. 20479-20484.

74. Duina, A.A., et al., *The peptidyl-prolyl isomerase domain of the Cyp-40 cyclophilin homolog Cpr7 is not required to support growth or glucocorticoid receptor activity in Saccharomyces cerevisiae*. J. Biol. Chem., 1998. **273**: p. 10819-10822.

75. Pratt, W.B., *The Role of Heat Shock Proteins in Regulating the Function, Folding, and Trafficking of the Glucocorticoid Receptor*. J. Biol. Chem., 1993. **268**: p. 221455-21458.

76. Pratt, W.B., et al., *The hsp56 immunophilin component of steroid receptor heterocomplexes: could this be the elusive nuclear localization signal-binding protein?* J. Steroid Biochem. Mol. Biol., 1993. **46**: p. 269-279.

77. Galigniana, M.D., et al., *Evidence that the peptidylprolyl isomerase domain of the hsp90-binding immunophilin FKBP52 is involved in both dynein interaction and glucocorticoid receptor movement to the nucleus*. J. Biol. Chem., 2001. **276**: p. 14884-14889.

78. Chinkers, M., *Protein phosphatase 5 in signal transduction*. Trends. Endocrinol. Metab., 2001. **12**: p. 28-32.

79. Shao, J., S.D. Hartson, and R.L. Matts, *Evidence that protein phosphatase 5 functions to negatively modulate the maturation of the Hsp90-dependent heme-regulated eIF2alpha kinase*. Biochemistry, 2002. **41**: p. 6770-6779.

80. Ballinger, C.A., et al., *Identification of CHIP, a novel tetratricopeptide repeat-containing protein that interacts with heat shock proteins and negatively regulates chaperone functions*. Mol. Cell. Biol., 1999. **19**: p. 4535-4545.

81. Jiang, J., et al., *CHIP is a U-box-dependent E3 ubiquitin ligase: identification of Hsc70 as a target for ubiquitylation*. J. Biol. Chem., 2001. **276**: p. 42938-42944.

82. Connell, P., et al., *The co-chaperone CHIP regulates protein triage decisions mediated by heat-shock proteins*. Nat. Cell. Biol., 2001. **3**: p. 93-96.

83. Smith, K.F., L.E. Faber, and D.O. Toft, *Purification of unactivated progesterone hormone receptor and identification of novel receptor associated proteins*. J. Biol. Chem., 1990. **265**: p. 3996-4003.

84. Johnson, J.L., et al., *Characterization of a novel 23-kilodalton protein of inactive progesterone receptor complexes*. Mol. Cell. Biol., 1994. **14**: p. 1956-1963.

85.   Forsythe, H.L., et al., *Stable association of hsp90 and p23, but Not hsp70, with active human telomerase.* J. Biol. Chem., 2001. **276**: p. 15571-15574.

86.   Bohen, S.P., *Genetic and biochemical analysis of p23 and ansamycin antibiotics in the function of Hsp90-dependent signaling proteins.* Mol. Cell. Biol., 1998. **18**: p. 3330-3339.

87.   Fang, Y., et al., *SBA1 encodes a yeast hsp90 cochaperone that is homologous to vertebrate p23 proteins.* Mol. Cell. Biol., 1998. **18**: p. 3727-3734.

88.   Weaver, A.J., et al., *Crystal structure and activity of human p23, a heat shock protein 90 co-chaperone.* J. Biol. Chem., 2000. **275**: p. 23045-23052.

89.   Johnson, J.L. and D.O. Toft, *Binding of p23 and hsp90 during assembly with the progesterone receptor.* Mol. Endocrinol., 1995. **9**: p. 670-678.

90.   Young, J.C. and F.U. Hartl, *Polypeptide release by Hsp90 involves ATP hydrolysis and is enhanced by the co-chaperone p23.* Embo J., 2000. **19**: p. 5930-5940.

91.   Zhang, X. and G.L. Verdine, *Mammalian DNA cytosine-5 methyltransferase interacts with p23 protein.* FEBS Lett., 1996. **392**: p. 179-183.

92.   Tanioka, T., et al., *Molecular identification of cytosolic prostaglandin E2 synthase that is functionally coupled with cyclooxygenase-1 in immediate prostaglandin E2 biosynthesis.* J. Biol. Chem., 2000. **275**: p. 32775-32782.

93.   Reed, S.I., *The selection of S. cerevisiae mutants defective in the start event of cell division.* Genetics, 1980. **95**: p. 561-577.

94.   Brugge, J.S., *Interaction of the Rous sarcoma virus protein pp60^{src} with the cellular proteins pp50 and pp90.* Curr. Top Microbiol and Immunol, 1986. **123**: p. 1-22.

95.   Stancato, L.F., et al., *Raf Exists in a native heterocomplex with hsp90 and p50 that can be reconstituted in a cell-free system.* J. Biol. Chem., 1993. **268**: p. 21711-21716.

96.   Cutforth, T. and G.M. Rubin, *Mutations in hsp83 and cdc37 impair signalling by the sevenless receptor tyrosine kinase in Drosophila.* Cell, 1994. **77**: p. 1027-1036.

97.   Gerber, M.R., et al., *Cdc37 is required for association of the protein kinase Cdc28 with G1 and mitotic cyclins.* Proc. Natl. Acad. Sci. U.S.A., 1995. **92**: p. 4651-4655.

98.   Schutz, A.R., et al., *The yeast CDC37 gene interacts with MPS1 and is required for proper execution of spindle pole body duplication.* J. Cell. Biol., 1997. **136**: p. 969-982.

99.   Grammatikakis, N., et al., *p50cdc37 acting in concert with hsp90 is required for raf-1 function.* Mol. Cell. Biol., 1999. **19**: p. 1661-1672.

100.   Shao, J., et al., *Hsp90 Regulates p50^{cdc37} Function during the Biogenesis of the Active Conformation of the Heme-regulated eIF2α Kinase.* J. Biol. Chem., 2001. **276**: p. 206-214.

101.   Stepanova, L., et al., *Mammalian p50-Cdc37 is a protein kinase-targeting subunit of hsp90 that binds and stabilizes Cdk4.* Genes Dev., 1996. **10**: p. 1491-1502.

102.   Siligardi, G., et al., *Regulation of Hsp90 ATPase activity by the co-chaperone Cdc37p/p50cdc37.* J. Biol. Chem., 2002. **277**(23): p. 20151-20159.

103. Scholz, G.M., K. Cartledge, and N.E. Hall, *Identification and characterization of Harc: A novel Hsp90 associating relative of Cdc37.* J. Biol. Chem., 2001. **276**: p. 30971-30979.

104. DeBoer, C., et al., *Geldanamycin, a new antibiotic.* J. Antibiot. (Tokyo), 1970. **23**: p. 442-447.

105. Omura, S., et al., *Herbimycin, a new antibiotic produced by a strain of Streptomyces.* J. Antibiot. (Tokyo), 1979. **32**: p. 255-261.

106. Uehara, Y., et al., *Screening of agents which convert 'transformed morphology' of Rous sarcoma virus-infected rat kidney cells to 'normal morphology': identification of an active agent as herbimycin and its inhibition of intracellular src kinase.* Jpn. J. Cancer Res., 1985. **76**: p. 672-675.

107. Kondo, K., et al., *Induction of in vitro differentiation of mouse embryonal carcinoma (F9) and erythroleukemia (MEL) cells by herbimycin A, an inhibitor of protein phosphorylation.* J. Cell. Biol., 1989. **109**: p. 285-293.

108. Whitesell, L., et al., *Benzoquinoid ansamycins possess selective tumoricidal activity unrelated to src kinase inhibition.* Cancer Res., 1992. **52**: p. 1721-1728.

109. Uehara, Y., et al., *Phenotypic change from transformed to normal induced by benzoquinoid ansamycins accompanies inactivation of p60src in rat kidneys infected with Rous sarcoma virus.* Mol. Cell. Biol., 1986. **6**: p. 2198-2206.

110. Whitesell, L., et al., *Inhibition of heat shock protein hsp90-pp60^{v-src} heteroprotein complex formation by benzoquinone ansamycins: Essential role for stress proteins in oncogenic transformation.* Proc. Natl. Acad. Sci. U.S.A., 1994. **91**: p. 8324-8328.

111. Panaretou, B., et al., *ATP binding and hydrolysis are essential to the function of the hsp90 molecular chaperone in vivo.* EMBO J., 1998. **17**: p. 4829-4836.

112. Hudziak, R.M., J. Schlessinger, and A. Ullrich, *Increased expression of the putative growth factor receptor p185HER2 causes transformation and tumorigenesis of NIH 3T3 cells.* Proc. Natl. Acad. Sci. U.S.A., 1987. **84**: p. 7159-7163.

113. Li, P., et al., *Raf-1: a kinase currently without a cause but not lacking in effects.* Cell, 1991. **64**: p. 479-482.

114. Dittmer, D., et al., *Gain of function mutations in p53.* Nat. Genet., 1993. **4**: p. 42-46.

115. Muthuswamy, S.K. and W.J. Muller, *Activation of the Src family of tyrosine kinases in mammary tumorigenesis.* Adv. Cancer Res., 1994. **64**: p. 111-123.

116. Moasser, M.M., et al., *Inhibition of Src kinases by a selective tyrosine kinase inhibitor causes mitotic arrest.* Cancer Res., 1999. **59**: p. 6145-6152.

117. Lewis, J., et al., *Disruption of hsp90 function results in degradation of the death domain kinase, receptor-interacting protein (RIP), and blockage of tumor necrosis factor-induced nuclear factor-kappaB activation.* J. Biol. Chem., 2000. **275**: p. 10519-10526.

118. Loo, M.A., et al., *Perturbation of Hsp90 interaction with nascent CFTR prevents its maturation and accelerates its degradation by the proteasome.* EMBO J., 1998. **17**: p. 6879-6887.

119. Schulte, T.W., et al., *Disruption of the Raf-1-Hsp90 Molecular Complex Results in Destabilization of Raf-1 and Loss of Raf-1-Ras Association.* J. Biol. Chem., 1995. **270**: p. 24585-24588.

120. Whitesell, L., et al., *Geldanamycin-stimulated destabilization of mutated p53 is mediated by the proteasome in vivo.* Oncogene, 1997. **14**: p. 2809-2816.

121. Nimmanapalli, R., E. O'Bryan, and K. Bhalla, *Geldanamycin and its analogue 17-allylamino-17-demethoxygeldanamycin lowers Bcr-Abl levels and induces apoptosis and differentiation of Bcr-Abl-positive human leukemic blasts.* Cancer Res., 2001. **61**: p. 1799-1804.

122. Blagosklonny, M.V., et al., *The Hsp90 inhibitor geldanamycin selectively sensitizes Bcr-Abl-expressing leukemia cells to cytotoxic chemotherapy.* Leukemia, 2001. **15**: p. 1537-1543.

123. Yufu, Y., J. Nishimura, and H. Nawata, *High constitutive expression of heat shock protein 90 alpha in human acute leukemia cells.* Leuk. Res., 1992. **16**: p. 597-605.

124. Ferrarini, M., et al., *Unusual expression and localization of heat-shock proteins in human tumor cells.* Int. J. Cancer., 1992. **51**: p. 613-619.

125. Neckers, L., *Hsp90 inhibitors as novel cancer chemotherapeutic agents.* Trends Mol. Med., 2002. **8**: p. S55-S61.

126. June, C.H., et al., *Inhibition of tyrosine kinase phosphorylation prevents T-cell receptor-mediated signal transduction.* Proc. Natl. Acad. Sci. U.S.A., 1990. **87**: p. 7722-7726.

127. Yorgin, P.D., et al., *Effects of geldanamycin, a heat-shock protein 90-binding agent, on T cell function and T cell nonreceptor protein tyrosine kinases.* J. Immunol., 2000. **164**: p. 2915-2923.

128. Gillis, S., et al., *T cell growth factor: parameters of production and a quantitative microassay for activity.* J. Immunol., 1978. **120**: p. 2027-2032.

129. Weiss, A. and J.D. Stobo, *Requirement for the coexpression of T3 and the T cell antigen receptor on a malignant human T cell line.* J. Exp. Med., 1984. **160**: p. 1284-1299.

130. Matts, R.L., et al., *Interactions of the heme-regulated eIF-2α kinase with heat shock proteins in rabbit reticulocyte lysates.* J. Biol. Chem., 1992. **267**(25): p. 18160-18167.

131. Shaw, A.S., et al., *The lck tyrosine protein kinase interacts with the cytoplasmic tail of the CD4 glycoprotein through its unique amino-terminal domain.* Cell, 1989. **59**(4): p. 627-36.

132. Danielian, S., et al., *The lymphocyte-specific protein tyrosine kinase p56^{lck} is hyperphosphorylated on serine and tyrosine residues within minutes after activation via T cell receptor or CD2.* Eur. J. Immunol., 1989. **19**: p. 2183-2189.

133. Degen, J.L., et al., *Regulation of protein synthesis in mitogen-activated bovine lymphocytes.* J . Biol. Chem., 1983. **258**: p. 12153-12162.

134. Schnaider, T., et al., *The Hsp90-specific inhibitor, geldanamycin, blocks CD28-mediated activation of human T lymphocytes.* Life Sci, 1998. **63**(11): p. 949-54.

135. Hermiston, M.L., et al., *Reciprocal regulation of lymphocyte activation by tyrosine kinases and phosphatases.* J. Clin. Invest., 2002. **109**: p. 9-14.

153

136. Rudd, C.E., et al., *The CD4 receptor is complexed in detergent lysates to a protein-tyrosine kinase (pp58) from human T lymphocytes.* Proc. Natl. Acad. Sci. US.A., 1988. **85**: p. 5190-5194.

137. Barber, E.K., et al., *The CD4 and CD8 antigens are coupled to a protein-tyrosine kinase (p56lck) that phosphorylates the CD3 complex.* Proc. Natl. Acad. Sci. U.S.A., 1989. **86**: p. 3277-3281.

138. Hartson, S.D. and R.L. Matts, *Association of hsp90 with cellular src-family kinases in a cell-free system correlates with altered kinase structure and function.* Biochemistry, 1994. **33**: p. 8912-8920.

139. Bijlmakers, M.-J.J.E. and M. Marsh, *Hsp90 is essential for the synthesis and subsequent membrane association, but not the maintenance, of the src-kinase p56^{lck}.* Mol. Biol. Cell., 2000. **11**: p. 1585-1595.

140. Brugge, J.S., E. Erikson, and R.L. Erikson, *The specific interaction of the Rous sarcoma virus transforming protein, pp60^{src}, with two cellular proteins.* Cell, 1981. **25**: p. 363-372.

141. Scholz, G., et al., *p50^{cdc37} can Buffer the Temperature-sensitive Properties of a Mutant of Hck.* Mol. Cell. Biol., 2000. **20**: p. 6984-6995.

142. Mimnaugh, E.G., C. Chavany, and L. Neckers, *Polyubiquitination and proteasomal degradation of the p185c-erbB-2 receptor protein-tyrosine kinase induced by geldanamycin.* J. Biol. Chem., 1996. **271**: p. 22796-22801.

143. Scholz, G.M., et al., *The molecular chaperone Hsp90 is required for signal transduction by wildtype Hck and maintenance of an oncogenic mutant of Hck.* Cell Growth and Differentiation, 2001. **12**: p. 409-417.

144. Schulte, T.W., W.G. An, and L.M. Neckers, *Geldanamycin-induced destabilization of Raf-1 involves the proteasome.* Biochem. Biophys. Res. Commun., 1997. **239**: p. 655-659.

145. Schneider, C., et al., *Pharmacologic shifting of a balance between protein refolding and degradation mediated by hsp90.* Proc. Natl. Acad. Sci., 1996. **93**: p. 14536-14541.

146. Oda, H., S. Kumar, and P.M. Howley, *Regulation of the Src family tyrosine kinase Blk through E6AP-mediated ubiquitination.* Proc. Natl. Acad. Sci. U.S.A., 1999. **96**: p. 9557-9562.

147. Rao, N., et al., *Negative regulation of Lck by Cbl ubiquitin ligase.* Proc. Natl. Acad. Sci. U.S.A., 2002. **99**: p. 3794-3799.

148. Bijlmakers, M.J. and M. Marsh, *Trafficking of an acylated cytosolic protein: newly synthesized p56(lck) travels to the plasma membrane via the exocytic pathway.* J. Cell. Biol., 1999. **145**: p. 457-468.

149. Laing, J.G., et al., *Degradation of connexin43 gap junctions involves both the proteasome and the lysosome.* Exp. Cell. Res., 1997. **236**: p. 482-492.

150. Xu, W., et al., *Sensitivity of mature Erbb2 to geldanamycin is conferred by its kinase domain and is mediated by the chaperone protein Hsp90.* J. Biol. Chem., 2001. **276**: p. 3702-3708.

151. Levkowitz, G., et al., *c-Cbl/Sli-1 regulates endocytic sorting and ubiquitination of the epidermal growth factor receptor.* Genes Dev., 1998. **12**: p. 3663-3674.

152. Lill, N.L., et al., *The evolutionarily conserved N-terminal region of Cbl is sufficient to enhance down-regulation of the epidermal growth factor receptor.* J. Biol. Chem., 2000. **275**: p. 367-377.

153. Citri, A., et al., *Drug-induced ubiquitylation and degradation of ErbB receptor tyrosine kinases: implications for cancer therapy.* Embo J, 2002. **21**(10): p. 2407-17.

154. Matsuda, S., et al., *Temperature-sensitive Zap70 mutants degrading through a proteasome-independent pathway.* J. Biol. Chem., 1999. **274**: p. 3415-3418.

155. Bergman, L.W. and W.M. Kuehl, *Formation of an Intrachain Disulfide Bond on Nascent Immunoglobulin Light Chains.* J Biol Chem, 1979. **254**: p. 8869-8879.

156. Fedorov, A.N., et al., *Folding on the Ribosome of Escherichia coli Tryptophan Synthase Beta Subunit Nascent Chains Probed with a Conformation-Dependent Monoclonal Antibody.* J. Mol. Biol., 1992. **228**: p. 351-358.

157. Friguet, B., et al., *A Radioimmunoassay-Based Method for Measuring the True Affinity of a Monoclonal Antibody with Trace Amounts of Radioactive Antigen: Illustration with the Products of a Cell-Free Protein Synthesis System.* Anal. Biochem., 1993. **210**: p. 344-350.

158. Frydman, J., et al., *Folding of nascent polypeptide chains in a high molecular mass assembly with molecular chaperones.* Nature, 1994. **370**: p. 111-117.

159. Netzer, W.J. and F.U. Hartl, *Recombination of Protein Domains Facilitated by Co-translational Folding in Eukaryotes.* Nature, 1997. **388**: p. 343-349.

160. Sala-Newby, G., N. Kalsheker, and A.K. Campbell, *Removal of Twelve C-Terminal Amino Acids from Firefly Luciferase Aboloishes Activity.* Biochem. Biophys. Res. Commun., 1990. **172**: p. 477-482.

161. Makeyev, E.V., V.A. Kolb, and A.S. Spirin, *Enzymatic Activity of the Ribosome-Bound Nascent Polypeptide.* FEBS Letters, 1996. **378**: p. 166-170.

162. Kolb, V.A., E.V. Makeyev, and A.S. Spirin, *Folding of Firefly Luciferase During Translation in a Cell-Free System.* EMBO J., 1994. **13**: p. 3631-3637.

163. Kudlicki, W., et al., *Folding of an Enzyme Into an Active Conformation While Bound as Peptidyl-tRNA to the Ribosome.* Biochemistry, 1995. **34**: p. 14284-14287.

164. Komar, A.A., et al., *Cotranslational folding of globin.* J. Biol. Chem., 1997. **272**: p. 10646-106551.

165. Hardesty, B. and G. Kramer, *Folding of a Nascent Peptide on the Ribosome.* Prog. Nucleic Acid Res. Mol. Biol., 2001. **66**: p. 41-66.

166. Beckman, R.P., L.A. Mizzen, and W.J. Welch, *Interaction of hsp70 with newly synthesized proteins: Implications for protein folding and assembly.* Science, 1990. **248**: p. 850-854.

167. Frydman, J. and F.U. Hartl, *Principles of chaperone-assisted protein folding: differences between in vitro and in vivo mechanisms.* Science, 1996. **272**: p. 1497-1502.

168. Hansen, W.J., N.J. Cowan, and W.J. Welch, *Prefoldin-Nascent Chain Complexes in the Folding of Cytoskeletal Proteins.* J. Cell Biol., 1999. **145**: p. 265-277.

169. Kudlicki, W., et al., *Chaperone-dependent Folding and Activation of Ribosome-bound Nascent Rhodanese: Analysis by Fluorescence.* J. Mol. Biol., 1994. **244**: p. 319-331.

155

170. Bukau, B., T. Hesterkamp, and L. J., *Growing Up in a Dangerous Environment: a Network of Multiple Targeting and Folding Pathways for Nascent Polypeptides in the Cytosol.* Trends Cell Biol, 1996. **6**: p. 480-486.

171. Nathan, D.F., M.H. Vos, and S. Lindquist, *In vivo functions of the Saccharomyces cerevisae Hsp90 chaperone.* Proc. Natl. Acad. Sci. U.S.A., 1997. **94**: p. 1249-12956.

172. Uma, S., et al., *Hsp90 is obligatory for the heme-regulated eIF-2α kinase to aquire and maintain an activable conformation.* J. Biol. Chem., 1997. **272**: p. 11648-11656.

173. Kreig, P.A. and D.A. Melton, *Functional messenger RNAs are produced by SP6 in vitro transcription of cloned cDNAs.* Nuc. Acids Res., 1984. **12**: p. 7057-7070.

174. Thulasiraman, V., *Role of Heat Shock Proteins In Protein Synthesis, Folding, and Renaturation,* in *Biochemistry and Molecular Biology.* 1996, Oklahoma State University: Stillwater. p. 163.

175. Nelson, R.J., et al., *The translation machinery and 70 kd heat shock protein cooperate in protein synthesis.* Cell, 1992. **71**: p. 97-105.

176. Pfund, C., et al., *The molecular chaperone Ssb from Saccharomyces cerevisiae is a component of the ribosome-nascent chain complex.* EMBO J., 1998. **17**: p. 3981-3989.

177. Blobel, G. and D. Sabatini, *Dissociation of Mammalian Polyribosomes into Subunits by Puromycin.* Proc. Natl. Acad. Sci. U.S.A., 1971. **68**: p. 390-394.

178. Faust, C.H. and H. Matthaei, *A Systematic Study of the Isolation of Murine Plasma Cell Ribosomal Subunits, Their Sedimentation Properties and Activity in Polyphenylalanine Synthesis.* Biochemistry, 1972. **11**: p. 2682-2690.

179. Uma, S., V. Thulasiraman, and R.L. Matts, *Dual role for Hsc70 in the biogenesis and regulation of the heme-regulated kinase of the α subunit of eukaryotic translation initiation factor 2.* Mol. Cell. Biol., 1999. **19**: p. 5861-5871.

180. Hansen, W.J., V.R. Lingappa, and W.J. Welch, *Complex environment of nascent polypeptide chains.* J. Biol. Chem., 1994. **269**: p. 26610-26613.

181. Hightower, L., *Cultured Animal Cells Exposed to Amino Acid Analogues or Puromycin Rapidly Synthesize Several Polypeptides.* J. Cell. Physiol., 1980. **102**: p. 407-427.

182. Thulasiraman, V. and R.L. Matts, *Effect of geldanamycin on the kinetics of chaperone-mediated renaturation of firefly luciferase in rabbit reticulocyte lysate.* Biochemistry, 1996. **35**: p. 13443-13450.

183. O'Keeffe, B., et al., *Requirement for a kinase-specific chaperone pathway in the production of a Cdk9/cyclin T1 heterodimer responsible for P-TEFb-mediated Tat stimulation of HIV-1 transcription.* J. Biol. Chem., 2000. **275**: p. 279-287.

184. Smith, D.F., et al., *Reconstitution of Progesterone Receptor with Heat Shock Proteins.* Mol. Endo., 1990. **4**: p. 1704-1711.

185. Scherrer, L.C., et al., *Structural and functional reconstitiutioin of the glucocorticoid receptor-hsp90 complex.* J. Biol. Chem., 1990. **265**: p. 21397-21400.

186. Smith, D.F., et al., *Assembly of progesterone receptor with heat shock proteins and receptor activation are ATP mediated events.* J. Biol. Chem., 1992. **267**: p. 1350-1356.

156

187. Yorgin, P.D., et al., *Effects of Geldanamycin, a Heat-Shock Protein 90-Binding Agent, On T Cell Function and T cell Nonreceptor Protein Tyrosine Kinase.* J. Immuol., 2000. **164**: p. 2915-2923.

188. Renoir, J.-M., et al., *The non-DNA binding hetereomeric form of mammalian steroid hormone recptors contains a hsp90-bound 59-kDa protein.* J. Biol. Chem., 1990. **265**: p. 10740-10745.

189. Matts, R.L. and R. Hurst, *Evidence for the association of the heme-regulated eIF-2α kinase with the 90-kDa heat shock protein in rabbit reticulocyte lysate in situ.* J. Biol. Chem., 1989. **264**: p. 15542-15547.

190. Cooper, J.A., et al., *Phosphorylation Sites in Enolase and Lactate Dehydrogenase Utilized by Tyrosine Protein Kinases in Vivo and in Vitro.* J. Biol. Chem., 1984. **259**: p. 7835-7841.

191. Craig, D., et al., *Plasmid cDNA-directed protein synthesis in a coupled eukaryotic in vitro transcription-translation system.* Nucleic Acids Res., 1992. **20**: p. 4987-4995.

192. Smith, D.F., et al., *Progesterone receptor structure and function altered by geldanamycin, an hsp90-binding agent.* Mol. Cell. Biol., 1995. **15**: p. 6804-6812.

193. Hess, R., W. Staubli, and W. Riess, *Nature of the hepatomegalic effect produced by ethyl-chlorophenoxy-isobutyrate in the rat.* Nature, 1965. **208**: p. 856-858.

194. Fairhurst, A.S., G. Kent, and R.E. Purdy, *Clofibrate and vascular smooth muscle: actions on rabbit aorta preparations.* Eur. J. Pharmacol., 1981. **72**: p. 323-329.

195. Lake, B.G., et al., *The effect of hypolipidaemic agents on peroxisomal beta-oxidation and mixed-function oxidase activities in primary cultures of rat hepatocytes. Relationship between induction of palmitoyl-CoA oxidation and lauric acid hydroxylation.* Xenobiotica, 1984. **14**: p. 269-276.

196. Reddy, J.K., et al., *Transcription regulation of peroxisomal fatty acyl-CoA oxidase and enoyl-CoA hydratase/3-hydroxyacyl-CoA dehydrogenase in rat liver by peroxisome proliferators.* Proc. Natl. Acad. Sci. U.S.A., 1986. **83**: p. 1747-1751.

197. Gottlicher, M., et al., *Fatty acids activate a chimera of the clofibric acid-activated receptor and the glucocorticoid receptor.* Proc. Natl. Acad. Sci. U.S.A., 1992. **89**: p. 4653-4657.

198. Issemann, I. and S. Green, *Activation of a member of the steroid hormone receptor superfamily by peroxisome proliferators.* Nature, 1990. **347**: p. 645-650.

199. Zhang, B., et al., *Identification of a peroxisome proliferator-responsive element upstream of the gene encoding rat peroxisomal enoyl-CoA hydratase/3-hydroxyacyl-CoA dehydrogenase.* Proc. Natl. Acad. Sci. U.S.A., 1992. **89**: p. 7541-7545.

200. Takenaka, I.M., et al., *Hsc70-binding peptides selected from a phage display peptide library that resemble organellar targeting sequences.* J. Biol. Chem., 1995. **270**: p. 19839-19844.

201. Thulasiraman, V., et al., *Differential Inhibition of Hsc70 Activities by Two Hsc70-Binding Peptides.* Biochemistry, 2002. **41**: p. 3742-3753.

202. Hanks, S.K. and T. Hunter, *Protein kinases 6. The eukaryotic protein kinase superfamily: kinase (catalytic) domain structure and classification.* FASEB J., 1995. **9**: p. 576-596.

203. Hutchison, K.A., et al., *Reconstitution of the multiprotein complex of pp60^{src}, hsp90, and p50 in a cell-free system.* J. Biol. Chem., 1992. **267**: p. 2902-2908.

204. Fang, Y., et al., *Hsp90 regulates androgen receptor hormone binding affinity in vivo.* J. Biol. Chem., 1996. **271**: p. 28697-28702.

205. Xu, Z., et al., *The role of the 90-kDa heat-shock protein and its associated cohorts in stabilizing the heme-regulated eIF-2alpha kinase in rabbit reticulocye lysates during heat stress.* Eur. J. Biochem., 1997. **246**: p. 461-470.

206. Whitelaw, M.L., K. Hutchison, and G.H. Perdew, *A 50-kDa cytosolic protein complexed with the 90-kDa heat shock protein (hsp90) is the same protein complexed with pp60^{v-src} hsp90 in cells transformed by the Rous sarcoma virus.* J. Biol. Chem., 1991. **266**: p. 16436-16440.

207. Stancato, L.F., et al., *The native v-Raf-hsp90-p50 heterocomplex contains a novel immunophilin of the FK506 binding class.* J. Biol. Chem., 1994. **269**: p. 22157-22161.

208. Hunter, T., *A tail of two src's: mutatis mutandis.* Cell, 1987. **49**(1): p. 1-4.

209. Xu, W., S.C. Harrison, and M.J. Eck, *Three-dimensional structure of the tyrosine kinase c-Src.* Nature, 1997. **385**: p. 595-602.

210. Sicheri, F., I. Moarefi, and J. Kuriyan, *Crystal structure of the Src family tyrosine kinase Hck.* Nature, 1997. **385**: p. 602-609.

211. Rutherford, S.L. and S. Lindquist, *Hsp90 as a capacitor for morphological evolution.* Nature, 1998. **639**: p. 336-342.

VITA ♂

Bradley Todd Scroggins

Candidate for the Degree of

Doctor of Philosophy

Thesis: THE ROLE OF HEAT SHOCK PROTEINS IN p56^{lck} KINASE FOLDING AND FUNCTION

Major Field: Biochemistry and Molecular Biology

Biographical:

Personal Data: Born in Tulsa, Oklahoma, 1973, the son of Lee R. and Mary Lou Scroggins.

Education: Graduated from Collinsville High School, Collinsville, Oklahoma in May 1991; received Bachelor of Science in Chemistry from Oklahoma Baptist University, Shawnee, Oklahoma in May 1995; completed requirements for the Doctor of Philosophy Degree at Oklahoma State University in July 2002.

Experience: Undergraduate research fellow, University of Oklahoma, Department of Chemistry, 1994; Research Assistant, Oklahoma State University, Department of Biochemistry and Molecular Biology, 1995 to present.

Honors and Organizations: American Institute of Chemists Foundation Award for Outstanding Undergraduate Senior in Chemistry, 1995; Member of American Chemical Society 1994-1995.